A Dissertation for the Degree of Doctor of Philosophy

Precision Hydroponic Nutrient Solution Management System based on Ion-Specific and Crop Growth Sensing

개별 이온 및 작물 생육 센싱 기반의 정밀

수경재배 양액 관리 시스템

August 2020

Graduate School of
College of Agriculture and Life Sciences
Seoul National University
Major in Biosystems Engineering

Woo-Jae Cho

Precision Hydroponic Nutrient Solution Management System based on Ion-Specific and Crop Growth Sensing

Advisor: Hak-Jin Kim

Submitting a Ph.D. Dissertation of Biosystems Engineering
August 2020

Graduate School of
College of Agriculture and Life Sciences
Seoul National University
Major in Biosystems Engineering

Woo-Jae Cho

Confirming the Ph.D. Dissertation written by Woo-Jae Cho
July 2020

Chair	Joong Yong Rhee	(Seal)
Vice Chair	Hak-Jin Kim	(Seal)
Examiner	Ghisepk Kim	(Seal)
Examiner	Young-Yeol Cho	(Seal)
Examiner	Soo Hyun Park	(Seal)

Precision Hydroponic Nutrient Solution Management System based on Ion-Specific and Crop Growth Sensing

Woo-Jae Cho

ABSTRACT

In current closed hydroponics, the nutrient solution monitoring and replenishment are conducted based on the electrical conductivity (EC) and pH, and the fertigation is carried out with the constant time without considering the plant status. However, the EC-based management is unable to detect the dynamic changes in the individual nutrient ion concentrations so the ion imbalance occurs during the iterative replenishment, thereby leading to the frequent discard of the nutrient solution. The constant time-based fertigation inevitably induces over- or under-supply of the nutrient solution for the growing plants. The approaches are two of the main causes of decreasing water and nutrient use efficiencies in closed hydroponics. Regarding the issues, the precision nutrient solution management that variably controls the fertigation volume and corrects the deficient nutrient ions individually would allow both improved efficiencies of fertilizer and water use and increased lifespan of the nutrient solution. The objectives of this study were to establish the precision nutrient solution management system that can automatically and variably control the fertigation volume based on the plant-growth information and supply the individual nutrient fertilizers in appropriate amounts to reach the optimal compositions as nutrient solutions for growing plants. To achieve the goal, the sensing technologies for the varying requirements of water and nutrients were investigated and validated. Firstly, an on-the-go monitoring system was constructed

to monitor the lettuces grown under the closed hydroponics based on the nutrient film technique for the entire bed. The region of the lettuces was segmented by the excess green (ExG) and Otsu method to obtain the canopy cover (CC). The feasibility of the image processing for assessing the canopy (CC) was validated by comparing the computed CC values with the manually analyzed CC values. From the validation, it was confirmed the image monitoring and processing for the CC measurements were feasible for the lettuces before harvest. Then, a transpiration rate model using the modified Penman-Monteith equation was fitted based on the obtained CC, radiation, air temperature, and relative humidity to estimate the water need of the growing lettuces. Regarding the individual ion concentration measurements, two-point normalization, artificial neural network, and a hybrid signal processing consisting of the two-point normalization and artificial neural network were compared to select an effective method for the ion-selective electrodes (ISEs) application in continuous and autonomous monitoring of ions in hydroponic solutions. The hybrid signal processing showed the most accuracy in sample measurements, but the vulnerability to the sensor malfunction made the two-point normalization method with the most precision would be appropriate for the long-term monitoring of the nutrient solution. In order to determine the optimal injection amounts of the fertilizer salts and water for the given target individual ion concentrations, a decision tree-based dosing algorithm was designed. The feasibility of the dosing algorithm was validated with the stepwise and varying target focusing replenishments. From the results, the ion-specific replenishments formulated the compositions of the nutrient solution successfully according to the given target values. Finally, the proposed sensing and control techniques were integrated to implement the precision nutrient solution management, and the performance was verified by a closed lettuce cultivation test. From the application test, the fertigation volume was reduced by 57.4% and the growth of the lettuces was promoted in comparison with the constant timer-based fertigation strategy.

Furthermore, the system successfully maintained the nutrient balance in the recycled solution during the cultivation with the coefficients of variance of 4.9%, 1.4%, 3.2%, 5.2%, and 14.9%, which were generally less than the EC-based replenishment with the CVs of 6.9%, 4.9%, 23.7%, 8.6%, and 8.3% for the NO_3, K, Ca, Mg, and P concentrations, respectively. These results implied the developed precision nutrient solution management system could provide more efficient supply and management of water and nutrients than the conventional methods, thereby allowing more improved water and nutrient use efficiencies and crop productivity.

Keyword : Automated system, Closed-loop control, Closed hydroponics, On-the-go crop monitoring, Precision nutrient solution supply, Ion-specific nutrient solution replenishment

Student Number : 2015-30385

TABLE OF CONTENTS

LIST OF FIGURES

LIST OF TABLES

CHAPTER 1. INTRODUCTION

BACKGROUND

Hydroponics, also called as soilless cultivation, can be defined as a cultivation technique that produces plants in soilless conditions in which the supply of water and minerals is carried out in nutrient solutions with or without a growing medium (e.g. stone wool, peat, perlite, pumice, coir, etc.) (Maucieri et al., 2019). Hydroponics has been widely utilized in greenhouses or plant factories because of the advantages such as the absence of soil-borne pathogens, efficient use of water, energy, space, and cost for growing plants (P Agung Putra & Henry Yuliando, 2015; F. X. Rius-Ruiz et al., 2014). Furthermore, hydroponics has the capacity for increased yield, which could be about 10 times higher than the conventional production (Barbosa et al., 2015a; Sambo et al., 2019).

In hydroponics, fertigation is the preferred approach to supplying nutrients and water, which is achieved by dissolving the soluble fertilizers in the irrigation water using injection equipment. This type of irrigation with the nutrient solution is called “fertigation” and it is one of the most important factors that are closely related to the crop yield and quality (Incrocci et al., 2017; P Agung Putra & Henry Yuliando, 2015; Raviv et al., 2019).

Fundamentally, fertigation makes the water and nutrients supply inextricable in hydroponics. Although the combined supply usually allows more efficient nutrient and water use in plant production than the soil-based cultivation, the discharge of nutrient solutions from the soilless culture systems can be a threat of environments (Ahn & Son, 2019; D. H. Jung et al., 2015). The wasted nutrients and water are higher in the open hydroponic system where the nutrient solution flows through the growing bed and is discarded. For the reason, closed hydroponics that recirculates and reuses nutrient solutions is compulsory by legislation in many countries, particularly in environmentally protected areas, or those suffering the scarcity of

water resources (Gieling et al., 2005; W. Voogt & C. Sonneveld, 1997; Zekki et al., 1996).

Despite the advantages of closed hydroponic systems such as less pollution of ground and surface water, less waste of water and nutrients, and lower costs in crop production, the nutrient and water use efficiencies of closed soilless cultivation are aggravated (Matthew Bamsey et al., 2012; D. H. Jung et al., 2015; Meric et al., 2011). Two of the main reasons are ion imbalance and fertigation scheduling.

NUTRIENT IMBALANCE

In closed hydroponic systems, the primary difficulty in managing the nutrient solutions is the imbalance of nutrient ions in the recycled nutrient solutions, which can induce the worsening of the edible parts' quality and productivity (Matthew Bamsey et al., 2012; Sambo et al., 2019). In current hydroponic systems, pH and electrical conductivity (EC) of the solutions are usually monitored to evaluate the nutrient status of recirculating hydroponic solutions (Domingues et al., 2012; N. Katsoulas et al., 2015; Kozai et al., 2018; Son et al., 2020). The main problem with this practice is that because EC measurements provide no information on the concentrations of individual ions, real-time individual corrections to each nutrient are not possible (Cloutier et al., 1997). Since plants require varying concentrations of nutrient ions for their growth and environmental conditions, such an EC-based control may lead to accumulation or deficiency of certain nutrients (Matthew Bamsey et al., 2012; Gieling et al., 2005; Zheng, 2017). In actual, several studies reported the nutrient imbalance in nutrient solutions after recirculation (Ahn & Son, 2019; Myat Thaint Ko et al., 2014; M. T. Ko et al., 2013; F. X. Rius-Ruiz et al., 2014).

One of the most common practices for managing the nutrient solutions based on individual nutrient ions is a periodical adjustment of recycled nutrient solutions, but it cannot help farmers to respond rapidly to unexpected changes in nutrient

ratios in hydroponic solutions (Matthew Bamsey et al., 2012). As a result, it would require frequent replacement of the nutrient solution, thereby reducing the nutrient and water use efficiencies.

Benchtop or portable analyzers equipped with ion-selective electrodes (ISEs) also could be used to measure the concentrations of individual ions in hydroponic solutions with the advantages such as rapid response, direct measurement of the analyte, low cost, and portability (Matthew Bamsey et al., 2012; Cloutier et al., 1997; Gutierrez et al., 2007; H. J. Kim et al., 2013). However, for on-site nutrient monitoring, which requires frequent immersions of the ISEs in solutions, the accuracy of the determination of nutrient concentrations is strongly affected by the signal drift and reduced sensitivity over time, which could be caused by manual calibrations, sampling, and the maintenance involved in the operation of ISEs (Caceres et al., 2017; H. J. Kim et al., 2017; F. X. Rius-Ruiz et al., 2014; Vardar et al., 2015). In this regard, the ideal way to solve the nutrient imbalance is to use a feedback control system, which can conduct automatic corrections to each deficient nutrient based on the measurement of individual nutrient concentrations, thereby allowing both improved efficiency of fertilizer use and increased time of use of the nutrient solution (Dorneanu et al., 2005; D. H. Jung et al., 2015; Zheng, 2017).

FERTIGATION SCHEDULING

Irrigation management is directly related to water use efficiency in agriculture. Under-irrigation usually results in reduced crop yield and quality and over-irrigation decreases the nutrient use efficiency of the crop and its vulnerability to diseases, the energy costs for water pumping (Pardossi et al., 2009), Therefore, efficient irrigation is important in horticulture, considering its implications on the success of the crop cultivation. Regarding the irrigation efficiency, two of the most important factors are the amount of water to be applied to the crop and the timing for application. In addition, not only irrigation but also fertilization is accomplished

by fertigation in hydroponics. It makes the scheduling of the fertigation more crucial in hydroponics.

In hydroponics, most fertigation has been automated, but it does not mean the efficient fertigation is achieved (F. F. Montesano et al., 2018). The most common and relatively easy method is automation using timers based on grower's experience without measurements to assess the adequate water inputs (Nemali et al., 2007; Nikolaou et al., 2019; Romero et al., 2012).

More efficient fertigation could be achieved by applying a feedback based closed-loop fertigation system or a feed-forward control system (Kläring, 2001). The closed-loop system can evaluate the percentage of drainage or plant water status to manage the fertigation interval (Rodríguez et al., 2015). In the feed-forward system, the crop water uptake is predicted by using growth and transpiration models (Prenger et al., 2005). However, the application of both systems usually depends on environmental variables, such as sunlight, humidity, and soil water content, which is not directly related to the plant responses (Baek et al., 2018). Those conventional approaches cannot respond to the varied plants' growth and physiology, thereby limiting efficient fertigation (Del Amor et al., 2010; Prenger et al., 2005).

Recently, several studies have reported the applicability of the remote sensing technology for plant-based irrigation strategies by monitoring the plant status such as leaf water potential, canopy temperature, crop reflectance, or biomass (Daniel G Fernández-Pacheco et al., 2014; Incrocci et al., 2017; F. F. Montesano et al., 2018; Nikolaou et al., 2019; Prenger et al., 2005). Furthermore, machine-vision based approaches could give various and useful information including the morphology (size, shape, and texture), spectrum (color, temperature, and water contents) and temporal variations (growth rate, flowering, and fruiting) (Chen et al., 2016; Hu et al., 2018; Joo & Jeong, 2017; Lati et al., 2013; Li et al., 2014; Story & Kacira, 2015; Te et al., 2011; Yeh et al., 2014). The vision-based crop management also has

been tried by several agricultural industries. For example, the HortiMaX (http://www.hortimax.com) developed a CropView system, which can provide real-time monitoring of plant canopy and the Priva (http://www.priva-international.com) developed a TopCrop Monitor that can estimate the plant transpiration by measuring the crop activity in the greenhouse based on plant temperature. However, the systems can only provide the information of plants within the image, not the entire plant canopy due to the fixed location. Also, little work has been done to correlate the obtained data with crop management (Nikolaos Katsoulas et al., 2016). Therefore, more researches on the imaging techniques are required for more efficient and practical agricultural application. In this context, the development of non-destructive, rapid, and reliable estimation methodology for the water needs of the growing plants based on the vision system would allow the optimization of the fertigation intervals, leading to improved water and nutrient use efficiencies.

The current practices and the issues of the closed hydroponics are summarized in Table 1.1.

Table 1.1. Current practices of closed hydroponics in nutrient solution replenishment and the fertigation scheduling

Category	Method	Limitation	Applied system
Nutrient solution replenishment	EC-based replenishment	● Lack of information about the individual ion concentration and balance ● Need of periodical sample analysis ● Need of periodical renewal of the nutrient solution	● NFT (nutrient film technique) ● Aeroponics ● DFT (deep flow technique) ● Ebb and flow ● Drip system
Fertigation scheduling	Time clock	● No considerations for the varied plant water uptake	● NFT (nutrient film technique) ● Aeroponics ● DFT (deep flow technique) ● Ebb and flow ● Drip system
	Climate monitoring (e.g., evapotranspiration, solar radiation)	● Indirect relationship to the plant responses	● NFT (nutrient film technique) ● Aeroponics ● DFT (deep flow technique) ● Ebb and flow ● Drip system
	Substrate monitoring (e.g., volumetric water content, percentage of drainage)	● Indirect relationship to the plant responses ● Limited applicability for the water culture	● Drip system
	Phyto-sensing (e.g., leaf water potential, canopy temperature, sap flow, crop reflectance)	● Specific to each plant ● Lack of information for entire plants	● NFT (nutrient film technique) ● Aeroponics ● DFT (deep flow technique) ● Ebb and flow ● Drip system

OBJECTIVES

The overall objectives of this research were 1) to establish a variable fertigation system that can measure the canopy covers of plants and adjust the fertigation volumes to be supplied based on the varying canopy covers and aerial environmental factors, and 2) to develop an automatic system that can measure the varied ion concentrations in the reused nutrient solution and replenish the nutrients for each deficient ion, thereby allowing more efficient management of nutrients and water in closed hydroponic systems.

The specific objectives were as follows.

1) To construct an on-the-go crop monitoring system that could collect the images of growing lettuces and compute the canopy cover, and characterize the transpiration rate of the growing lettuces using the canopy cover, air temperature, relative humidity, and radiation for adaptive fertigation strategy.
2) To evaluate two or more types of signal processing methods for ion-selective sensors to compensate the signal drifts over time and interferences from other ions present in hydroponic solutions, and select the effective method for application in continuous and autonomous monitoring of ions in hydroponic solutions.
3) To develop an ion-specific nutrient dosing algorithm that could efficiently maintain the target concentrations of individual nutrients and employ the closed control scheme by evaluating the nutrient solution after the replenishment and carrying out additional injections for more accurate nutrient management.
4) To testify the precision hydroponic nutrient solution management with the lettuce cultivation by adjusting the fertigation volumes to be supplied based on the estimated transpiration rate from the canopy cover of the growing lettuces in conjunction with the prevailing greenhouse

environment and correcting the ion concentrations in the recycled nutrient solution for deficient ions.

ORGANIZATION OF THE DISSERTATION

The organization of the dissertation is as follows.

Chapter 2 provides literature reviews for related researches.

Chapters 3, 4, and 5 describe the subsystems or the technologies for the precision nutrient solution supply and management system.

In Chapter 3, the overall structure of the experimental hydroponic system was introduced. Then, an on-the-go canopy cover (CC) monitoring system and environmental sensors for the estimation of the transpiration rate using the modified Penman-Monteith equation were described with image acquisition and processing procedures for assessing the canopy cover of the growing lettuces. Finally, the performance of the CC and the transpiration rate estimation was discussed.

In Chapter 4, three signal processing methods including the two-point normalization (TPN), artificial neural network (ANN), and a hybrid method that employed both the TPN and the ANN, were compared to select the most applicable method for using an array of the ion-selective electrodes in hydroponic solutions. For the comparison of the three signal processing methods, the predictability of the ISE array was tested using 27-artificial samples and 8-real hydroponic samples, and the applicability was discussed.

In Chapter 5, a decision tree (DT)-based dosing algorithm was designed to determine the proper amount of fertilizer salts to manage the ion concentrations close to the preset concentrations. Then, an ion-specific nutrient management system was developed using the DT-based dosing algorithm with a closed-loop control scheme to achieve the accurate resulting concentrations. The DT-based dosing algorithm was validated by the five replenishments for the randomly

determined three level-concentrations of NO_3^-, K^+, and Ca^{2+}, and the results were compared with those obtained by the conventional simplex-based dosing algorithm. In addition, the Ca^{2+}-focused replenishment scenario was conducted to clarify the system responses to the Ca concentrations, which would be smaller than the other measurable ions, i.e., K^+ and NO_3^-.

Finally, in Chapter 6, the introduced subsystems and technologies were integrated and a lettuce cultivation test was conducted with the nutrient solution supply and management by the integrated system. The effectiveness of the system was investigated in two aspects. Regarding the nutrient solution supply, the efficiency of fertigation control based on the estimated water need was compared with the fertigation based on the timer. For evaluating the nutrient management performance, the nutrient ion balance during the cultivation was compared with the EC-based replenishment and the ion-specific replenishment.

The general conclusions and further studies are explained in Chapter 7.

For simplicity in describing the contents of the dissertation, the ions will hereafter be written without the charges.

CHAPTER 2. LITERATURE REVIEW

VARIABILITY OF NUTRIENT SOLUTIONS IN HYDROPONICS

In hydroponic cultivation systems, plants' uptakes of water and nutrients are fully dependent on the nutrient solutions. For efficient plant growth, there would be optimal compositions and concentrations. Steiner investigated the optimal ratios of cations and anions with fixed levels of EC and pH for nutrient solutions. He tested 1,600 combinations of the main nutrient ions (NO_3, H_2PO_4, SO_4, K, Ca, and Mg) and proposed a method to calculate the proper ion ratios for the optimized nutrient composition (Steiner, 1961). In 1966, Steiner verified the effects of the optimized nutrient compositions by applying the various nutrient solutions that were more than 10 combinations for soilless cultivations of tomato plants (Steiner, 1966).

Wiser and Blom (2016) reported that the ion ratios of NO_3, NH_4, and P differently influenced on crop growth and height among marigolds, sunflowers, and tomatoes, indicating the optimal compositions would be varied for crop species .

Schippers (1979) analyzed the concentrations of N, P, and K in the nutrient solutions of tomatoes, cucumbers, and lettuce, and confirmed the need for periodic analysis of nutrient solutions because the degree of ion absorption in the nutrient solution for each crop changed according to the growth of the crops .

Terabayashi et al. (2004) confirmed that the maximum yield of tomato appeared when applying the varied nutrient compositions for each growth stage.

J. Y. Lee et al. (2017) analyzed the changes of individual ion concentrations in nutrient solutions for tomato, and the uptake patterns could be divided into 5 stages of transplanting, adaptation, flowering, fruiting, and harvest.

Nutrient solution compositions should be adjusted considering the environmental factors such as temperature, humidity, and light conditions. For example, the nutrient uptakes of radish were varied according to the seasonal change, which

might be due to the different light, temperature, and humidity conditions (Sonneveld & Van den Bos, 1995).

Morimoto et al. (1996) observed daily changes in nutrient concentration of the solution in hydroponic tomato cultivation and reported the complex interactions in nutrient concentrations and environments.

Noh et al. (2011) also configured the significant correlation ($p \leq 0.01$) between the light intensity and the nutrient uptake of Kalanchoe in an ebb and flow based soilless cultivation system.

The aforementioned researches show the variability of the ion concentrations in nutrient solutions. Therefore, it is necessary to replenish the nutrients and water for nutrient solutions for maintaining the concentration of these nutrients in solution at proper levels for the success of closed hydroponic cultivation.

LIMITATIONS OF CURRENT NUTRIENT SOLUTION MANAGEMENT IN CLOSED HYDROPONIC SYSTEM

In general, nutrient management in closed hydroponics is conducted based on electrical conductivity (EC) and pH measurements. EC of the nutrient solutions is proportional to the total ions present, so it can be an indirect indicator of nutrient concentrations within nutrient solutions (Domingues et al., 2012; N. Katsoulas et al., 2015; Kozai et al., 2018; Son et al., 2020). pH determines the availability of nutrient ions for plants, and the proper level of pH for nutrient uptake is usually between pH 5.5 and pH 6.5 (G. De Rijck & Schrevens, 1997; Resh, 2016).

Based on the EC and pH, Zekki et al. (1996) manually replenished the nutrient solutions every day and compared the productivity of the closed cultivation to the productivity of the open cultivation . He reported there was an accumulation of several nutrients such as K_2SO_4 and $MgSO_4$, thereby reducing the total productivity in closed hydroponics.

In 1999, Savvas and Manos developed a computer algorithm that could

perform replenishment and reuse of the drain nutrient solution in close hydroponic systems while maintaining a target electrical conductivity in the nutrient solution. From the application tests for growing roses, gerbera, chrysanthemum, and carnation, they showed the reused nutrient solution could be corrected efficiently in terms of EC, but a nutrient imbalance occurred after a fortnight of drain solution reuse (D Savvas & Manos, 1999).

Savvas (2002) improved the capability of maintaining the nutrient balance by supplying freshwater or adopting the ion uptake ratio, but these strategies limited by the water quality and imposed a partial discharge of nutrient solution.

Ahn et al. (2010) monitored the reused nutrient solution of closed-hydroponic paprika using the EC based system and reported the deviation of nutrient ratio was proportional to the recycling rate of the drainage.

Ko et al. (2013) also investigated the nutrient composition in the recycled nutrient solution and reported the significant reductions in NO_3, K, Ca, and Mg, and the accumulation of SO_4, Cl, and Na.

The nutrient imbalance issue when reusing nutrient solution based on EC is still ongoing. Therefore, hydroponic growers who want to manage their nutrient solutions based on individual nutrient species and extend the lifespan of the nutrient solution, depend on relatively infrequent (e.g., 1–3 weeks) off-line analysis by manually sampling and mailing the nutrient solution to laboratories with huge and expensive analytical instruments such as a colorimetric spectrophotometer, an AAS (Atomic Absorption Spectrophotometer) analyzer, an ICP (Inductively Coupled Plasma) spectrometer, or ion chromatography system (M. Bamsey et al., 2012; Gieling et al., 2005; W. Voogt & C. Sonneveld, 1997). In addition, the relatively low adjustment frequency of recycled nutrient solutions based on standard analysis could reduce the stability and operational cost in closed hydroponics. In this regard, automatic corrections to each deficient nutrient based on the measurement of individual nutrient concentrations would allow both

improved efficiency of fertilizer use and increased time of use of the nutrient solution.

ION-SPECIFIC NUTRIENT MONITORING AND MANAGEMENT IN CLOSED HYDROPONICS

The need for individual nutrient monitoring has led to the application of ion-selective electrode (ISE) technology to measure hydroponic macronutrients due to several advantages of ISEs over standard chemical analytic techniques, such as rapid response, direct measurement of the analyte, low cost, and portability.

In 1988, Bailey et al. developed an automated measuring system that could monitor pH, nitrate, potassium, calcium, sodium, and chloride in nutrient film solutions using ISEs. The accuracies of nitrate, sodium, and potassium measurements were within 10%, although the deviations of calcium and chloride were more than 20%. Based on the results, they concluded the ISEs would be applicable in horticulture, but frequent and regular calibrations should be conducted to accommodate the drift and extend the life of the ISE.

Cloutier et al. (1997) evaluated the potential of the ISEs application in closed hydroponics. They found the sensitivities of the Ca, K, NH_4, and NO_3 varied by -134%, -20.2%, -26.5%, and -12.0% over the 24 hours, respectively, indicating the significant automation requirements for the ISE calibration.

Gieling et al. (2005) employed an array of ISEs and ion-selective field-effect transistor (ISFET) to measure the concentration of the individual ions in the drainage water and controlled the injection pumping times of the liquid single element nutrients. Although the concentrations of Ca, K, and NO_3 in the drain were kept reasonably well at the set values, the feasibility was only validated for 6-days.

Gutierrez et al. (2007) developed an electronic tongue with an array of solid-state ISEs that could measure NH_4, K, Na, Cl, and NO_3, and applied a multilayer artificial neural network (ANN) model to enhance the predictability of the system

by compensating the strong interfering effects. However, the effect of response drifts of the sensor array was found. After 1 year, although they supplemented PO_4 electrodes to the electronic tongue system and validated the feasibility of the system in real greenhouse samples, the problems of the low reliability of PO_4 electrodes and the drifts in the sensor array were not solved (Gutierrez et al., 2008).

Kim et al. (2013) fabricated NO_3, K, and Ca ISEs and constructed a test stand with an array of ISEs which automatically conduct rinsing, normalization, sample injection, and sample analysis for hydroponic solutions. They reported the two-point normalization was effective in minimizing potential drift and bias that might occur during continuous, thereby improving the applicability of the ISEs for hydroponic nutrients in greenhouses.

In 2014, Rius-Ruiz et al. (2014) developed an analytical platform with K, NO_3, Ca, and Cl solid-state electrodes to monitor the nutrient compositions in hydroponic solutions and replenish the solutions as optimal concentrations manually for 120 days. Specifically, they verified the two-point calibration was more effective in improving sample measurement accuracy than the one-point calibration.

Jung et al. (2015) improved the system developed by Kim et al. (2013) by adding the control logic to measure the NO_3, K, and Ca in the closed hydroponic system and manage the ion concentrations automatically using the three single element nutrients. Although the three ions were controlled to reach target concentrations of 280, 140, and 70 $mg \cdot L^{-1}$ within errors of -7.7±28.1, 20.8±28.5, and -5.6±8.2 $mg \cdot L^{-1}$ for NO_3, K, and Ca ions, respectively, during the lettuce cultivation, the fertilization was limited by the coupled compositions of the nutrients. In 2019, the system was modified to manage the P and Mg concentrations by injecting the nutrients proportional to the supply of and NO_3 and Ca ions, respectively, and the feasibility of the cobalt electrodes to measure P concentrations was evaluated. However, the effectiveness of the proportional

injection of Mg and P was not clear and the dosing algorithm was insufficiently analyzed.

As described above, various hydroponic applications using ISEs for individual ionic concentration measurement and nutrient solution management were achieved. However, the electrode drift and the absence of the reliable ionophore that could measure the main nutrient ions of P, Mg, and SO_4 hinder the application of ISEs in the hydroponic application. Specifically, P ion has various forms according to the pH of the solution and could be easily affected by other interfering ions (Gutierrez et al., 2008; H.-J. Kim et al., 2007). Mg and S ionophores developed until now have limitations of very low selectivity and sensitivity, so there is no successful application case in hydroponics (H. J. Kim et al., 2013; Lomako et al., 2006).

The table below summarizes the researches on nutrient solution measurement and control (Table 2.1).

Table 2.1. Researches on hydroponic systems for nutrient solution monitoring and management

Author (Year)	Plant species	Nutrient solution sensor	Nutrient solution management	Limitations
Zekki et al. (1996)	Tomato (Capello)	EC, pH	Manual adjustment	Accumulation of SO_4
Savvas & Manos (1999)	Roses, gerbera, chrysanthemum and carnation	EC, pH	Stock solution injection based on the computer algorithm	Accumulation of Na, Cl, Ca, Mg, and SO_4 Reduction of P, Zn, Mn, K, Fe, NO_3, B
Savvas (2002)	Chrysanthemum	EC, pH	Stock solution injection based on the computer algorithm	Accumulation of Ca and Mg Reduction of K
Bailey et al. (1988)	Tomato	ISEs (NO_3, K, Ca, Na, Cl, pH)	Manual adjustment	Low accuracy Low lifetime Bubbles in flow cell
Gieling et al. (2005)	Plant (Not described)	ISE and ISPET	Single element nutrients injection	Short-monitoring Deviation of NH_4 and Ca
Gutierrez et al. (2007)	Rose (Rosa indica L. cv. Lovelly Red)	ISEs (NH_4, K, Na, Cl, and NO_3)	Monitoring	Drifts in sensor array Low accuracy in Cl
Gutierrez et al. (2008)	Rose (Rosa indica L. cv. Lovelly Red)	ISEs (NH_4, K, Na, Cl, NO_3, and PO_4)	Monitoring	Drifts in sensor array Low accuracy in PO_4
Kim et al. (2013)	Paprika	ISEs (NO_3, K, and Ca)	Analysis	Off-line analysis Low selectivity in Ca ISE
Rius-Ruiz et al. (2014)	Tomato (Solanum lycopersicum)	ISEs (NO_3, K, Ca and Cl)	Monitoring, manual adjustment	Low stability in NO_3, Cl
Jung et al. (2015)	Lettuce	ISEs (NO_3, K, and Ca)	NO_3, K, and Ca salt solution injection	Limited fertilization Low K estimation
Jung et al. (2019)	Lettuce	ISEs (NO_3, K, and Ca)	NO_3, K, Ca, Mg, and P salt solution injection	Unclear performance of Mg and P management Low stability of cobalt electrodes

REMOTE SENSING TECHNIQUES FOR PLANT MONITORING

In hydroponics, the supply of water and nutrients is dependent on the fertigation, so the efficient use of water and nutrient could be achieved by optimizing the fertigation. Precision fertigation, which provides water based on the water needs of the plant, would be an effective approach for saving water and nutrient while maximizing yield (Abioye et al., 2020; Jones, 2004; Zeng et al., 2009). To achieve precision fertigation, there is a need to assess the status of plants to adjust the fertigation at an appropriate level (Nikolaos Katsoulas et al., 2016). Machine vision would be an effective, non-invasive, and non-destructive sensing technology for measuring morphological and spectral characteristics in plant growth monitoring, post−harvest grading, transplant detection, and disease diagnosis (Kacira & Ling, 2001).

He et al. (2003) developed a stereovision system using two cameras and constructed three-dimensional (3D) color images of the transplant population from pairs of two-dimensional (2D) color images to estimate average height, leaf area, fresh mass, and dry mass determined from destructive measurements. From the results, the estimated values were correlated closely with the values determined from destructive measurements (R^2: 0.7-0.9).

Yeh et al. (2014) showed a more advanced stereo-vision system which could obtain the images of lettuces growing in the vertical bed automatically. They reported the system could enable the continuous and non-destructive estimation of the plant projected leaf area, height, and volume index.

Recently, Hu et al. (2018) reported the newly developed depth camera could easily give information of the plant projected leaf area, fresh weight, and height that had high determination coefficients of 0.9 versus the standard analysis .

A vision-based assessment of the crop water needs also has been widely investigated. One of the most important vision-based plant properties is the canopy cover (CC), which is also called the percentage of ground cover of vegetation

(PGC) (Allen et al., 1998; Daniel G. Fernández-Pacheco et al., 2014; Stojanova et al., 2010). CC is defined as “the vertical projection of the plant canopy onto an imaginary horizontal surface” (Stojanova et al., 2010). This parameter is a key component for estimating the crop water requirements using FAO-56 methodology due to its strong linear relationship with the leaf area index (Allen et al., 1998; Baret et al., 2000; Córcoles et al., 2013; Escarabajal-Henarejos et al., 2015; García-Mateos et al., 2015; Gitelson et al., 2003; Lati et al., 2013; J. Y. Lee et al., 2017).

Fernández-Pacheco et al. applied digital photography in plant growth monitoring and obtained the CC of the lettuces growing in the field. Then, they estimated the crop height using the CC and computed the crop coefficient K_c from the CC and the crop height. From the validation test, the linear regression analysis between the estimated K_c and the actual K_c showed a slope of the linear regression line very similar to 1 (0.966) and a squared correlation coefficient of 0.977, indicating the vision approach could be used to determine the crop water requirements. Similarly, González-Esquiva et al. (2017) reported that the canopy cover (CC) of the growing lettuces obtained from the digital photography could be utilized to calculate the crop coefficient below 1% of error.

Story and Kacira (2015) developed a plant monitoring system that could dynamically collect the canopy images using color, near-infrared (NIR), and thermal cameras. From these three types of images, they showed the system could determine the water stress level as well as the plant morphology (top projected plant and canopy area).

Nutrient uptakes and requirements of crops are also crucial considerations for the precision fertigation. Elvanidi et al. (2018) tried to detect the nitrogen deficiency in hydroponically grown tomatoes using a hyperspectral machine vision sensor. Through the background adjusted nitrogen index, they confirmed the possibility of the reflectance-based detection of nitrogen stress.

Sun et al. (2018) suggested temporal dynamics of rice leaf in morphology and

color to identify NPK deficiencies. The results showed there were distinct leaf responses to NPK deficiencies. However, it would be difficult to independently distinguish the influences of NPK deficiencies on leaf extension and senescence.

Nguyen et al. also investigated the hyperspectral remote sensing to assess nutrient status in bok choy and spinach grown under greenhouse conditions. The results demonstrated that individual spectral bands in three spectral regions (700–709 nm, 780–787 nm, and 817–821 nm) were significantly correlated with leaf contents of N, K, Mg and Ca, thereby allowing more efficient fertilizer regimes.

Although the studies showed a potential of the remote sensing for the plant nutrient uptakes and requirements, further studies are needed to use the remote sensing in agricultural application due to the variations in the reflectance according to the light conditions, ambient conditions, growth stages, or nutrient compositions in hydroponic solutions. Therefore, the fertigation control based on the crop water needs would be only possible as the first step for the precision fertigation.

FERTIGATION CONTROL METHODS BASED ON REMOTE SENSING

In practice, several studies reported the fertigation control using the vision-based estimation of the water needs of plants reduced water consumption and improved productivity.

Prenger et al. (2005) estimated the crop evapotranspiration (ET) based on the crop water stress index (CWSI) using infrared thermometry (IRT) measurement of plant canopy temperature. When applying the closed-loop proportional irrigation control based on the estimated ET, only 52% of the water used for the conventional system was used while the height, fresh mass, and dry mass were not significantly different (95% confidence interval).

Seeling et al. (2012) automated the irrigation control for growing cowpea based on the dynamics of leaf thickness and reported that between 25 and 45% of irrigation water could be conserved compared with a typical timed irrigation

schedule.

Osroosh et al. (2016) variably controlled the irrigation for apple trees based on CWSI and weather and confirmed the strategy substantially reduced water applied (70%) while maintaining the stem water potential within the non-stressed range.

By computer processing of digital photographs of vegetation cover, Escarabajal-Henarejos et al. (2015) built a model for estimating the crop coefficient and validated the model performance during the subsequent 2 years. Furthermore, they applied the model to schedule crop irrigation and reported a 6.93% increase in production and a 17.80% reduction in water consumption compared to the grower's irrigation control.

Up to now, the fertigation control based on plant status measured by the remote sensing methods has been mainly investigated for the open field cultivations. In general, fertigation under the soilless culture requires a much more frequent control due to the small volume occupied by the root system and low water-holding capacities (M. Gallardo et al., 2013). Therefore, a fast and on-the-go monitoring of plant responses is necessary to accomplish precision fertigation in hydroponic cultivation.

CHAPTER 3. ON-THE-GO CROP MONITORING SYSTEM FOR ESTIMATION OF THE CROP WATER NEED

ABSTRACT

Precision fertigation in soilless cultivation is an important task to secure sustainable water use. However, the difficulty in assessing the water needs of the plants due to the varied plant growth and the environmental information hinders the establishment of the precision fertigation. In this study, an estimation model for the transpiration rate of the plants growing in hydroponics was characterized using the modified Penman-Monteith equation. Furthermore, an on-the-go crop monitoring system that can compute the canopy cover of the growing plants was established using a two-axis guided moving camera for monitoring the entire growing bed and sensors for measuring ambient conditions in the greenhouse. From the application test to the lettuces growing in the nutrient film technique cultivation, the developed system showed a high accuracy of 98.5 ±1.7% for the canopy cover measurements besides the saturated period, indicating the feasibility of estimating the growth information of the lettuces in hydroponics. In addition, the system showed high predictability for the transpiration rate with a highly linear relationship of a slope of 0.91, coefficient of determination (R^2) >0.9, and standard error of the regression (SER) of <0.51 in comparison to the direct measurement. The results indicate the developed model could provide the water needs of the growing lettuces in a simple and real-time manner, thereby allowing more efficient and effective fertigation in hydroponics.

INTRODUCTION

The scarcity of water poses a limitation on agricultural water utilization, so there is a growing demand for developing efficient water management techniques

(García et al., 2020; Romero et al., 2012; Sesma et al., 2015). Specifically, irrigation or fertigation (i.e., irrigation combined with fertilization) is the greatest water user in agriculture (F. F. Montesano et al., 2018). However, irrigation or fertigation practices are generally based on the personal experience of the grower without considering the water needs of the growing plant (Bonachela et al., 2006; Chauhan et al., 2013). This approach usually causes over- or under-irrigation for crops, thereby leading to higher water consumption and less yield and quality of crops (Bonachela et al., 2006; Liu & Xu, 2018; Prenger et al., 2005). For these reasons, precision irrigation, which is a technique that provides water based on the water needs of the plant at the desired location, has been emerged and widely investigated in the last years (Mafuta et al., 2013; F. F. Montesano et al., 2018; Smith & Baillie, 2009).

To achieve precision irrigation, an accurate and fast assessment of the water needs of the plants should be conducted. However, traditional estimations usually suffer from an inaccurate estimate of the crop water need because the crop water need is often affected by the climatic conditions and crop growth (Kläring, 2001; Prenger et al., 2005; Rodríguez et al., 2015). Moreover, all direct methods of measuring the crop growth are extremely laborious, destructive, site-specific, and costly in terms of time and money (Jiang et al., 2018; Nikolaos Katsoulas et al., 2016; Kirk et al., 2009; Sigrimis et al., 2001).

In this context, a vision-based approach would be an effective tool for obtaining the various parameters related to plant growth and water status in real-time (González-Esquiva et al., 2017; Lorente et al., 2012). Specifically, the most applicable parameter from the vision sensors for estimating the plant growth is the leaf area index, which has a linear relationship with the canopy cover (CC) (Córcoles et al., 2013). It could estimate the water need of plants because it is directly related to evapotranspiration (Escarabajal-Henarejos et al., 2015; Daniel G Fernández-Pacheco et al., 2014).

As one of the transpiration rate estimation methods using the LAI, the Penman-Monteith (P-M) equation has been widely used (Ahn & Son, 2019; Allen et al., 1998; Baille et al., 1994; J. W. Lee et al., 2013). In this regard, the estimation of the transpiration rate based on the automated measurement of the CC of the growing plants would allow the precision fertigation approach for hydroponic growers, thereby improving the water use efficiency.

In this study, a P-M equation-based estimation model for the transpiration rates of the growing plants in hydroponics was developed. Specifically, the model used the CC obtained from an on-the-go image monitoring system and the environmental sensors to respond to the varied water needs of the plants according to the ambient conditions and the growing days. Crop cultivation test was carried out with lettuces (*Lactuca sativa*) which is one of the most popular vegetables and is the most consumed salad crop (Ryder, 1999). The specific objectives were to (1) develop an on-the-go crop monitoring system that can collect the environmental conditions and RGB images of the plants grown in hydroponics for computing the CC, (2) characterize the P-M equation-based crop water need estimation model in conjunction with the sensor data of the temperature, relative humidity, radiation, and CC, and (3) evaluate the performance of the model by comparing the estimated transpiration rate with the actual transpiration rate of the lettuces grown in the recirculating nutrient film technique (NFT) bed.

MATERIALS AND METHODS

HYDROPONIC GROWTH CHAMBER

The experimental growth chamber is an even-span plastic greenhouse (Fig. 3.1 a). The bottom area is approximately 7.44 m^2, and the heights of the wall and top are 1.3 m and 2.2 m, respectively. In the growth chamber, a nutrient film technique (NFT)-based growing bed is installed with evenly-distributed 25 fluorescent lamps as shown in Figs. 3.1(b) and 3.1 (d). A total of 45 growing holes are prepared for

the growing bed with a distance of 0.02 m (Fig. 3.1c), which is constructed according to the hydroponic culture guideline for the lettuces of the RDA (Rural Development Administration, South Korea). During the cultivation, growing plants would be suspended on the holes while the growing bed is supported by eight poly(vinyl) chloride (PVC) cylinders. To equally supply hydroponic nutrient solutions over the growing bed, eight distribution nozzles were applied with a circulation pump (PP50Y, Hwarang System Co., Ltd., Incheon, South Korea). The leachate flows into a drainage hole located on the opposite side of the injection nozzles.

The experimental growth chamber is located in the experimental room of Seoul National University (Seoul, Republic of Korea, latitude 37.45786°N, longitude 126.94845°E). Although there is no precise environmental control or the bio-filtration system in the room, it can provide the circumstance that is sufficiently out of the climatic elements (e.g. wind, rain, and sunlight) with the prevention of pest intrusion. The detailed structures and dimensions of the growth chamber are shown in Fig 3.1.

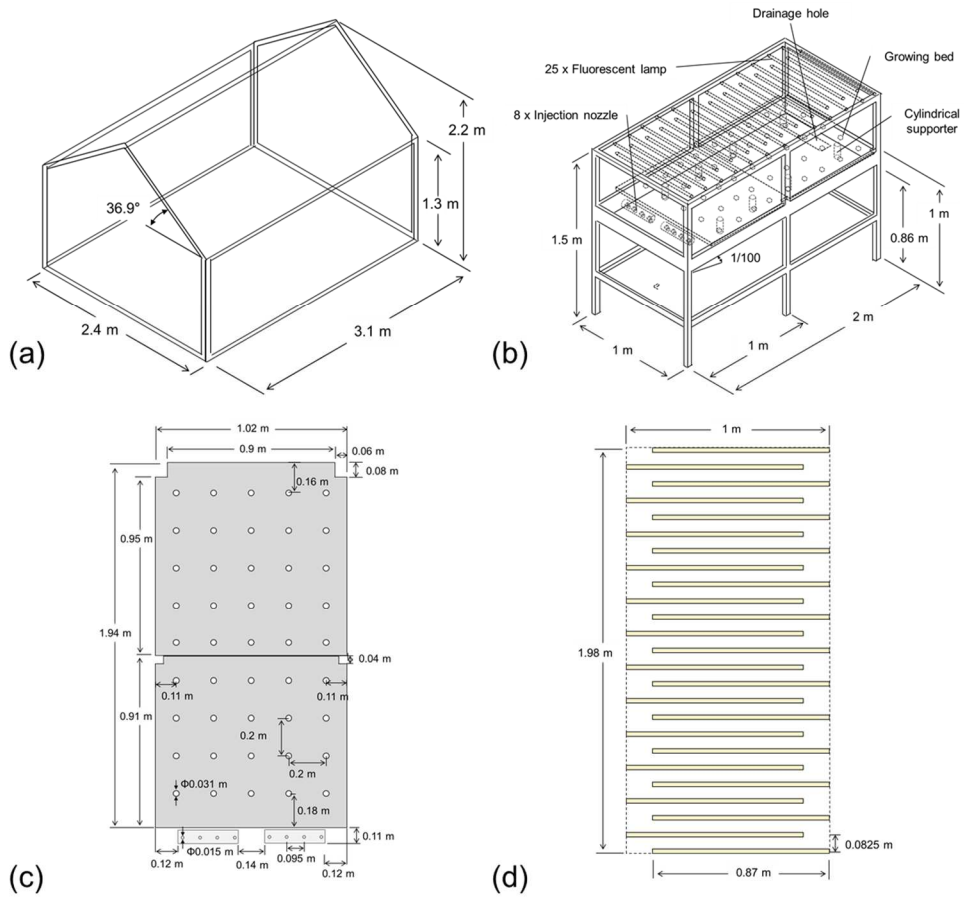

Fig. 3.1. Structures and dimensions of the experimental growth chamber: (a) Growth chamber; (b) Growing bed frame; (c) Growing bed; (d) 25-fluorescent lamps. There are 8 cylindrical supporters for the growing bed.

CONSTRUCTION OF AN ON-THE-GO CROP MONITORING SYSTEM

Considering the varied growth status according to the sites due to the different microclimates, light conditions, or the different growing days, an on-the-go monitoring system was necessary to observe the growing plants for the entire bed.

In this study, the on-the-go crop image monitoring system was modified for the CC measurements based on the XY camera-guided system developed in the previous study (Jiang et al., 2018). Briefly, the XY camera-guided system consisted of a motion controller (MoonWalker MW DCM02, NTREX, South Korea), two motor servo drivers (MoonWalker i-servo SBL24D200U-B, NTREX, South

Korea), two step motors (BLM57090-1000, Leadshine, China), and two linear belt-type actuators (MoonWalker MW-EQB40, NTREX, South Korea).

The position of the camera and environmental sensors were determined considering several practical issues. The XY camera-guided system and the camera were installed at the height of 0.4 m from the growing bed to avoid any damage to the growing lettuces during the movement. A pyranometer (SP-110, Apogee Instruments Inc., USA) was placed on the side of the growing bed to prevent the effect of the shadow made by the leaves. For monitoring the air conditions, air temperature and humidity sensor (HD9008TRR, Delta Ohm, Italy), and CO_2 sensor (GMT220, Vaisala, Finland) were installed in the center of the growth chamber.

Fig. 3.2 shows the constructed crop monitoring system in the growth chamber with the sensor data flow.

For the RGB image acquisition of the growing lettuces, a low-cost web camera (c270, Logitech, Switzerland) was applied to the moving frame. Specifically, the movement of the camera was controlled by pulse signals from the servo drivers and the spatial resolution of the system was 0.0127 mm · $pulse^{-1}$. Based on the resolution, the XY moving pulse signals were calculated to determine the image acquisition for the entire growing bed. In addition, the single image frame was 0.339 m × 0.226 m (the dimension was 640 × 480 pixels) and the dimension of the growing bed was 1.02 m × 1.86 m, so 3 × 8 images would be necessary to monitor the entire bed. Finally, a total of 24 positions for the image acquisitions were determined, and a reversed N-shaped route was employed for the effective camera movement (Fig. 3.3). After the one cycle of the image monitoring was ended, the camera was returned to the initial point and waited for the next monitoring.

The camera control and computation were conducted using a program based on Python 3.7.3 programming language with several third-party libraries. The source code of the software is displayed in A1. The main system was programmed using LabVIEW (v2015, National Instruments, TX, USA).

The detailed specifications of the crop-monitoring system and the environmental sensors are shown in Table 3.1.

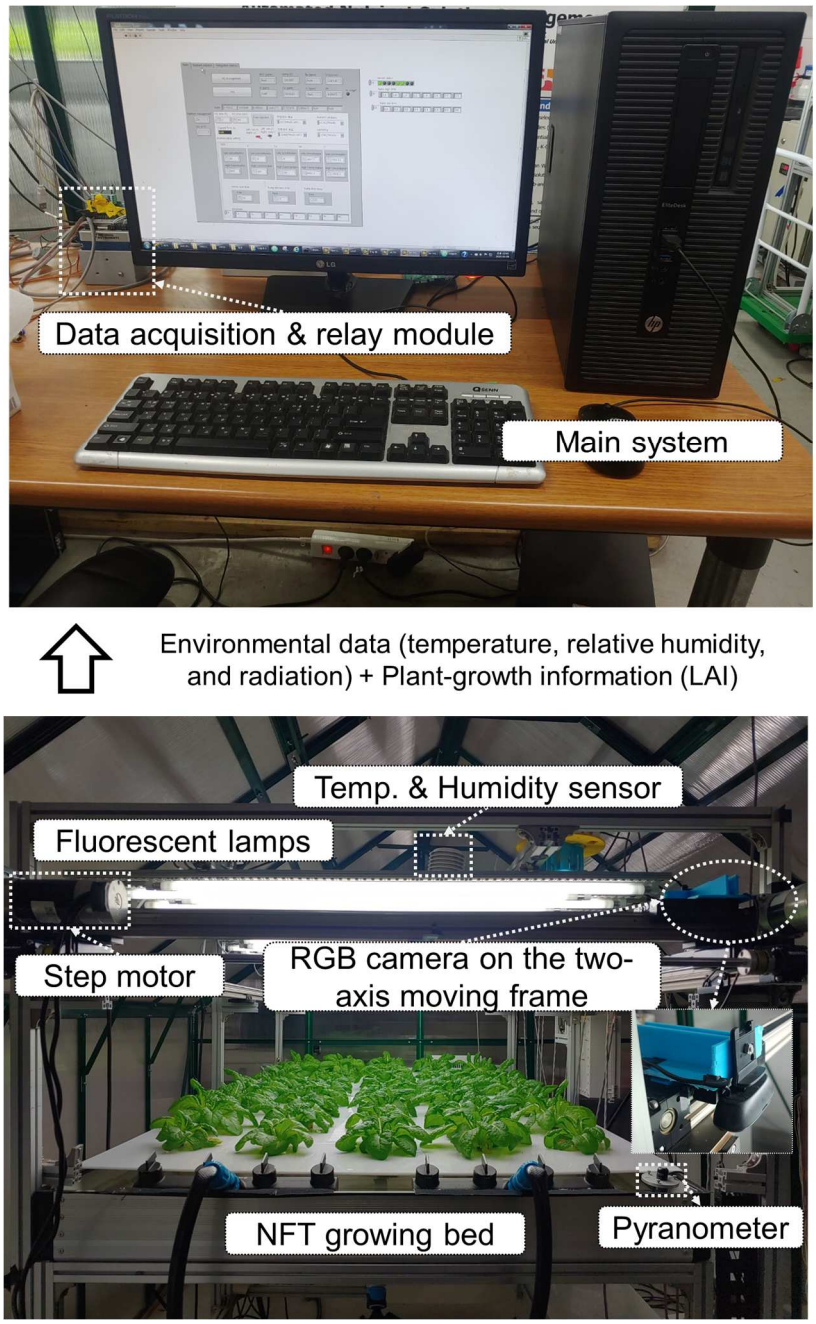

Fig. 3.2. View of the crop monitoring system in conjunction with the control system

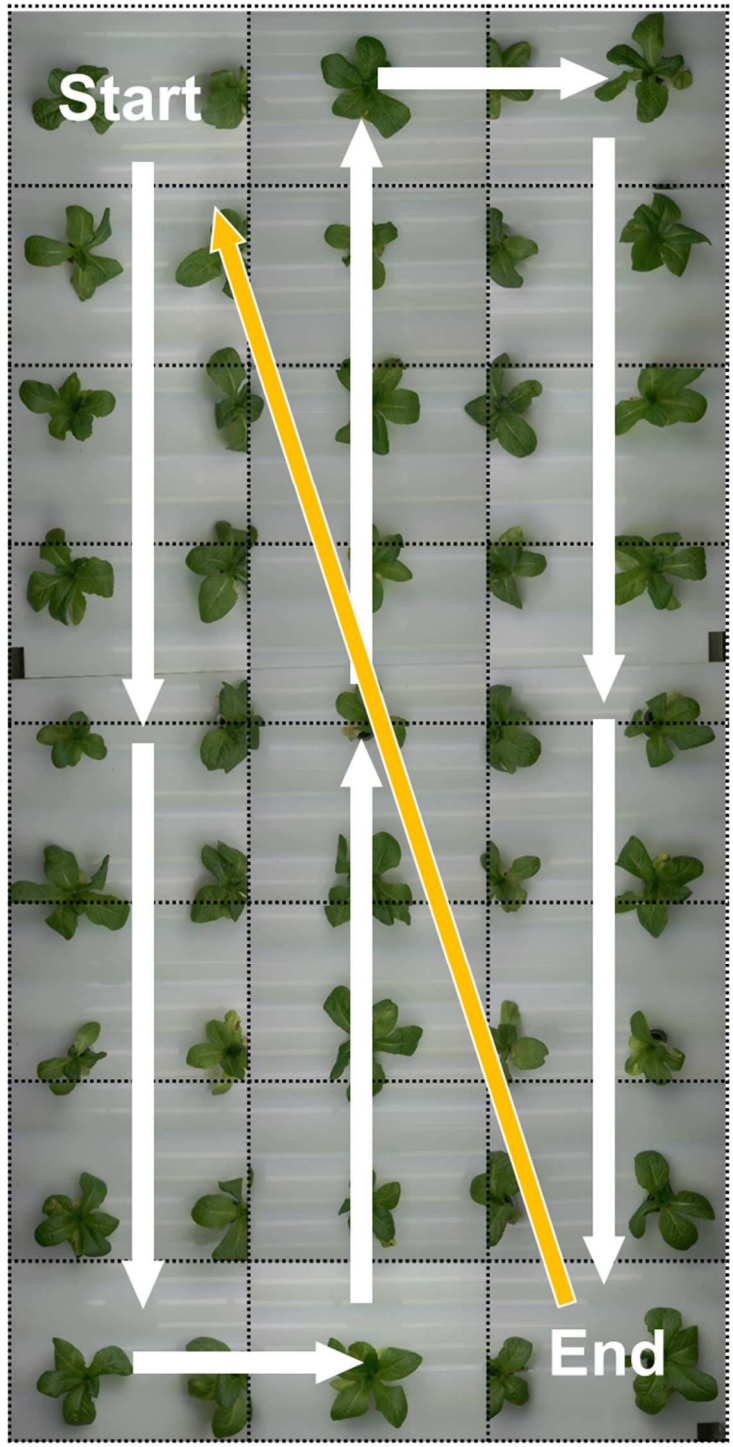

Fig. 3.3. Moving route of the image monitoring system. White arrows indicate the route for image acquisition, and yellow arrow indicates the route for the return.

Table 3.1. Specifications of components of the on-the-go monitoring system and the environmental sensors

Component	Specification	Manufacturer/Model
Data acquisition board	A/D converter for atmosphere sensor signal Input channel: 16 bit analog input 32 ch. Input range: ± 10 V Sampling rate: 250 $kS \cdot s^{-1}$	National Instrument (TX, USA), NI-9205
Air temperature and humidity sensor	Temperature measurement range: -40-80 °C Relative humidity measurement range: 5-98 % Power: 10-30 VDC	Delta Ohm (Caselle di Selvazzano, Italy), HD9008TRR
CO_2 probe	Measurement range: 0-2000 ppm Output range: 0-10 VDC Power: 24 VDC	Vaisala (Vantaa, Finland), GMT220
Pyranometer	Spectral range: 360-1120 nm Measurement range: 0-2000 $W \cdot m^{-2}$ Output range: 0-0.4 VDC Power: Self-powered	Apogee Instruments Inc. (Logan, USA), SP-110
Camera	RGB camera Fixed focus Maximum resolution: 1280 x 720 pixels Field of View: 60° Power: 5 VDC (USB)	Logitech (Lausanne, Switzerland), c270
Servo motor	Rotational speed: 0–3000 rpm Nominal torque: 0.29 NM Power: 36 VDC	Leadshine (Shenzhen, China), BLM57090
Belt-type actuator	Max Load: 8 kg Max speed: 1 $m \cdot s^{-1}$ Power: 100 W	NTREX (Incheon, South Korea), MW-EQB40
Motor driver	PWM modulation: 20 kHz Encoder: 1,000,000 pulse/rev Power: 24 VDC	NTREX (Incheon, South Korea), SBL24D200U-B
Motion controller	PID position controller USB based data transfer PWM control range: 18-40 kHz	NTREX (Incheon, South Korea), MW-DCM02

IMAGE PROCESSING FOR CANOPY COVER ESTIMATION

To compute the CC of the growing lettuces, a series of image processing was conducted. The flow of the CC computation is as follows.

First, the obtained RGB image was converted to the Excess Green Index (ExG)

for identifying the vegetation fractions of plants in the obtained image. The ExG, which was first examined by Woebbecke et al., (1995), could be calculated using the following equation 1 (Woebbecke et al., 1995).

$$\mathrm{ExG} = 2\mathrm{g} - \mathrm{r} - \mathrm{b} \qquad (3.1)$$

where r, g, and b are the chromatic coordinates obtained by eq. 3.2.

$$\mathrm{r} = \frac{R^*}{(R^*+G^*+B^*)}$$

$$\mathrm{g} = \frac{G^*}{(R^*+G^*+B^*)} \qquad (3.2)$$

$$\mathrm{b} = \frac{B^*}{(R^*+G^*+B^*)}$$

where R*, G* and B*, are the normalized RGB (Red, Green and Blue) values, which are computed by dividing the actual pixel values of R, G and B by the maximum value of 255 for an 8-bit color channel (eq. 3.3).

$$R^* = \frac{R}{255}$$

$$G^* = \frac{G}{255} \qquad (3.3)$$

$$B^* = \frac{B}{255}$$

The ExG indices enhance the contrast between the plant area and the non-plant area, so it could be used to segment the plants from the background (D.-W. Kim et al., 2018; Riehle et al., 2020).

Then, a threshold for the plant segmentation was calculated based on the Otsu method, which automatically calculates optimal threshold values, thereby minimizing inter-class variance and maximizing intra-class variance (Otsu, 1979). The basic principle used in the process was an assumption that dense green vegetation produces a high value, while background has a low value. Therefore, the ExG image could be converted to a binary image based on the Otsu’s threshold, which would be classified into two groups, i.e., plant or non-plant.

After the segmentation, the CC of the image was calculated as the ratio of the number of pixels segmented as a crop to the number of total pixels following

equation 3.4 (Escarabajal-Henarejos et al., 2015; D.-W. Kim et al., 2018).

$$\mathrm{CC} = \frac{Number\ of\ pixels\ determined\ as\ a\ plant\ in\ a\ frame}{Number\ of\ total\ pixels\ in\ a\ frame} \quad (3.4)$$

The system calculated the CCs for all images, and the average value of the CCs was assumed as the representative growth status of the lettuces in the growth chamber. Fig. 3.4 shows the flow of the image processing for CC calculation.

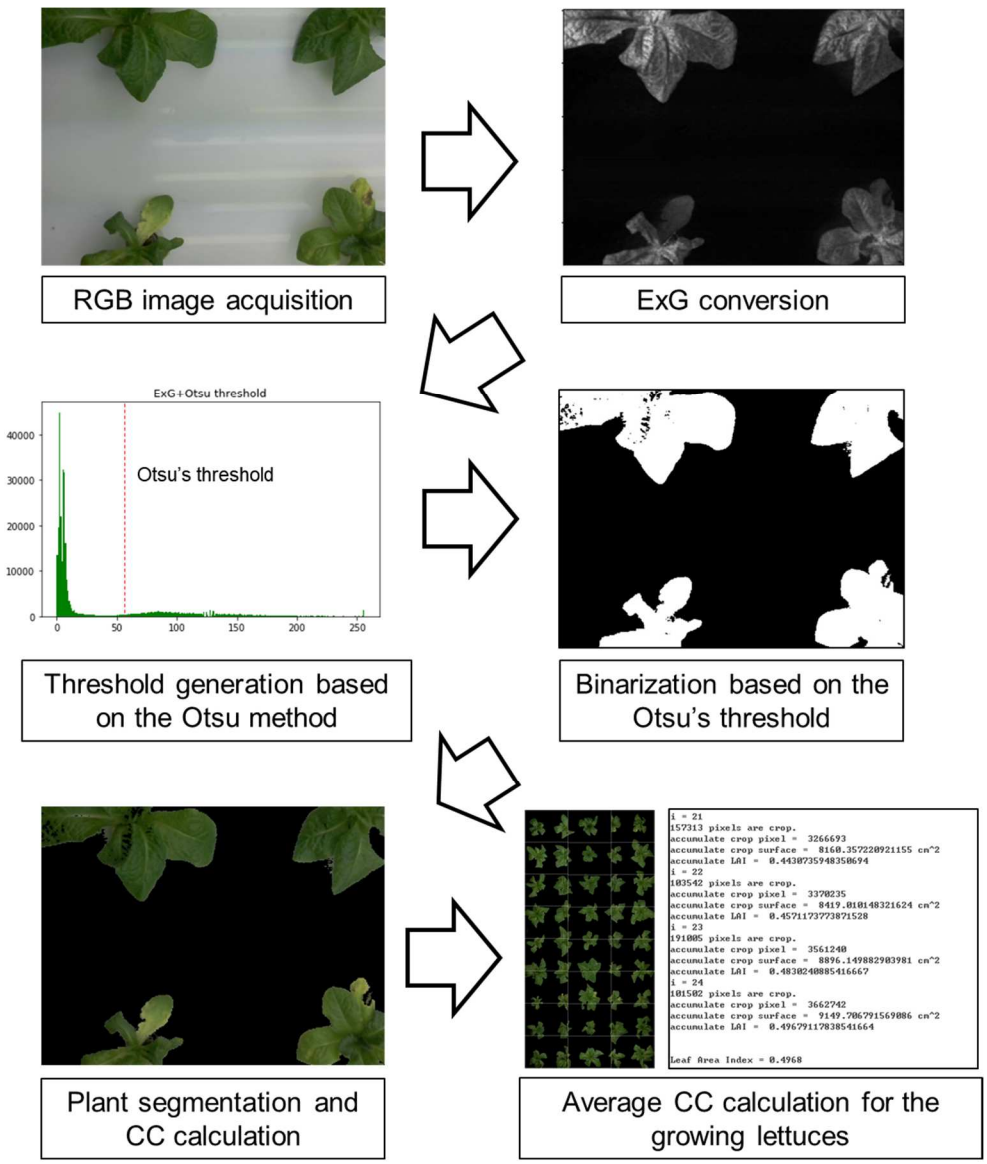

Fig. 3.4. Process of the CC calculation for the crop growth estimation

EVALUATION OF THE CC CALCULATION PERFORMANCE

Accuracy of the crop segmentation method applied in the study was assessed by comparing with manually segmented crop pixel numbers using the commercial software (ENVI v5.4, L3Harris Geospatial, CO, USA) (eq. 3.5).

$$\text{Accuracy}\ (\%) = 100 - \frac{1}{n} * \sum_{i=1}^{n} \left(100 \times \left| \frac{CC_{ExG-Otsu} - CC_{manual}}{CC_{manual}} \right|_i \right) \qquad (5)$$

where n is the number of frames from the monitoring system, $CC_{Exg\text{-}Otsu}$ is the CC determined by the ExG-Otsu based segmentation, and CC_{manual} is the CC determined by the manual segmentation.

ESTIMATION MODEL FOR TRANSPIRATION RATE

In this study, a simplified Penman-Monteith model modified by Baille at al. (1994) was used to estimate the transpiration rate of the growing lettuce (eq. 3.6) (Baille et al., 1994).

$$E_t = a * \left(1 - e^{-k*LAI}\right) * RAD_{in} + b * LAI * VPD \qquad (3.6)$$

where E_t is the estimated transpiration rate ($g \cdot h^{-1}$), k is the light extinction coefficient, LAI is the leaf area index ($m^2 \cdot m^{-2}$), RAD_{in} is the radiation ($W \cdot m^{-2}$), VPD is the vapor pressure deficit (kPa), and a ($g \cdot J^{-1} \cdot m^2$) and b ($g \cdot h^{-1} \cdot kPa^{-1}$) are regression parameters.

In the case of the LAI, it could be substituted by the CC because the CC has a highly linear relationship with the LAI (Escarabajal-Henarejos et al., 2015; García-Mateos et al., 2015). Then, the light extinction coefficient (k) was obtained based on the approximation equation (eq. 3.7) described in the previous study (Nobel et al., 1993).

$$k * CC = \ln(RAD_{Top}/RAD_{Bottom}) \qquad (3.7)$$

where RAD_{Top} ($W \cdot m^{-2}$) is the radiation measured at the top of the canopy and RAD_{Bottom} ($W \cdot m^{-2}$) is the radiation measured at the bottom of the canopy.

The VPD in the growing chamber was computed from equations 3.8 and 3.9

(Abtew & Melesse, 2013).

$$e_s = 0.611 * \exp(\frac{17.27*T}{T+237.3}) \quad (3.8)$$

$$VPD = e_s \left(1 - \frac{RH}{100}\right) \quad (3.9)$$

where e_s is the saturation vapor pressure (kPa), T is the air temperature (°C), and RH is the relative humidity (%).

DETERMINATION OF THE PARAMETERS OF THE TRANSPIRATION RATE MODEL

For the determination of the constant parameters (i.e., k, a, and b), 45 lettuces were planted on a bed of 1.02 m×1.86 m with a distance of 0.2 m. The lighting period was introduced as a 12h light/12h dark alternation. 65 L of nutrient solution was prepared based on the composition of the modified Hoagland's hydroponic nutrient solution (Table 3.2) (Hoagland & Arnon, 1950), and supplied to the growing bed by a relay-based circulation pump with a constant timer-based fertigation cycle of a 3 min on/7 min off cycle (PP50Y, Hwarang System Co., Ltd., Incheon, South Korea).

To manage the recycled nutrient solution, electrical conductivity (EC) and pH of the recycling nutrient solution were monitored by an in-line EC probe (HI7635, Sistemes Electrònics Progrés S. A., Lleida, Spain) and a pH probe (HI1001, Hanna instruments, RI, USA), respectively. In addition, a reflective ultrasonic water-level transmitter (EchoPod UG01, Flowline, Inc., CA, USA) was employed to measure the remaining volume of the nutrient solution. Based on the status of the nutrient solution (i.e., EC, pH, and volume), the system replenished the nutrient solution every day using the calculation method reported in the previous study (D Savvas & Manos, 1999).

Table 3.2. Composition of the Hoagland's nutrient solution (Hoagland & Arnon, 1950)

Solution	Substance	Amount ($mg \cdot L^{-1}$ of water)
A	$Ca(NO_3)_2 \cdot 4H_2O$	472.3
	KNO_3	151.65
	Fe(EDTA)	21.055
B	KNO_3	151.65
	$MgSO_4 \cdot 7H_2O$	246.48
	$MnCl_2 \cdot 4H_2O$	0.905
	$ZnSO_4 \cdot 7H_2O$	0.11
	$NH_4H_2PO_4$	57.53
	H_3BO_3	1.43
	$CuSO_4 \cdot 5H_2O$	0.01
	$Na_2MoO_4 \cdot 2H_2O$	0.01

The light extinction coefficient, k was determined by calculating the averaged k for the growing lettuces in initial, mid, and end day during the cultivation based on equation 3.7. For the determination of the regression parameters (i.e., a and b), the transpiration rates of the lettuces were investigated during the growing period for regression. The regression analysis was conducted using SIGMA Plot 12.0 (Systat Software Inc., London, UK).

During the cultivation, three of the growing lettuces were transferred to beakers with nutrient solutions individually, then they were grown for 1 hour under the growth chamber. The changed weight of the beaker was assumed as the evapotranspiration rate (Fig. 3.5a). And a beaker without lettuce was also measured in the same way to measure the evaporation rate (Fig. 3.5b). Finally, the transpiration rate of the growing lettuce was computed by subtracting the estimated evaporation rate from the estimated evapotranspiration rate. It was assumed that there was no effect from the different evaporation surfaces with or without the lettuce, or the spatial variation in the growing bed. During the night period, the transpiration rate would be small, so the variation in the coefficient was not

considered. Based on the procedure described above, the transpiration rate in the daytime was calculated almost every day.

The experiment was carried out until the CC of the lettuces were saturated.

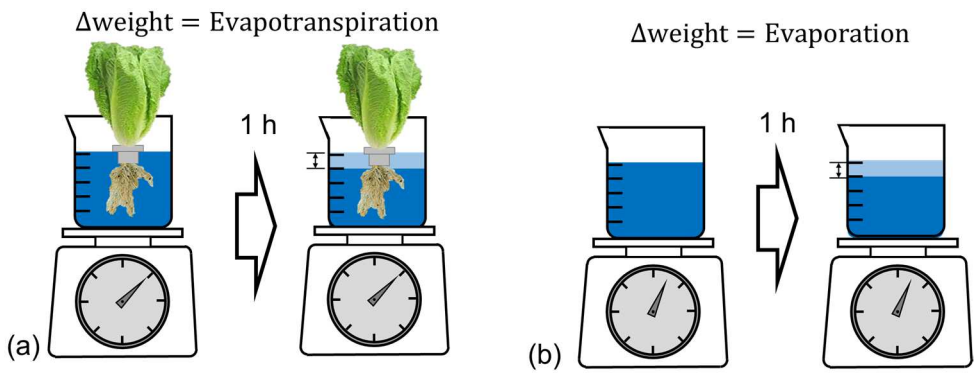

Fig. 3.5. Schematic of calculating the evapotranspiration rate of the growing lettuce (a) and the evaporation rate of the nutrient solution (b). The actual transpiration rate could be obtained by subtracting the evaporation rate from the evapotranspiration rate.

RESULTS AND DISCUSSION

PERFORMANCE OF THE CC MEASUREMENT BY THE IMAGE MONITORING SYSTEM

Fig. 3.6 shows the measured CC by the automated image monitoring system and the manual segmentation during the experimental period. The $CC_{ExG\text{-}Otsu}$ showed a highly linear relationship for the CC_{manual} with a slope of 0.834 and a high coefficient of determination (R^2) of 0.94 during the growing period (Fig. 3.6a). However, there were several underestimations from the ExG+Otsu method, which would induce a decrease of the linearity of the relationship. Specifically, the values of the $CC_{ExG\text{-}Otsu}$ after the DAT 24 were underestimated when compared to the CC_{manual}, thereby deteriorating the accuracy of the CC measurements (Fig. 3.6b). Excluding the values after the DAT 24, the linear relationship between the plant pixels segmented by the ExG+Otsu method and manual operation was improved by a slope of 0.99 and an R^2 of 0.99.

The underestimation would be related to the vulnerability of the ExG+Otsu

method to the saturated color index or reflections in the vegetation, which was reported by other authors (García-Mateos et al., 2015; Riehle et al., 2020). As an example, a growing lettuce image obtained from the DAT 25 was investigated (Fig. 3.7). The raw RGB image shows the lettuces were almost full (Fig. 3.7a), so the lettuce image segmented based on the ExG+Otsu should be also full. However, the ExG+Otsu method counted the part of lettuces as the background, thereby making holes in the lettuces (Fig. 3.7b).

The ExG calculation uses the color values. The veins or the surfaces reflecting the light for the lettuce had color values close to white color, so they were regarded as the background, not lettuces. As the result, the accuracy of the ExG+Otsu method was decreased after the DAT 24, as shown in Fig. 3.8. However, the saturation effect of the CC measurement appeared in the late growth stage, just before harvest, so the application would be feasible considering the fertigation control would be necessary for the growing stage, not the harvesting stage. The accuracy of the CC estimation was 98.5 ±1.7 % until the saturation.

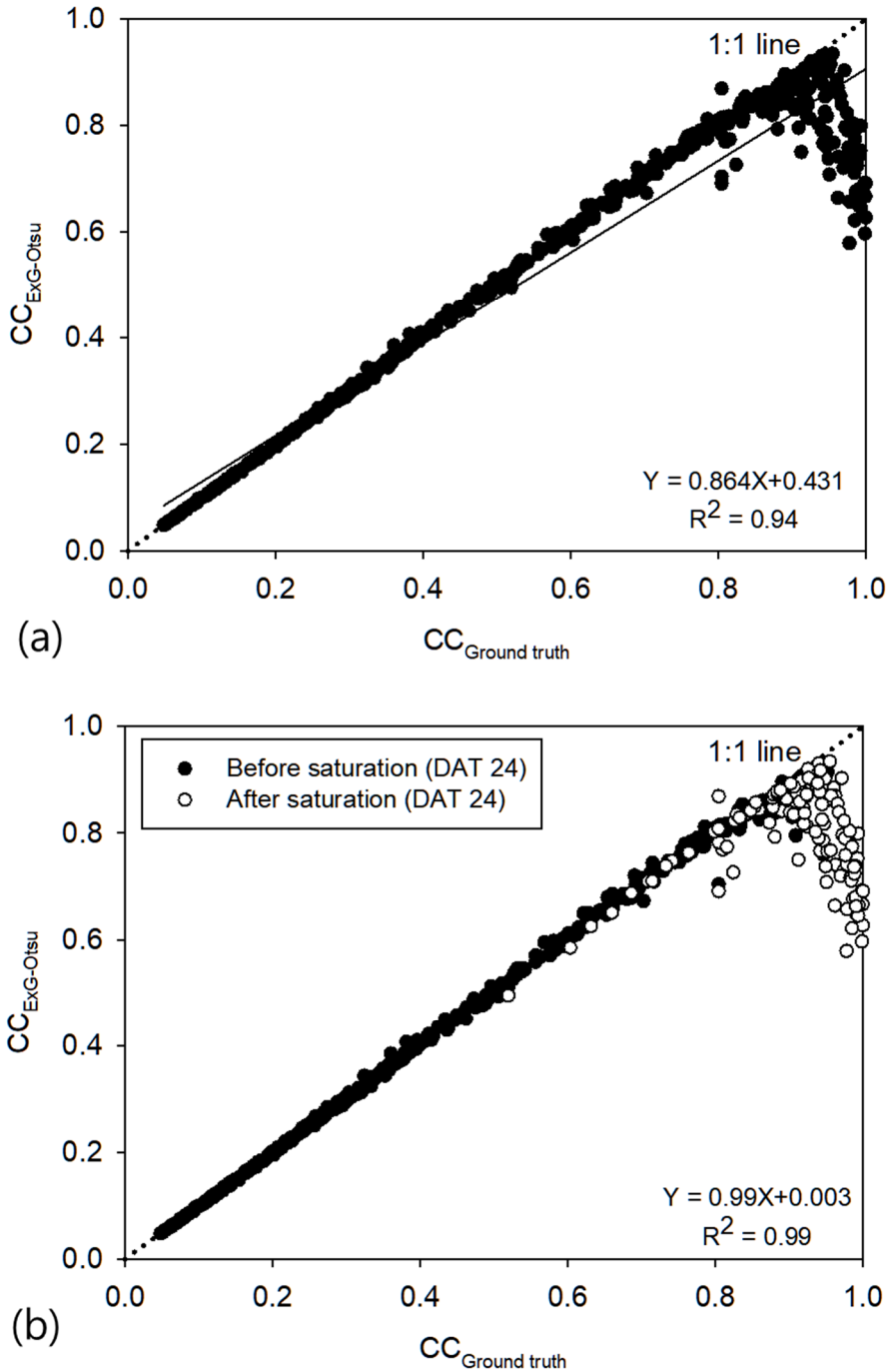

Fig. 3.6. Relationships between the CCs of the lettuces determined by ExG+Otsu method and the manual segmentation method during (a) the 27-day lettuce growing period and (b) the 23-day lettuce growing period

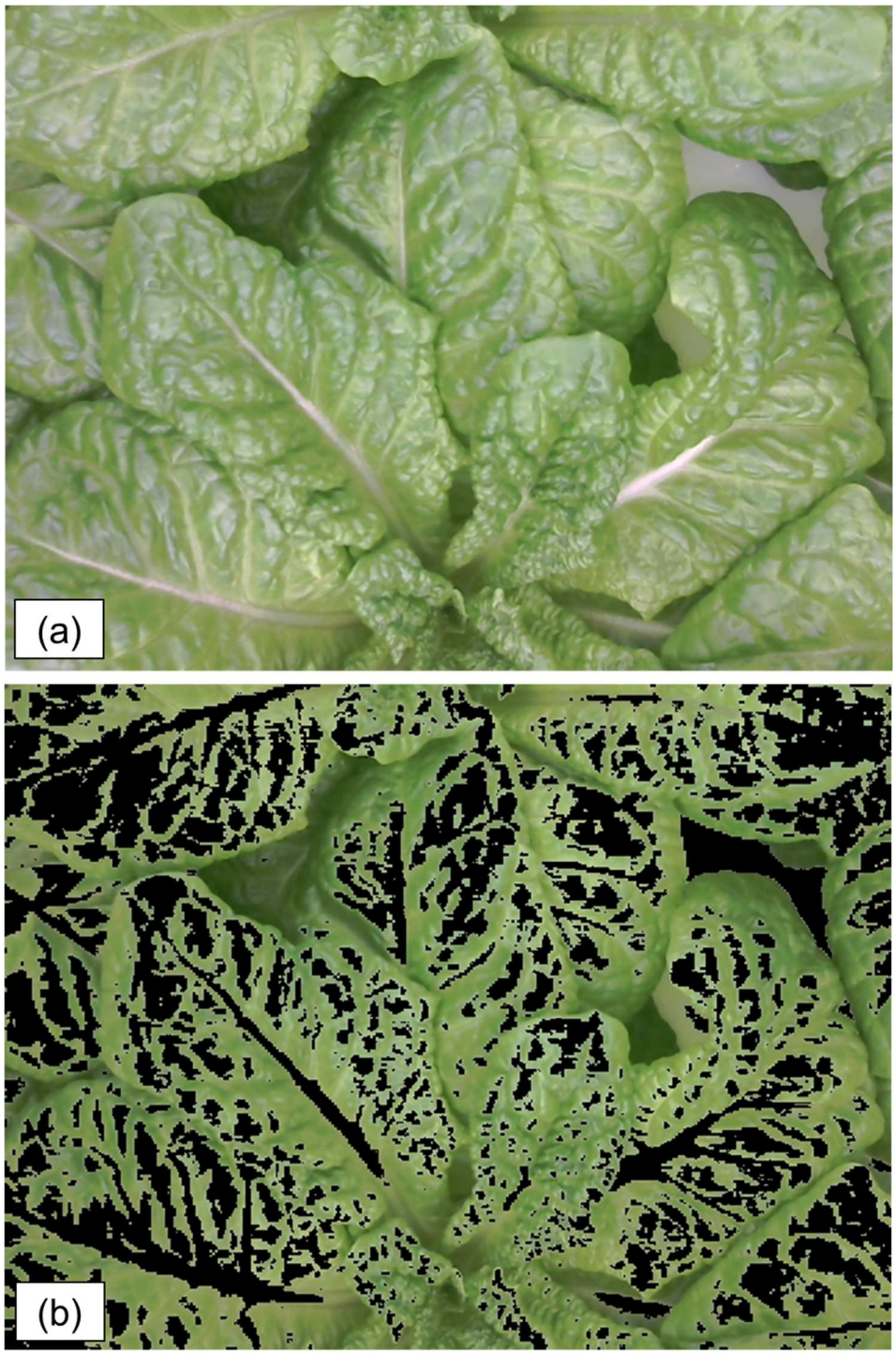

Fig. 3.7. An example of the saturated lettuce image obtained from the DAT 25: (a) raw image; (b) ExG+Otsu based segmented image

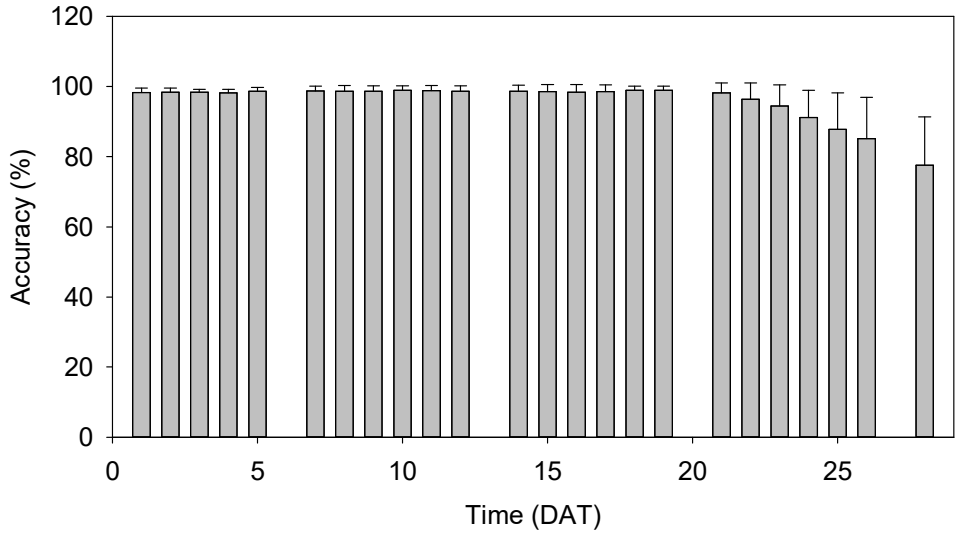

Fig. 3.8. Accuracy of the CC estimation during the cultivation. Error bars denote the standard deviation of the analyzed images.

PLANT GROWTH MONITORING IN CLOSED HYDROPONICS

Fig. 3.9 shows the automated vision-based plant growth monitoring system could monitor the growth information of the growing lettuces during the cultivation period. Although the holes induced by the saturated lettuces were displayed in Figs. 3.9e and 3.9f, the increase of the lettuces according to the growing period could be configured through the segmented images. In addition, the collected images could provide information on the spatial-temporal variations in lettuce's growth. Fig. 3.10 shows the spatial map of the CC on the growing bed for DAT 11, 16, 22, and 25. In DAT 11, the CCs of the lettuces at the left and right sides of the bed were slightly higher than the CCs of the top and bottom sides of the bed (Fig. 3.10a). The trend was consistent with the DAT 16 (Fig. 3.10b). However, the distributions of the CCs in DAT 22 and 25 became different for the DAT 11 and 16, indicating the growth of the lettuces would be varied according to the growing positions though the cultivation was conducted at the same bed and chamber (Figs. 3.10c and 3.10d).

The spatial variation would be caused by the different microclimates or light

distribution in the growth chamber. In particular, the spatial variation might be generated consistently in greenhouses or plant factories where the year-round production is conducted. The results showed the on-the-go monitoring scheme could detect the spatial variation during cultivation, thereby enabling the adaptive crop management for the spatial variation.

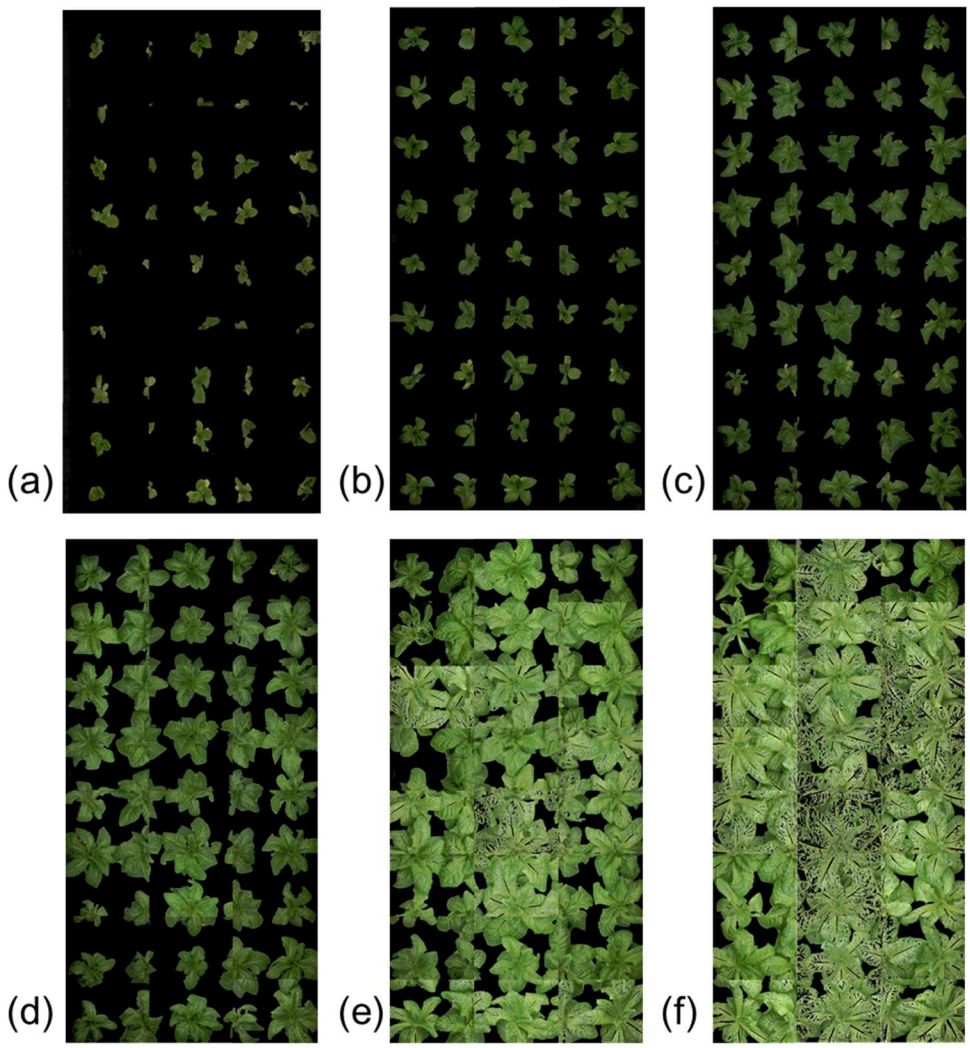

Fig. 3.9. Panoramic images of the growing lettuces segmented from the background: (a) DAT 1; (b) DAT 5; (c) DAT 11; (d) DAT 16; (e) DAT 22; (f) DAT 25

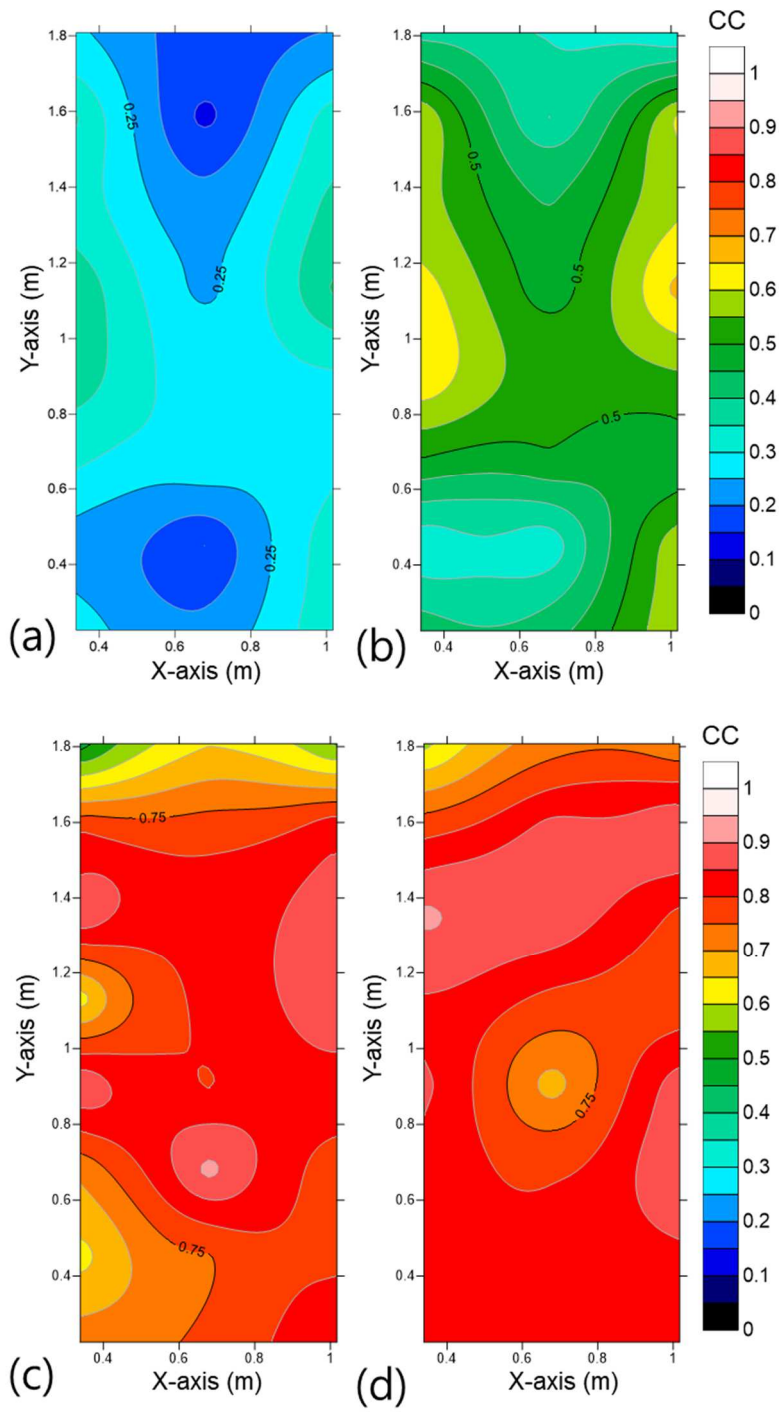

Fig. 3.10. Spatial map of the CC on the growing bed: (a) DAT 11; (b) DAT 16; (c) DAT 22; (d) DAT 25

In this study, an average CC of the growing bed was used as a representative

growth parameter for the growing lettuces. The average CC obtained by the on-the-go crop monitoring system shows the growth curve of the lettuces during the cultivation period (Fig. 3.11). Although there were underestimations in the late period, it happened in the harvesting time for the lettuces, so the CC measurement by the monitoring system would be applicable in estimating the growth of the lettuces as mentioned above. In addition, the similarity in error bars of the measured CCs and the actual CCs indicated the spatial variation of the lettuces could be observed by the system with the accuracy comparable to the manual detection.

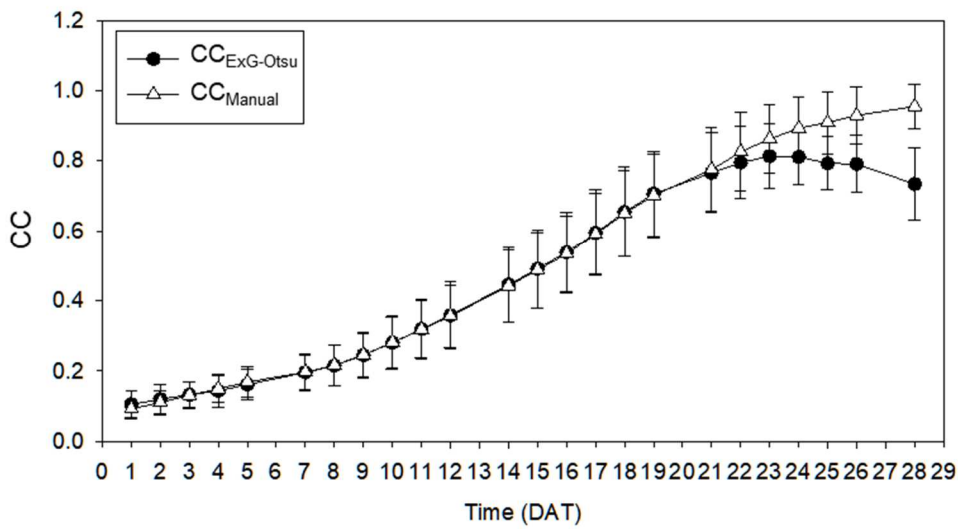

Fig. 3.11. Changes in the average CC of the lettuces according to the growing days. Error bars denote the standard deviation of the analyzed images.

EVALUATION OF THE CROP WATER NEED ESTIMATION

Fig. 4.11 shows the measured sensor data and the actual transpiration rate of the growing lettuce during the cultivation. The temperature, relative humidity, and radiation measured in the growth chamber were almost maintained at the constant levels during the experimental period (Figs. 4.11a, 4.11b, and 4.11d). Resultingly, the VPD, which was calculated from the temperature and relative humidity by

equations 3.8 and 3.9, also showed almost constant value during the period. On the other hand, the transpiration rate measured by the direct method was increased with the growing day, which was similar to the trend of the CC (Figs. 4.11e and 4.11f). The results indicate the transpiration rate of the lettuces would be strongly affected by the CC because they would uptake more water when they were grown. The result was corresponding to the result in the previous study (J. W. Lee et al., 2013).

From the experiment, the light extinction coefficient, k for the growing lettuces was determined as 3.318. Then, the regression parameters (i.e., a and b) were calculated as 0.056 and 1.466, respectively, from the regression analysis for the actual transpiration rate based on the estimated CC and the environmental conditions (i.e., temperature, relative humidity, and radiation) in the growth chamber (Fig. 4.12a). Specifically, the regression curve provided a highly linear relationship with a slope of 0.91, coefficient of determination (R^2) >0.9, and standard error of the regression (SER) of <0.51 (Fig. 4.12b). Therefore, the fitted transpiration estimation model based on the plant-growth information was expected to provide promising predictability for the water need of the growing lettuce.

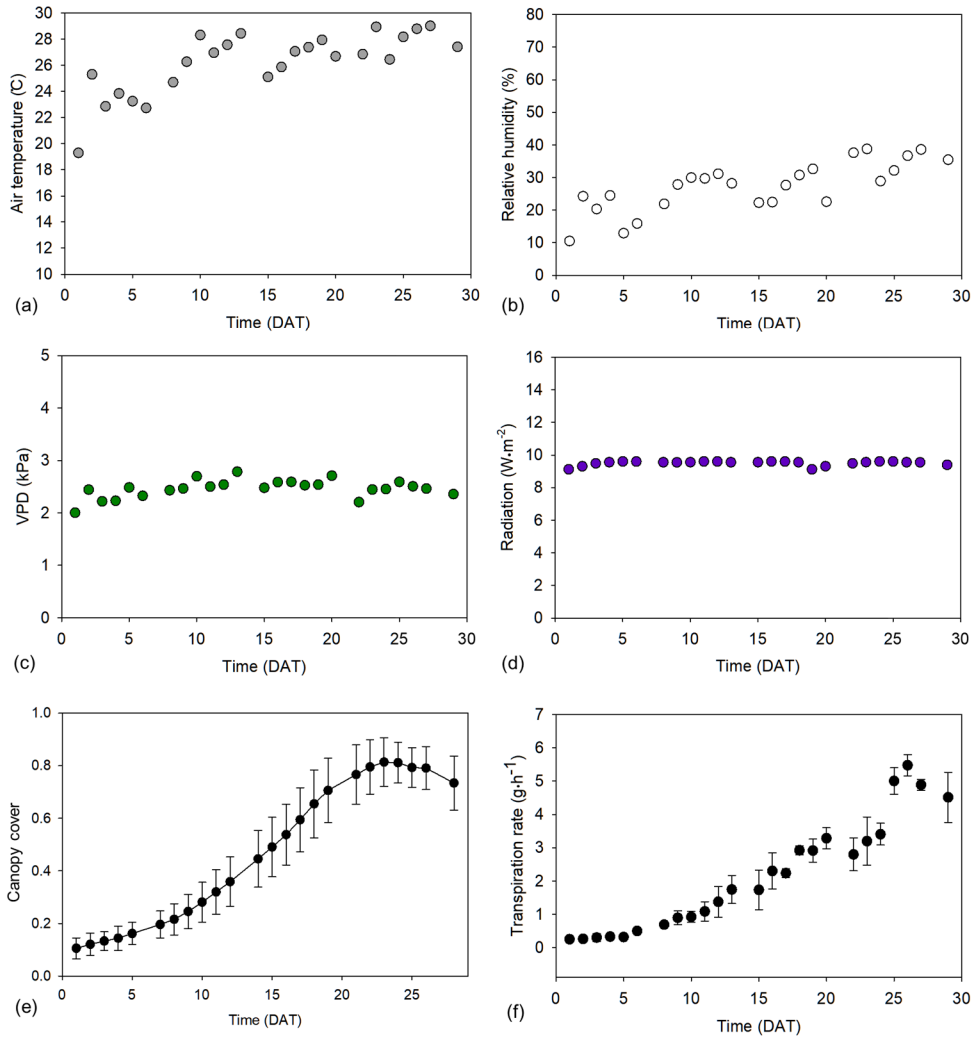

Fig. 3.12. Changes in the measured parameters during the cultivation: (a) air temperature; (b) relative humidity; (c) VPD; (d) radiation; (e) CC; (f) actual transpiration rates of three lettuces. Error bars denote the standard deviation of the three lettuces for the measured transpiration.

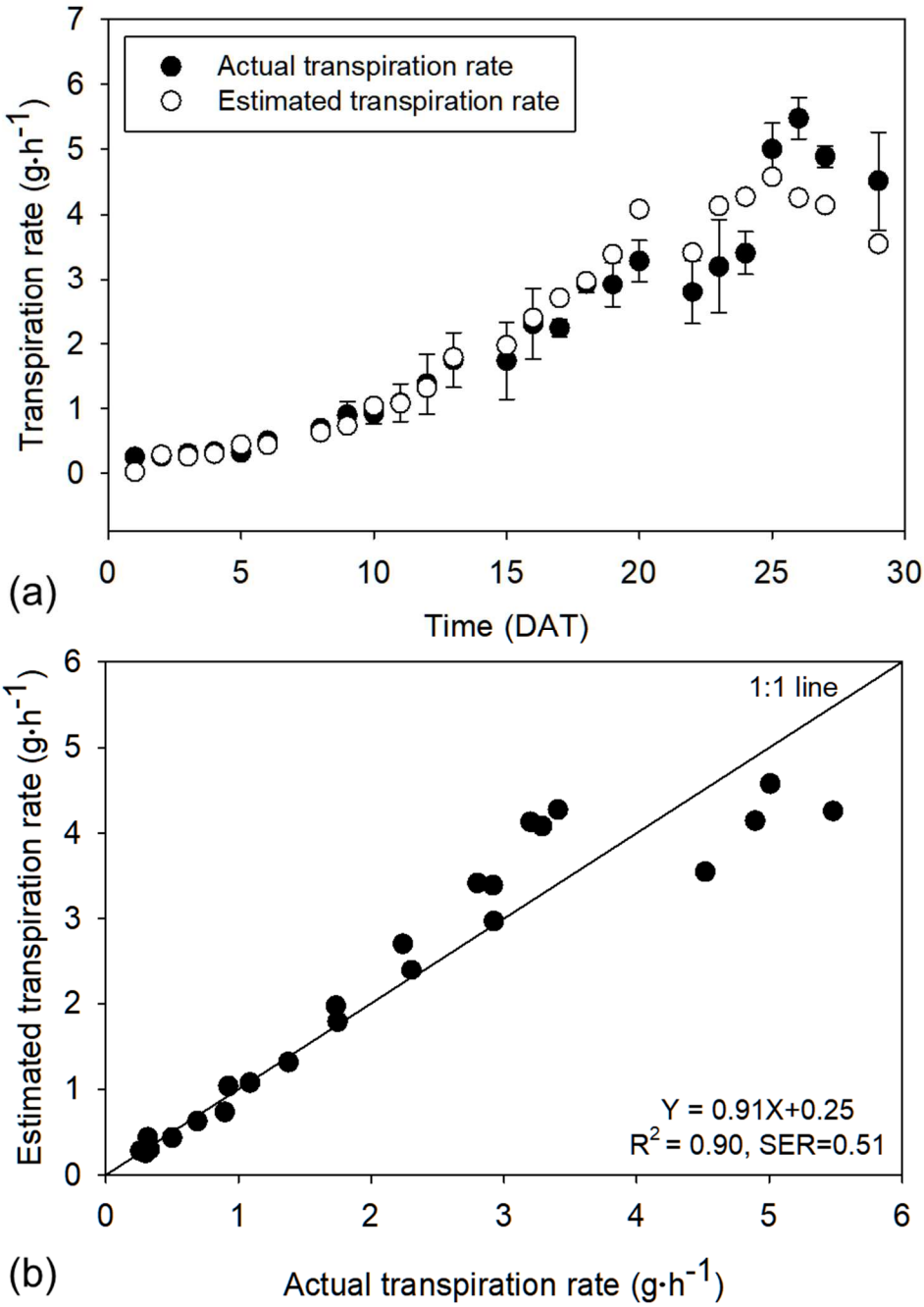

Fig. 3.13. (a) Comparison and (b) relationship of the actual transpiration rate and the estimated transpiration rate for one lettuce. Error bars denote the standard deviation of the three lettuces for the measured transpiration.

CONCLUSIONS

In this study, an on-the-go crop monitoring system for monitoring the plant CC and the ambient conditions was constructed.

From the real lettuce cultivation experiment, the on-the-go monitoring system showed a highly linear relationship between the measured plant area pixels and the actual plant area pixels with a slope of 0.99 and a coefficient of determination (R^2) of 0.99. In addition, the system proved the detectability for spatial-temporal variations of the growing lettuces. The accuracy of 98.5 ±1.7% besides the saturated period in estimating the CC showed the system could easily obtain the CC of the growing lettuces, thereby estimating the crop water needs of the growing plants for the entire bed based on the modified Penman-Monteith equation using the ambient conditions consisting of the air temperature, relative humidity, and radiation.

The crop water need estimation model calibrated using the experimental results showed a highly linear relationship with a slope of 0.91, a coefficient of determination (R^2) >0.9, and a standard error of the regression (SER) of <0.51 for the actual transpiration rate. Considering the high accuracy of the estimation model, it would be feasible for precision fertigation that conducts the fertigation based on the crop water need varying according to the growth and the environments of the plants grown in hydroponics.

However, no consideration for the crop water need varying according to the growth stage would limit the system availability to only the vegetative growth of the leafy vegetables. Specifically, the vulnerability of the ExG-Otsu method to the light conditions might make it difficult to segment the plant area from the growing bed under the greenhouses which have more dynamic light conditions. Further researches on the remote sensors and image processing would be required to assess the crop water needs for more various plants and greenhouse applications.

* Note: Ji-Song Jiang provided technical assistance for the construction of the XY camera-guided system. Dong-Wook Kim and Gyujin Jang shared their knowledge for programming of the plant segmentation. Yoon-Hong Yi helped the manual plant segmentation. The system construction was financially supported by the R&D center for Green Patrol Technologies, for KEITI (Korea Environmental Industry & Technology Institute), Republic of Korea. (E614-00184-0401-1). I would like to express my sincere gratitude to their support.

CHAPTER 4. HYBRID SIGNAL-PROCESSING METHOD BASED ON NEURAL NETWORK FOR PREDICTION OF NO_3, K, CA, AND MG IONS IN HYDROPONIC SOLUTIONS USING AN ARRAY OF ION-SELECTIVE ELECTRODES

ABSTRACT

In closed hydroponics, fast and continuous measurement of individual nutrient concentrations is necessary to improve water- and nutrient-use efficiencies and crop production. Ion-selective electrodes (ISEs) could be one of the most attractive tools for hydroponic applications. However, signal drifts over time and interferences from other ions present in hydroponic solutions make it difficult to use the ISEs in hydroponic solutions. In this study, hybrid signal processing combining a two-point normalization (TPN) method for the effective compensation of the drifts and a back propagation artificial neural network (ANN) algorithm for the interpretation of the interferences was developed. In addition, the ANN-based approach for the prediction of Mg concentration which had no feasible ISE was conducted by interpreting the signals from a sensor array consisting of electrical conductivity (EC) and ion-selective electrodes (NO_3, K, and Ca). From the application test using 8 samples from real greenhouses, the hybrid method based on a combination of the TPN and ANN methods showed relatively low root mean square errors of 47.2, 13.2, and 18.9 $mg \cdot L^{-1}$ with coefficients of variation (CVs) below 10% for NO_3, K, and Ca, respectively, compared to those obtained by separate use of the two methods. Furthermore, the Mg prediction results with a root mean square error (RMSE) of 14.6 $mg \cdot L^{-1}$ over the range of 10–60 $mg \cdot L^{-1}$ showed potential as an approximate diagnostic tool to measure Mg in hydroponic solutions. These results demonstrate that the hybrid method can improve the accuracy and feasibility of ISEs in hydroponic applications.

INTRODUCTION

Hydroponics is a cultivation method that grows plants using nutrient solutions composed of water and nutrient salts without soil. Recently, hydroponics has been widely and rapidly utilized in agricultural industries because it is the most intensive and effective production method that can be designed to support year-round production with high yields and good quality (Barbosa et al., 2015b; P. Agung Putra & Henry Yuliando, 2015).

Hydroponics is usually classified into open and closed types. In open hydroponics, the nutrient solution flows through the growing bed and is discarded, which can result in the pollution of ground- and surface water (Van Os, 1994; W Voogt & C Sonneveld, 1997). In closed hydroponics, which collects drainage solutions and reuses these by replenishing water and nutrients, the use and discharge of water and nutrients are less than for open hydroponics (M. T. Ko et al., 2013; Meric et al., 2011; Zekki et al., 1996). Therefore, a transition from open hydroponics to closed hydroponics is seen increasingly often due to the more environmentally-friendly aspect of closed hydroponics (Meric et al., 2011). However, current practices for closed hydroponics still have several limitations, as described below.

In closed hydroponics, the management of the reused solutions is mostly conducted by the conductivity and pH probes. However, the probes can only provide a total ion activity and pH, so the imbalance of nutrient ratios may occur in reused nutrient solutions due to the lack of information about the individual ion concentrations (Domingues et al., 2012; Gutierrez et al., 2007; D.-H. Jung et al., 2019; N. Katsoulas et al., 2015; Dimitrios Savvas & Gizas, 2002). This makes the crop quality and productivity decrease. Therefore, growers usually flush the nutrient solutions and replace all solutions periodically, despite the environmental pollution and loss of fertilizers (Gieling et al., 2005). Although growers can analyze the individual ion concentrations of the nutrient solutions by periodic laboratory analysis,

a time delay between the sampling and the analysis limits the instantaneous feedback control of the nutrient solution composition (Matthew Bamsey et al., 2012; Gutierrez et al., 2008). In this regard, fast and continuous measurement of individual nutrient concentrations is necessary for the precise correction of the reused nutrient solutions, thereby allowing both improved efficiency of fertilizer use and reduced environmental pollution (W. J. Cho et al., 2017; Gutierrez et al., 2007; Vardar et al., 2015).

Ion-selective electrodes (ISEs) could be one of the most attractive tools to measure the individual ion concentrations of hydroponic solutions due to their advantages such as simplicity of use, fast response time, direct measurement of analyte, sensitivity over a wide concentration range, and portability (Heinen & Harmanny, 1991; H. J. Kim et al., 2013; F Xavier Rius-Ruiz et al., 2014). Specifically, the concept of a sensor array makes it possible to simultaneously determine individual ion concentrations in complex samples (J. Gallardo et al., 2005; Gutierrez et al., 2007; Mimendia et al., 2010). However, several disadvantages of ISEs such as signal drift and distortions due to interfering ions make the application for hydroponics difficult (W. J. Cho et al., 2017; Gieling et al., 2005; Gutierrez et al., 2007; D. H. Jung et al., 2015). Therefore, it is essential to develop an effective data-processing method to compensate for the signal drift and interference (Bratov et al., 2010; Amy V Mueller & Hemond, 2016).

One such method is a two-point normalization (TPN) method in conjunction with the use of the Nernst equation that consists of a sensitivity adjustment followed by an offset adjustment applied to all of the signal data measured with the ISEs (D. H. Jung et al., 2015; H. J. Kim et al., 2017; H. J. Kim et al., 2013). In previous studies, the TPN method was employed and shown to be effective in compensating for the signal drifts of a sensor array consisting of NO_3, K, and Ca ISEs which were used for measuring hydroponic solutions (W.-J. Cho et al., 2018; W. J. Cho et al., 2017; D.-H. Jung et al., 2019; D. H. Jung et al., 2015; H. J. Kim et

al., 2017). However, the TPN method is relatively weak for the interference because the standard curve for the TPN is constructed based on the simplified Nernst equation. The simplified Nernst equation assumes the ion-selective membrane would be specific to the ion of interest, but the actual membrane responds to other interfering ions. As a result, electromotive forces (EMFs) generated from the ISEs are affected by the complex ion matrix in hydroponic solutions, thereby inducing errors in the ion concentrations predicted by the TPN method. In addition, use of the TPN method is still limited in measuring other ions, such as P and Mg, present in hydroponic solutions, because ionophores for selective recognition of the P and Mg with an acceptable level are not yet commercially available.

Considering the complexity of ions present in hydroponic solutions, an artificial neural network (ANN) would be a proper method for compensating for the interferences on ISEs because ANN conducts the processing of non-linear multivariate interactions based on knowledge storage and learning and its property of controlling the number of hidden neurons and hidden layers makes it more flexible than other machine-learning techniques (Baret et al., 2000; Gutierrez et al., 2008; Amy V. Mueller & Hemond, 2013; Amy V Mueller & Hemond, 2016; Ni et al., 2014). In addition, ANN could be utilized as a predictive tool through the reflection of inherent chemical relationships (Amy V. Mueller & Hemond, 2013). However, ANN is vulnerable to signal drifts. For example, drifts can make the signals different from the signals obtained during the training, then the predicted ion concentrations by the ANN model would deviate from the actual values. This indicates that the ANN model would be difficult to use in ISE measurements without the drift compensation (W. J. Cho et al., 2017).

Based on the complementary properties of the TPN and ANN methods, in this study, we proposed a hybrid signal processing approach to effectively compensate for the signal drifts and interferences from other ions, thereby improving the

accuracy of ISEs in hydroponic applications. The specific objectives of this study were (1) to evaluate the hybrid processing method when compared to the TPN or ANN methods using a sensor array consisting of ion-selective electrodes for macronutrients (NO_3, K, and Ca) and an electrical conductivity electrode, and (2) to investigate the possibility of an ANN-based prediction model for Mg concentration in hydroponic solutions, of which there are few robust ISEs.

MATERIALS AND METHODS

PREPARATION OF THE SENSOR ARRAY

For the measurement of NO_3 and K ions, two different polyvinyl chloride (PVC)-based ion-selective membranes were formulated based on the chemical compositions previously reported (Table 4.1) (D. H. Jung et al., 2015; H. J. Kim et al., 2017; H. J. Kim et al., 2013). The ion-selective membrane solutions were prepared by dissolving the chemicals with 2 mL of tetrahydrofuran (THF) solvent. The solutions were then poured into a 24-mm diameter glass ring (48953, Sigma-Aldrich, St. Louis, MO, USA) with a flat glass plate (48952, Sigma-Aldrich, St. Louis, MO, USA) and evaporated for 24 h at room temperature. When the solutions were evaporated, ion-selective membrane films were punched with a diameter of 2.5 mm. The punched films were attached to the ends of laboratory-made plastic bodies of 44 mm length using THF solvent. As a final step, the internal solutions, consisting of 0.01 M $NaNO_3$ + 0.01 M NaCl for NO_3 ISEs, and 0.01 M KCl for K ISEs, were filled.

For sensing Ca ions, a commercially available Ca ISE (Orion 9320BNWP, Thermo Fisher Scientific, Beverly, MA, USA) was used. A double junction glass electrode (Orion 900200, Thermo Fisher Scientific, Beverly, MA, USA) was used as the reference electrode for ISEs. In addition, a commercial conductivity probe (Orion 013610MD, Thermo Fisher Scientific, Beverly, MA, USA) was employed to measure the conductivity of the test samples.

Finally, the sensor array was composed of three ISEs for NO_3, three ISEs for K, two ISEs for Ca, one reference electrode, and one conductivity probe. It has been reported that the ISEs prepared in the study are applicable for hydroponic solutions (W.-J. Cho et al., 2018; W. J. Cho et al., 2017; D.-H. Jung et al., 2019; D. H. Jung et al., 2015; H. J. Kim et al., 2017; H. J. Kim et al., 2013). The performance characteristics of the ISEs reported in the previous studies are summarized in Table 4.2.

Table 4.1. Chemical compositions of NO_3 and K ion-selective electrode (ISE) membranes used in this study*

Component	NO_3		K	
	Reagent	Composition	Reagent	Composition
Ionophore	TDDA	4.0% (8 mg)	Valinomycin	2.0% (4 mg)
Plasticizer	NPOE	67.75% (135.5 mg)	Dos	64.7% (129.4 mg)
Matrix	PVC	28.25% (56.5 mg)	PVC	32.8% (65.6 mg)
Ionic additive			KTClPhB	0.5% (1 mg)

* TDDA = tetradodecylammonium nitrate, DOS = bis(2-ethyhexyl) sebacate, NPOE = 2-nitrophenyl octylether, PVC = high-molecular-weight polyvinyl chloride, and KTClPhB = potassium tetrakis(4-chlorophenyl)borate.

Table 4.2. Performance characteristics of the NO_3, K, and Ca ISEs reported in the previous studies

Sensor	Linear Range ($mg \cdot L^{-1}$)	Detection Limit ($mg \cdot L^{-1}$)	Response Time (s)	Lifetime (days)	References
NO_3	3–1600	3	~50	~60	(W.-J. Cho et al., 2018; W. J. Cho et al., 2017; D. H. Jung et al., 2015)
K	3–700	3	~50	~60	
Ca	3–700	3	~50	~40	

CONSTRUCTION AND EVALUATION OF DATA-PROCESSING METHODS

Two conventional processing methods (TPN and ANN) were used and compared to validate the feasibility of the hybrid processing method (TPN-ANN). The working principle of the TPN method is that individual sensitivity slopes of each of

the ISE electrodes are normalized by multiplying the EMF data by the ratio of a reference EMF difference to a measured EMF difference using two different solutions with known concentrations of the primary ion corresponding to the electrodes. Offsets are then adjusted by subtraction of the difference between the highest reference point and the modified highest concentration point (Fig. 4.1a). The EMF data modified by use of the TPN method are applied to the simplified Nernst equation (eq. 4.1).

$$\text{EMF} = E_O + E_J + S * \log a_i \qquad (4.1)$$

where E_O, E_J, S, and a_i are the standard potential (mV), the liquid-junction potential (mV), Nernstian slope ($59.16/z_i$ mV/decade change in concentration for H_2O at 25 °C and z_i is the charge number of the response ion i), and the activity of the response ion.

The parameters of calibration equations determined in the previous study (D. H. Jung et al., 2015), i.e., S, E_O, and E_J, could be utilized because the compositions of ISE membranes were the same (Table 4.3). The activity of the ion was assumed to be equal to the concentration. According to the procedures in previous studies (W.-J. Cho et al., 2018; W. J. Cho et al., 2017; D. H. Jung et al., 2015; H. J. Kim et al., 2017; H. J. Kim et al., 2013), the TPN was carried out prior to each sample measurement.

The structure of the ANN used in this study was a feed-forward backpropagation neural network, which consisted of an input layer, hidden layers, and an output layer (Fig. 4.1b). The numbers of neurons in the input layer and the output layer were 9 (signals from eight ISEs and one conductivity probe) and 4 (NO_3, K, Ca, and Mg), respectively. Although ANNs with multiple hidden layers and neurons have a stronger generalization ability, the training time is usually increased and more samples are required to avoid an over-fitting issue (Chai et al., 2019). Therefore, for the application of the ANN, the parameters of ANN such as the number of hidden layers or hidden neurons should be determined carefully.

The optimal numbers of hidden layers and neurons were determined via trial and error method. Briefly, the number of input neurons was fixed as 10 and the number of hidden layers was set to 1, 2, 3, 5, and 10. Three replicate results were then obtained for each layer number and their root mean square errors (RMSEs) were calculated and compared to select the optimal number of hidden layers. Similarly, the number of hidden neurons was tested using ranges of 8 to 16 with an interval of 2 because the neuron number is highly related to the predictability of the ANN model [31]. The model performance was evaluated based on RMSEs of three replicate training results.

During the learning process, the learning rate of 0.01 and the Levenberg-Marquardt algorithm, which is one of the optimizer algorithms for avoiding local minima and overfitting, were used (H. Yu & Wilamowski, 2011). The input data (X_s) for ANN was rescaled (X_r) using min-max scaling (eq. 4.2) to make each input have equal meanings and dimensions for the neural network.

$$X_r = \frac{X_S - X_{min}}{X_{max} - X_{min}} \qquad (4.2)$$

where X_{min} and X_{max} are the minimum value and the maximum value of the input dataset, respectively.

As a next step, a conversion of input values to output values was carried out to calculate the interconnections between input values and output values, which is called an activation function. Due to the non-linear interactions among the ISEs, non-linear activation functions such as the tanh (tansig) (Freeman & Skapura, 1991) and rectified linear unit (ReLU) (Hara et al., 2015; Nair & Hinton, 2010) were considered for the hidden layer. Specifically, the application of the tansig showed the high accuracy in ISE signal processing in the previous study (Gutierrez et al., 2007). However, the tansig function limits the output range as −1 to 1. As a result, the output would be diminished when the hidden layer number is increased, thereby reducing the predictability of the ANN model. This problem is called the "vanishing information problem" (Kamimura, 2016). ReLU makes the output

sparser so it can be effective in multi-layer neural networks (Freeman & Skapura, 1991; H. Yu & Wilamowski, 2011). Therefore, ReLU was used for the neural networks of the hidden layers of 5 and 10.

After the determination of the parameters for the ANN, the original ANN was trained using the raw EMFs from the sensor array. In the case of the hybrid method, the ANN was applied using the EMFs after the TPN to achieve the drift compensation for the enhancement of the signal processing (Fig. 4.1c).

For the data processing, Python 3.7.3 programming language and several third-party libraries were used. The performances of the constructed processing methods were evaluated by the determination coefficients (R^2) and RMSEs of the correlation between the predicted concentrations and the actual concentrations.

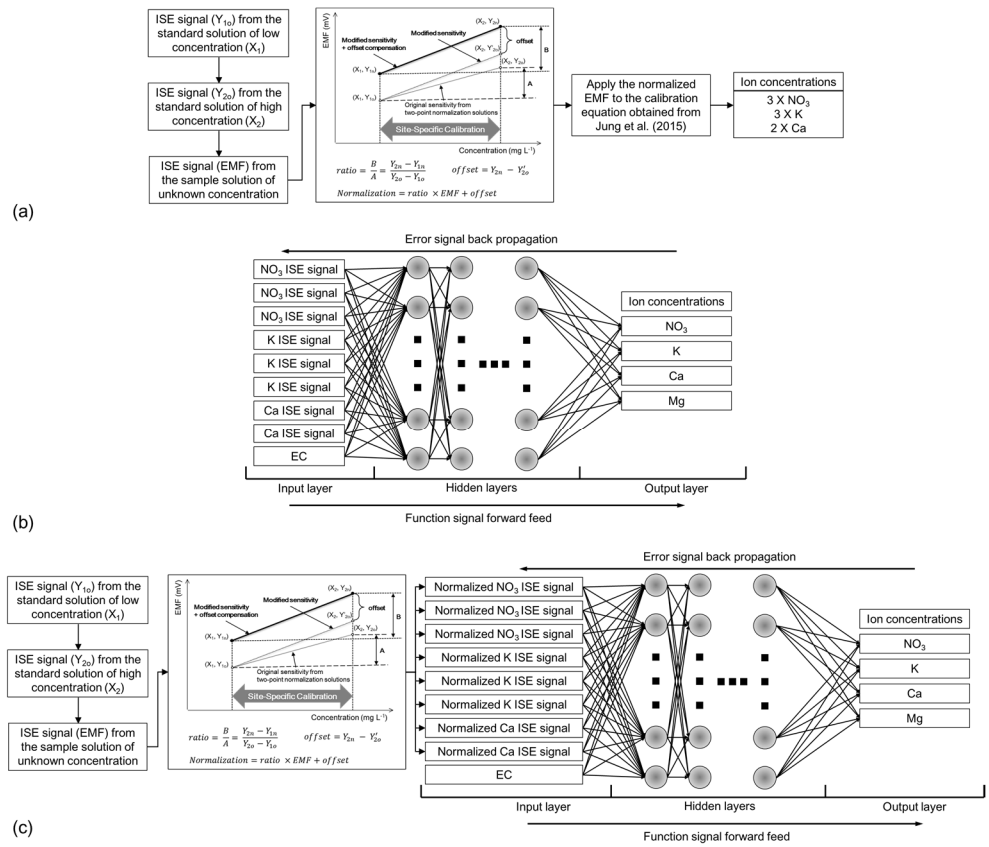

Fig. 4.1. Structures of the ISE data processing methods used in this study: (a) TPN;

(b) ANN; (c) hybrid method

Table 4.3. Calibration equations for NO_3, K, and Ca ISEs from the study of Jung et al. (2015)

Ion	Calibration equation*	Coefficient of determination (R^2)	Standard error of calibration (SEC)
NO_3	$EMF_{NO3} = -44.4 \times \log C_{NO3} + 257.3$	0.95	10.8
K	$EMF_K = 60.5 \times \log C_K - 49.6$	0.99	6.1
Ca	$EMF_{Ca} = 27.3 \times \log C_{Ca} - 50.3$	0.99	2.8

* C represents the concentration of the solution.

PREPARATION OF SAMPLES

Two-point normalization solutions and training samples were necessary to generate the primary information for the model training of TPN and ANN, respectively. Referring to the procedure described by the previous study (Gutierrez et al., 2007), 27 solutions were designed by a fractional factorial design with three levels of concentration and four factors (NO_3, K, Ca, and Mg) using a commercial statistical software (JMP, SAS Institute, Inc., Cary, NC, USA). Briefly, various mixtures of the primary ions (NO_3, K, Ca, and Mg) were prepared to have concentrations of 100–1000, 30–300, 24–240, and 10–100 $mg \cdot L^{-1}$ for NO_3, K, Ca, and Mg, respectively, by adding the calculated stock solutions of ammonium nitrate, magnesium sulfate, potassium sulfate, and calcium chloride to a base solution. In order to generate training samples with a similar background of real hydroponic solutions, a mixture of the modified Hoagland's hydroponic nutrient solution (Hoagland & Arnon, 1950) and tap water (1/1 (*v*/*v*)) was used as the base solution for the training samples. The samples of the lowest levels and the highest levels of NO_3, K, Ca, and Mg ions (i.e., 100 and 1000 $mg \cdot L^{-1}$, 30 and 300 $mg \cdot L^{-1}$, 24 and 240 $mg \cdot L^{-1}$, 10 and 100 $mg \cdot L^{-1}$, respectively) were additionally prepared for two-point normalization solutions.

For evaluating the feasibility of the processing methods in real hydroponic application, a total of 8 samples were manually collected from nutrient solution

mixing tanks of various hydroponic systems (Table 4.4). Specifically, the samples had different compositions for six kinds of plants (kale, *Atractylodes japonica*, *Glehnia littoralis*, beet, basil, and paprika), which spanned a wide range of ion concentrations.

The actual concentrations of the samples were determined by a standard soil-water testing laboratory (National Instrumentation for Environmental Management (NICEM), Seoul, South Korea) using an ion chromatograph (ICS-5000, Thermo Fisher Scientific, Waltham, MA, USA) with a low detection limit of 0.05 $mg \cdot L^{-1}$ for NO_3, and an inductively coupled plasma-optical emission spectrometer (iCAP 7400, Thermo Fisher Scientific, Waltham, MA, USA) with a detection limit of 0.6 $\mu g \cdot L^{-1}$ for K, Ca, and Mg, respectively. The measured ion concentrations of the samples are shown in A2.

Table 4.4. Hydroponic samples used in this study

Sample	Growing Period	Hydroponic System	Nutrient Solution Recipe	Sampling Sites
Basil 1	5 weeks	Deep Flow Technique (DFT) (closed)	Yamazaki's hydroponic nutrient solution	Experimental farm of Seoul National University (SNU)
Kale	3 weeks	Nutrient Film Technique (NFT) (closed)	Otsuka House's hydroponic nutrient solution	Smart farm of Korea Institute of Science and Technology (KIST)
Basil 2	5 weeks	DFT (closed)	Yamazaki's hydroponic nutrient solution	Experimental farm of SNU
Beet	5 weeks	NFT (closed)	Otsuka House's hydroponic nutrient solution	Smart farm of KIST
Atractylodes japonica	6 weeks	NFT (closed)	Hoagland's hydroponic nutrient solution	Plant factory of Jeju National University (JNU)
Glehnia littoralis 1	8 weeks	NFT (closed)	Hoagland's hydroponic nutrient solution	Plant factory of JNU
Paprika	14 weeks	Drip Irrigation (open)	Grodan's hydroponic nutrient solution	Smart farm of KIST
Glehnia littoralis 2	6 weeks	NFT (closed)	Hoagland's hydroponic nutrient solution	Plant factory of Chungbuk National University

PROCEDURE OF SAMPLE MEASUREMENTS

In order to accurately and simultaneously obtain the signals from the sensor array and effectively apply the TPN prior to each sample measurement, a laboratory-made automated test stand used in the previous study was used (W.-J. Cho et al., 2016). The schematic diagram of the automated test stand is shown in Fig. 4.2a. The test stand includes a Teflon-based sensor array chamber equipped with a servomotor, sample containers, a main computer system with a signal-conditioning data acquisition board, a motor controller, discrete pressure pumps for samples, and a control box for pump and motor operation (Fig. 4.2b).

For each sample measurement, about 50 mL of sample solution was automatically injected into the sample holder by the pressure pumps and stirred by

rotating the holder at approximately 30 rpm during data collection. Each test sequence began with a rinsing of the electrodes by introducing the distilled water (DW). Sixty seconds after the sample injection, the signals of the electrodes were logged with the mean of a 1 s burst of 1 kHz data. After each measurement, the holder was rinsed with distilled water and the rotational speed was increased to approximately 400 rpm to expel solutions centrifugally. The test sequence was controlled by software developed based on LabVIEW (A3). Fig. 4.3 represents the overall process of the sample measurements in this study. Three iterations were conducted for the prepared samples and Excel 2016's statistical tools (Microsoft, Redmond, WA, USA) were used to analyze the data. The specifications of components in the test stand are listed in Table 4.5.

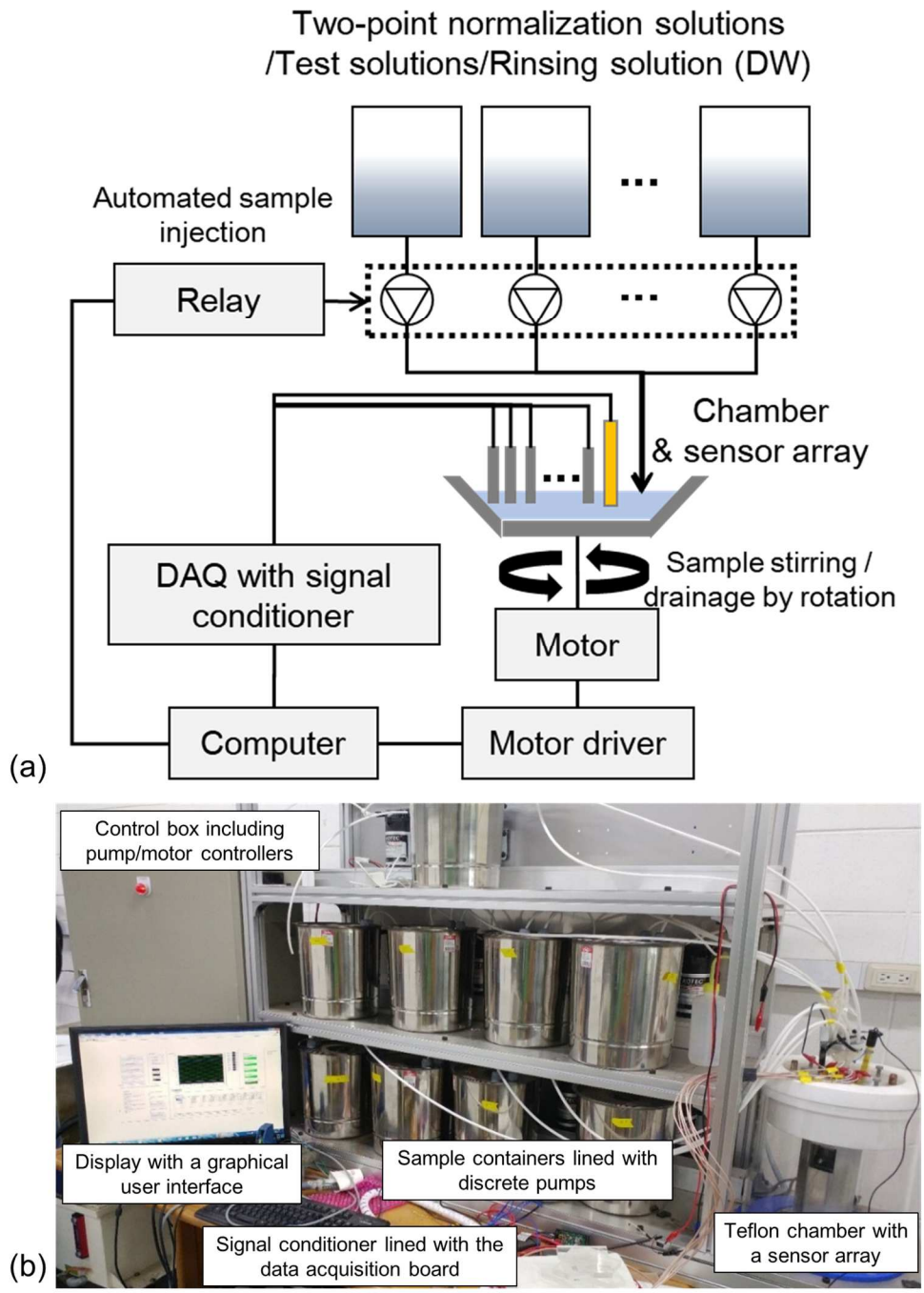

Fig. 4.2. View of the schematic diagram of the test stand (a) and the automated test stand (b)

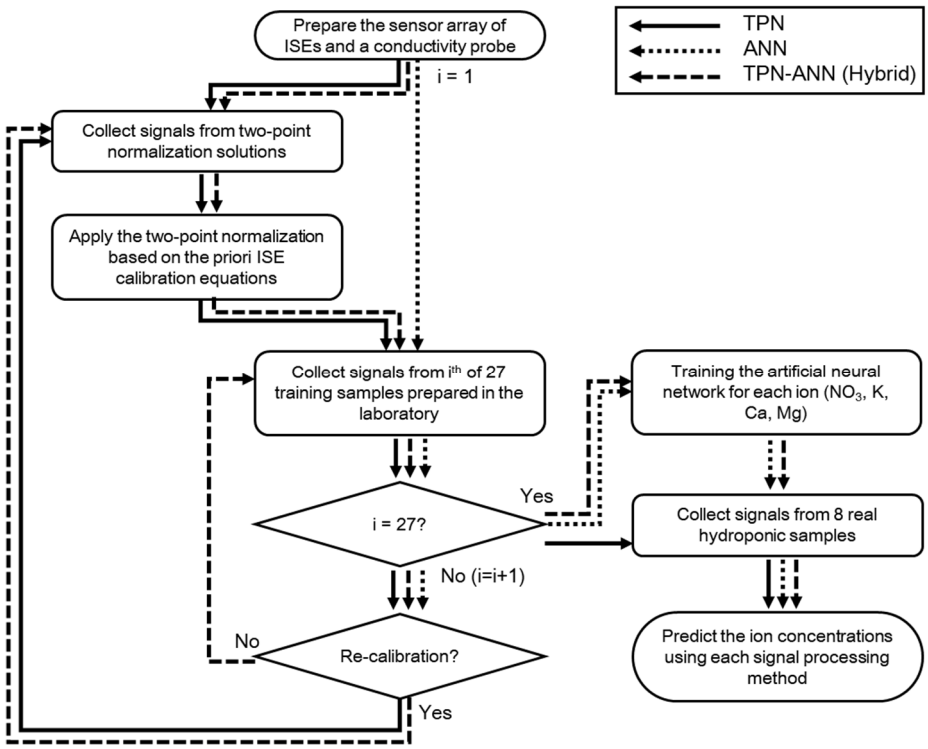

Fig. 4.3. Block diagram of the sample measurement process

Table 4.5. Specifications of components of the automated test stand

Component	Specification	Manufacturer/Model
Data acquisition board	A/D converter Input channel: 16 bit analog input Sampling rate: 250 $kS \cdot s^{-1}$	National Instrument (TX, USA), PCI-6221
Signal conditioner	Isolated analog input board for ISEs Input range: ± 10 V Gain: 1	National Instrument (TX, USA), SCC-AI13
Pump	Diaphragm pump Flow rate: 2-2.51 $L \cdot min^{-1}$ Maximum pressure height: 8.2 kgf/cm^2 Power: 24 VDC	KOTEC (Incheon, South Korea), R-1305
Servo motor	Rotational speed: 0–3000 rpm Power: 100 W	Mitsubishi (Tokyo, Japan), HG-MR
Motor controller	Speed frequency response: 2.5 kHz Encoder: 4,194,304 $pulse \cdot rev^{-1}$ Power: 200 VAC	Mitsubishi (Tokyo, Japan), MELSERVO-J4
Digital output controller	Pump relay control Digital I/O channel: Bidirectional 5 V/TTL 32 ch.	National Instrument (TX, USA), NI-9403
Solid state relay	Pump control Input voltage range: 4~32 VDC Output voltage range: 10~200 VDC	Woonyoung (Cheonan, South Korea), WYNSG1C205D4

RESULTS AND DISCUSSION

DETERMINATION OF THE ARTIFICIAL NEURAL NETWORK (ANN) STRUCTURE

The RMSEs according to the hidden layers and the hidden neurons are shown in Fig. 4.4. When the layer number was increased, the RMSEs of the prediction was increased (Fig. 4.4a). Specifically, the ANN with single-hidden layer shows significantly low average RMSEs when compared to the ANN with multi-hidden layer. Therefore, the optimization of neuron numbers was conducted using a single hidden layer. In the same way, the number of neurons in the hidden layer was determined to be 14. The final structure of ANN used in this study is shown in Fig. 4.5.

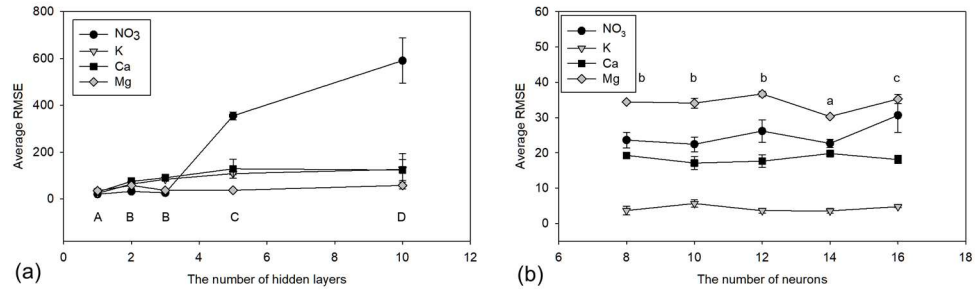

Fig. 4.4. Trends of the root mean square errors (RMSEs) according to the number of hidden layers (a) and hidden neurons (b). Error bars indicate the standard deviations of three replicates (n = 3, Duncan's multiple range test, a~c: $p < 0.05$, A~D: $p < 0.01$).

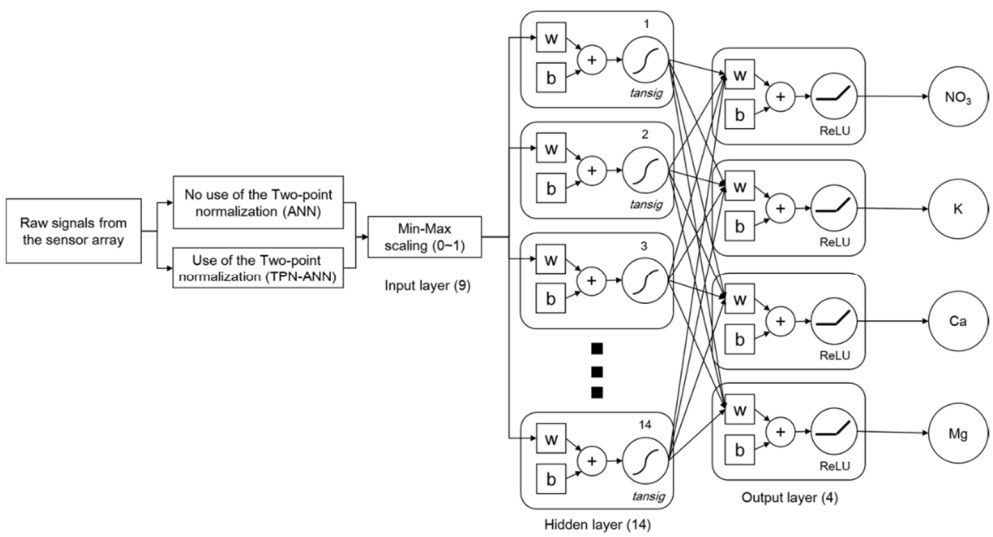

Fig. 4.5. Diagram of the determined neural network structure for the ANN and the hybrid method (w: weight value, b: bias)

EVALUATION OF THE PROCESSING METHODS IN TRAINING SAMPLES

In the training step, the performances of the ANN-based processing methods (ANN and TPN-ANN) training and the TPN method were evaluated. The prediction results according to the processing methods are shown in Fig. 4.6. In NO_3 prediction (Fig. 4.6a), the TPN showed a linear and accurate prediction result with R^2 of 0.99, a slope of 0.87, and a RMSE of 89.1 $mg \cdot L^{-1}$. In the case of the ANN and the hybrid method, there was no significant difference in the prediction

results despite the lower RMSE of the hybrid method (ANN: 22.3 mg·L^{-1}, TPN-ANN: 19.2 mg·L^{-1}). Specifically, the highly linear relationships with R^2 of 0.99 and slopes of 1.00 supported the proposition that the training of the ANN components would be well achieved.

The K prediction results showed similar trends in R^2, slopes, and RMSEs (Fig. 4.6b). The TPN method showed a good prediction result with an R^2 of 0.99, a slope of 1.01, and an RMSE of 9.3 mg · L^{-1}. In the ANN training, the RMSE was 26.3 mg · L^{-1}, which was slightly higher than the RMSE of the TPN. However, the R^2 of 0.97 and the slope of 0.94 showed the training was conducted at an acceptable level [29]. The TPN-ANN method showed improved training performance with a R^2 of 0.99, a slope of 1.00, and an RMSE of 3.7 mg·L^{-1}.

In the Ca prediction results, it was remarkable that the ANN-based approaches had more stable and linear responses when compared to the TPN-based approach (Fig. 4.6c). Specifically, the TPN showed a linear relationship with R^2 of 0.82 and a slope of 1.57, a RMSE of 93.0 mg·L^{-1}, which was relatively high considering the Ca concentration of training samples ranging from 30 to 300 mg·L^{-1}. The ANN-based methods showed better performances with R^2 of 0.97 and slopes of 0.97 and 0.96, and low RMSEs of 18.0 and 18.9 mg · L^{-1} for the ANN and the TPN-ANN methods, respectively.

The Mg prediction result (Fig. 4.6d) was only achieved by the ANN-based methods because the TPN has no predictability in ions without a directly related measurable sensor. The training results show that the ANN-based Mg prediction had a slope of 0.29, a R^2 of 0.51, and a RMSE of 29.3 mg · L^{-1}. The result of the hybrid processing method showed an improved slope, R^2, and RMSE, which were 0.4, 0.69, and 24.9 mg · L^{-1}, respectively. Although the values are somewhat subjective factors for evaluating the model performance, it would be possible to use the prediction model based on the hybrid method for the approximate quantitative prediction of Mg concentration according to the criteria of the previous

study (Baret et al., 2000). The correlation values between the predicted concentrations with the actual concentrations are presented in Table 4.6.

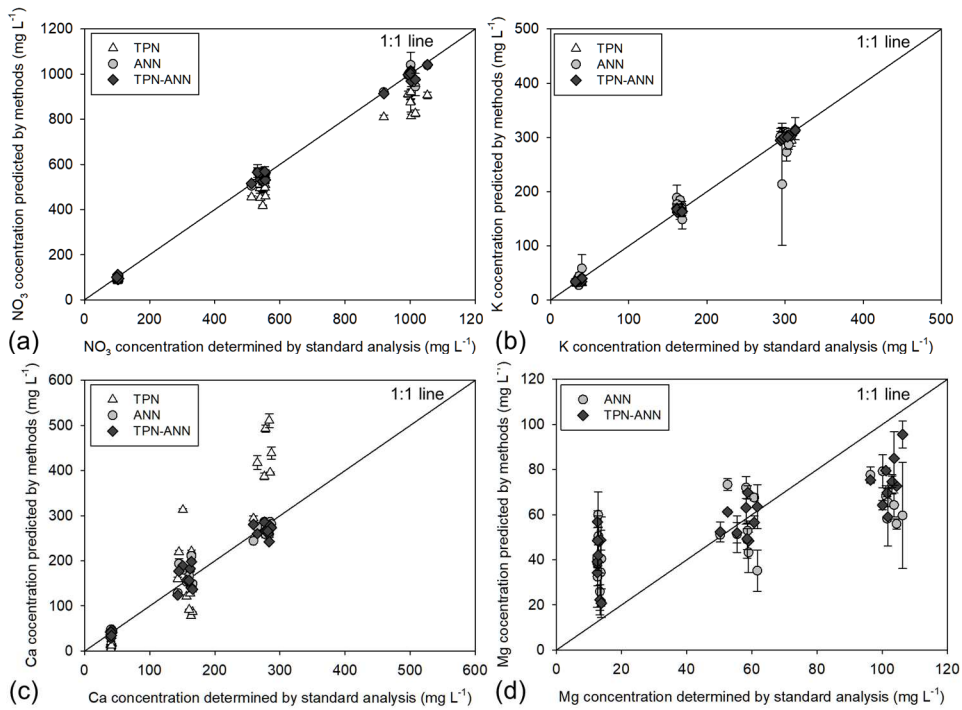

Fig. 4.6. Relationships between ion concentrations determined by the sensor array with three data processing methods and standard analyzers: (a) NO_3, (b) K, (c) Ca, and (d) Mg. Error bars indicate standard deviations of three replicates.

Table 4.6. Correlation between the predicted concentrations with the actual concentrations for NO_3, K, Ca, and Mg

Ion	Processing Method	Linear Relationship [*]	Confidence Intervals for Regression Slope		Coefficient of Determination (R^2)	RMSE [b] ($mg \cdot L^{-1}$)
			Lower 95%	Upper 95%		
NO_3	TPN	Y = 0.87X + 6.07	0.846	0.889	0.99	89.1
	ANN	Y = 1.00X + 0.52	0.984	1.014	0.99	22.3
	TPN-ANN	Y = 1.00X + 2.7	0.981	1.006	0.99	19.2
K	TPN	Y = 1.01X + 0.28	0.988	1.025	0.99	9.3
	ANN	Y = 0.94X + 7.18	0.884	1.005	0.97	26.3
	TPN-ANN	Y = 1.00X − 0.12	0.992	1.007	0.99	3.7
Ca	TPN	Y = 1.57X − 62.46	1.364	1.768	0.82	93.0
	ANN	Y = 0.97X + 6.4	0.918	1.02	0.97	18.0
	TPN-ANN	Y = 0.96X + 4.41	0.908	1.014	0.97	18.9
Mg	ANN	Y = 0.29X + 37.47	0.186	0.392	0.51	29.3
	TPN-ANN	Y = 0.4X + 34.79	0.306	0.485	0.69	24.9

[*] X represents the concentrations predicted by the processing methods and Y represents the concentrations determined by the standard analysis. [b] RMSE = $\sqrt{\frac{\sum_i^N (\hat{x_i} - x_i)^2}{N}}$; where $\hat{x_i}$: concentration estimated by ISE, x_i: actual concentration determined by standard instruments, N: number of sample measurements. TPN: two-point normalization

APPLICATION OF THE PROCESSING METHODS IN REAL HYDROPONIC SAMPLES

After the training and evaluation of the processing methods in laboratory-made samples, the applicability of the processing methods for the sensor array was validated by the prediction of the ion concentrations of real hydroponic samples. Fig. 4.7 shows the ion concentrations of the real hydroponic samples determined by the standard analyzers and the sensor array with the three processing methods. For NO_3 and K concentrations, the ANN-based prediction was less accurate than the TPN-based prediction. Specifically, the ANN-based prediction made significant deviations ($p < 0.01$) in most sample measurements comparing the actual concentrations (Fig. 4.7a and 4.7b). The hybrid method (TPN-ANN) predicted the concentration to be closer to the actual concentrations in NO_3 and K than other methods, which indicated that the hybrid method improved the accuracy of the sensor array by effectively processing the signals.

When comparing the RMSEs obtained with the three methods (Table 4.7), even

though the TPN showed lower RMSEs than those of the ANN (TPN: 75.4 and 19.8 $mg \cdot L^{-1}$, ANN: 133.5 and 144.7 $mg \cdot L^{-1}$ for NO_3 and K, respectively), the hybrid method (TPN-ANN) showed the best predictability with RMSEs of 47.2 and 13.2 $mg \cdot L^{-1}$, and coefficients of variation (CVs) below 10% for NO_3 and K, respectively. Moreover, in the Ca prediction (Fig. 4.7 and Table 4.7), the RMSE of 18.9 $mg \cdot L^{-1}$ obtained with the TPN-ANN was the lowest. In the Mg prediction, although the error bars showed relatively high CVs (26.6% and 28.6% for ANN and TPN-ANN methods), the Mg prediction results were almost comparable to the actual values, implying that the TPN-ANN method would offer the potential for use in hydroponic magnesium sensing.

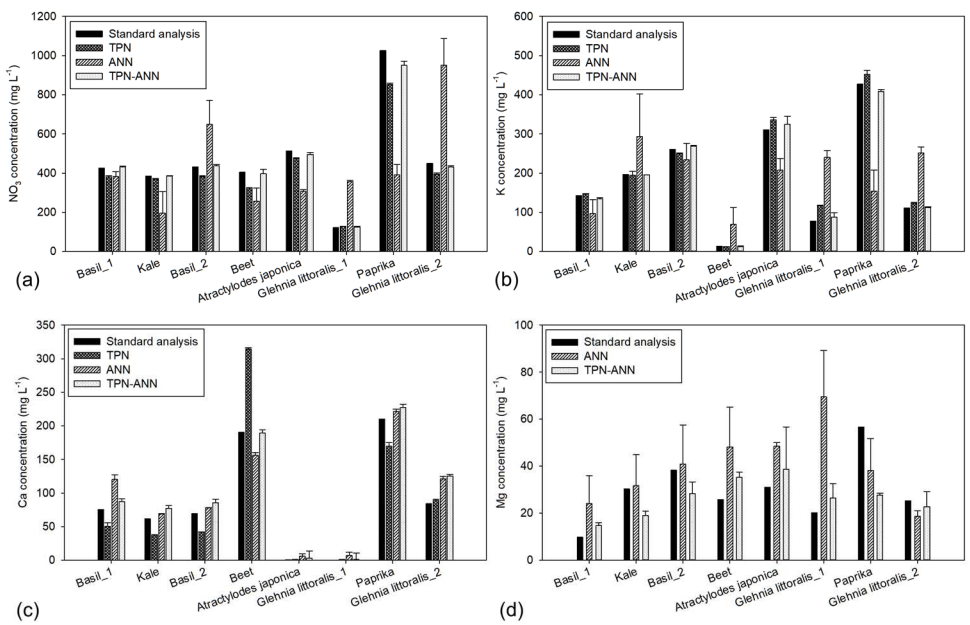

Fig. 4.7. Comparisons of the actual concentrations with the predicted concentrations by three signal-processing methods using 8 different hydroponic samples: (a) NO_3, (b) K, (c) Ca, and (d) Mg. Error bars indicate standard deviations of three replicates.

Fig. 4.8 shows changes in EMFs obtained with two-point normalization solutions (the high and low concentrations for NO_3 (Fig. 4.8a), K (Fig. 4.8b), and

Ca (Fig. 4.8c), respectively) during the ANN training. As shown in the figures, the EMFs were varied over time, indicating the need for compensating for sensitivity and offset changes over time. In addition, the EMF differences obtained with the low and high concentration solutions, i.e., sensitivities, were nearly constant, implying that the use of the two-point normalization method would be effective in minimizing the signal drifts of all of the tested ISEs during the measurement. This confirmed a reason of worse predictabilities of the ANN compared to those obtained with the TPN and TPN-ANN methods might be related to no use of the TPN.

Table 4.7. Comparison of processing methods to predict NO_3, K, Ca, and Mg concentrations in hydroponic samples

Predicted Ion	Conc. Range ($mg \cdot L^{-1}$)	Processing Method	Accuracy (RMSE, $mg \cdot L^{-1}$)	Precision (CV [a], %)
NO_3	120–1025	TPN	75.4	1.1
		ANN	133.5	17.9
		TPN-ANN	47.2	2.9
K	13–430	TPN	19.8	2.4
		ANN	144.7	30.1
		TPN-ANN	13.2	4.6
Ca	0–210	TPN	48.8	3.3
		ANN	26.1	13.8
		TPN-ANN	18.9	6.6
Mg	10–60	TPN	Not measurable	
		ANN	29.4	26.6
		TPN-ANN	14.6	28.6

[a] $\mathrm{CV} = \frac{SD}{\bar{x}} \times 100;\ \mathrm{SD} = \sqrt{\frac{\sum_i^N (\hat{x}_i - \bar{x}_{sample})^2}{N-1}}$;where $\hat{x}_i$: concentration estimated by ISE, $\bar{x}_{sample}$: average concentration estimated by ISE for each sample, N: number of sample measurements, $\bar{x}$: average concentration of N measurements

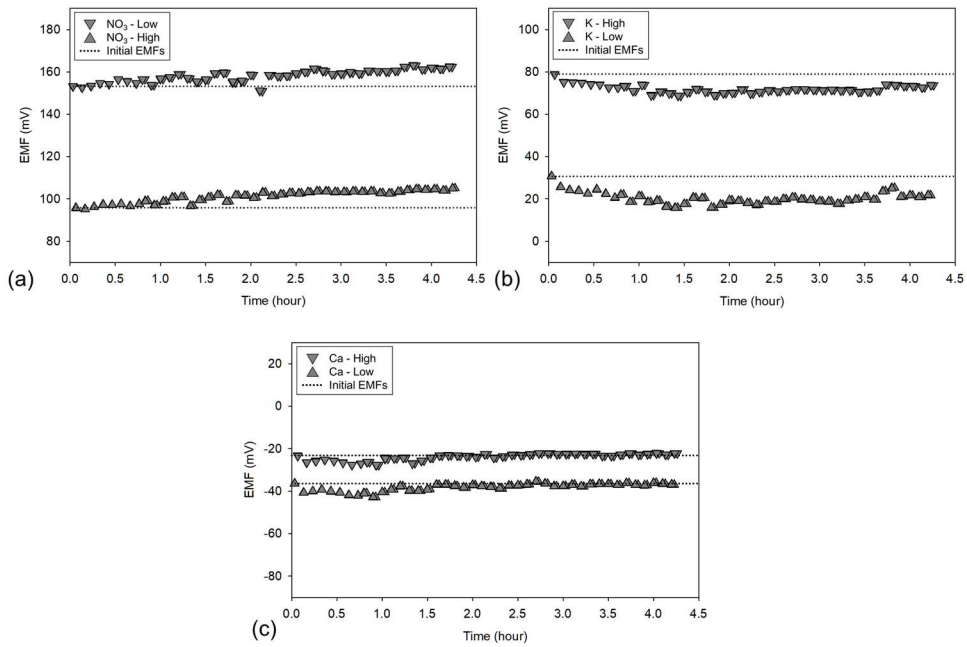

Fig. 4.8. Representative electromotive force (EMF) values showing drifts of (a) NO_3, (b) K, and (c) Ca ISEs from two-point normalization during the measurement ('Low' and 'High' in legends indicate the EMF values from the low and high concentrations of two-point normalization solutions, respectively).

In this study, we suggested a hybrid signal-processing method to improve the accuracy and feasibility of ISEs in hydroponic application by effectively compensating for the signal drifts and interferences from other ions.

The optimization results of the number of hidden layers showed a single hidden layer ANN had the lowest RMSE for NO_3, K, Ca, and Mg prediction (Fig. 4.4a). In actual fact, the ANN models with more hidden layers do not guarantee better performance than those with fewer layers if the number of hidden layers is sufficient for the given non-linear problem (J. Yu et al., 2019). Similarly, the performance of the ANN model was not increased according to the number of hidden neurons (Fig. 4.4b), as reported in the previous study (Baret et al., 2000).

In the training sample measurements (Fig. 4.6, Table 4.6), the application of the TPN showed a strongly linear relationship with R^2 of 0.99 despite a slight underestimation of NO_3 concentrations between the actual and predicted

concentrations similar to that reported in previous studies (W.-J. Cho et al., 2018; D. H. Jung et al., 2015; H. J. Kim et al., 2017). This might be caused by signal interferences from other ions, such as Cl and SO_4 in training samples. Moreover, TPN-based Ca prediction has a deviated slope of 1.57, which might be due to the presence of Mg ions, which have a similar chemical behavior to Ca ions (Saurina et al., 2002). The cross-interference would affect the Nernstian slope, thereby inducing inaccuracy in prediction (Wang et al., 2017).

To solve the interference issue, the ANN, which would possibly compensate for the interfering responses by training the various backgrounds, was employed and improved the performance of the actual test (Fig 4.6a and 4.6c). It supports the theory that ANN would be effective for the non-linear interference by adjusting the relationship as reported in the previous studies (Chai et al., 2019; Gutierrez et al., 2007, 2008; Amy V. Mueller & Hemond, 2013; Wang et al., 2017). In addition, we applied the ANN to predict the Mg concentration because we expected the ANN would extract the signals from the Mg ions through the training with defined background samples. Although the results were not satisfactory (Fig. 4.6d, Table 4.6), the ANN-based models could be used to discriminate between high and low concentrations of Mg according to the criterion of the previous study (Saeys et al., 2005).

In real sample application, the TPN-ANN was the best processing method, followed by TPN and ANN (Fig. 4.7, Table 4.7). As mentioned above, the Ca prediction by the TPN was vulnerable to interferences. Although the TPN made Ca predictions more precise than the ANN in several samples, e.g., Basil 1, *Atractylodes japonica*, *Glehnia littoralis* 1, and *Glehnia littoralis* 2, relatively high variations in Ca predictions depending on the samples showed that the TPN could be affected by the changes of background ions. In contrast, the ANN-based methods were effective in managing the interferences in actual tests, showing they were less affected by the samples in most cases (Fig. 4.7c). However, the ANN

method showed high RMSEs in the predictions of NO_3, K, and Mg. The main reason for the errors in the ANN-based prediction would be due to the signal drifts. This limitation of the ANN was similar to the results of several studies (Baret et al., 2000; Gutierrez et al., 2007, 2008).

The TPN method proved its effectiveness in drift compensation with improved accuracy. However, there were deviations in Ca prediction similar to those in the training sample measurement, which could be due to the interference by the various background ions.

The hybrid method showed the best predictability in real hydroponic sample application by successfully combining the strengths of the TPN and the ANN, as expected. It meant the hybrid method could compensate for the signal drifts and then calculate the concentrations considering the non-linear influences from the interference through the neural network. As a result, the hybrid method improved the accuracy and the precision of the prediction of the ion concentrations with the lowest RMSEs of 47.2, 13.2, and 18.9 $mg \cdot L^{-1}$ and CVs below 10% for NO_3, K, and Ca, respectively.

In Mg prediction, the RMSE of 29.4 $mg \cdot L^{-1}$ in the ANN-based prediction is high considering the range of 10–60 $mg \cdot L^{-1}$ in real samples. However, by applying the hybrid method, the RMSE of the prediction was reduced to 14.6 $mg \cdot L^{-1}$. Considering the lack of the ISEs for the direct measurement of Mg, it would be possible to improve the predictability by adding more ISEs which are more closely related to the Mg ion.

CONCLUSIONS

In this study, a hybrid signal-processing approach combining the TPN and the ANN was proposed to improve the applicability of the ISEs in hydroponics by effectively managing the signal drift and the interference. The parameters of the method were optimized by the 27 training samples, which imitated the hydroponic

background. The feasibility and the performance of the method was validated through eight of the real hydroponic sample applications.

From the results, the conventional processing methods such as the TPN and the ANN were sometimes unsatisfactory for prediction of the ion concentrations in hydroponic samples due to their vulnerability to the interference or the drift. The hybrid method improved the RMSEs to 47.2, 13.2, 18.9, and 14.6 $mg \cdot L^{-1}$, which were approximately half the values of the conventional methods, with CVs below 10% for NO_3, K, Ca, and Mg, respectively. Furthermore, the hybrid method showed potential as an approximate diagnostic tool for Mg prediction despite the lack of direct Mg ISEs in the sensor array.

The structure of the hybrid method can be utilized fundamentally for other ISEs. Therefore, the TPN-ANN method was proved to be possibility of use in the ISEs to measure the individual ions in hydroponic solutions while minimizing the effects of signal drifts and the interference. However, the input layer of nine sensor nodes could impose the use of the sensor array that were perfectly operated. On the contrary, the TPN can be used for each ISE and showed the best precision. Considering the long-term monitoring of the ISEs in hydroponic solutions, the stability and the reliability would be more important. Therefore, the TPN was chosen to be more feasible approach for the ISE array in aspect of the practical use.

* Note: Young-Yeol Cho, Jeju National University, Myung-Min Oh and Moon-Sun Yeom, Chungbuk National University, and Soo Hyun Park and Jai-Eok Park, Korea Institute of Science and Technology (KIST) donated the hydroponic samples used in this study. The development of the automated test stand was financially supported by the R&D center for Green Patrol Technologies, for KEITI (Korea Environmental Industry & Technology Institute), Republic of Korea. (E614-00184-0401-1) and the Rural Development Administration, Republic of Korea (PJ01385203201901). I would like to express my sincere gratitude to their support.

CHAPTER 5. DECISION TREE-BASED ION-SPECIFIC NUTRIENT MANAGEMENT ALGORITHM FOR CLOSED HYDROPONICS

ABSTRACT

The maintenance of ion balance in closed hydroponic solution is essential to improve the crop quality and the recycling efficiency of the nutrient solution. In the last decade, the ion-specific nutrient monitoring based on the ion-selective sensors has been implemented and shown potential in hydroponic applications. However, the absence of the robust ion sensors for several major ions such as P, Mg, and SO_4, and the coupling ions of the fertilizer salts make it difficult to efficiently manage the nutrient ions based on the measured ion concentrations. Therefore, it is necessary to develop an effective calculation process for formulating optimal compositions of fertilizer salts to replenish the recycled hydroponic solutions while minimizing the accumulation or deficiency of the ions which are not measurable. In this study, a decision tree-based closed control method was developed to calculate the optimal volumes of individual nutrient stock solutions to be supplied based on the measurement of present concentrations in a mixing tank. In a five stepwise test with the varying target concentrations and nutrient solution volumes, the system formulated the nutrient solutions according to the given target with the average relative errors of 10.6 ±8.0%, 7.9 ±2.1%, 8.0 ±11.0%, and 4.2 ±3.7%, respectively, for the Ca, K, and NO_3 concentrations and volume of the nutrient solution. The closed control logic conducted in the Ca focused management scenario showed more accurate ion-specific management would be possible, reducing the relative errors of Ca concentration and volume from -10.2% and -1.5% to -1.5% and -0.6%, respectively.

INTRODUCTION

When dealing with closed hydroponic solutions, the maintenance of ion balances in nutrient solutions is fundamental not only to ensure the productivity and quality of crops, but to elongate the recycling period of the nutrient solution for reducing the water and nutrient discharge, thereby allowing more economic and environmental benefits (Matthew Bamsey et al., 2012; Sambo et al., 2019).

Most soilless cultivation systems replenish the nutrient solution based on the pH and electrical conductivity (EC) of the solutions, which cannot cope with the varying concentrations of individual ions (Cloutier et al., 1997; Domingues et al., 2012; N. Katsoulas et al., 2015; Kozai et al., 2018; Son et al., 2020). However, the ion-specific nutrient management based on the ion-selective sensors has been investigated and showed potential in hydroponic applications (Matthew Bamsey et al., 2012; Gieling et al., 2005; Gutierrez et al., 2007, 2008; D.-H. Jung et al., 2019; D. H. Jung et al., 2015; H. J. Kim et al., 2013; F Xavier Rius-Ruiz et al., 2014; Vardar et al., 2015). Furthermore, several studies reported the development of the automated nutrient management system using ion-selective electrodes (ISEs) that could measure the concentrations of individual ions in hydroponic solutions and dose the nutrients according to each deficient ions (W. J. Cho et al., 2017; Gieling et al., 2005; D.-H. Jung et al., 2019; D. H. Jung et al., 2015; Xu et al., 2020). These are important developments that could allow both improved efficiency of fertilizer use and increased time of use of the nutrient solution in closed hydroponics.

However, it is difficult to conduct the ion-specific management exactly because there are few robust ISEs for several major ions such as P, Mg, and SO_4. In addition, the commercially available nutrients consist of coupled ions, thereby limiting the fully independent ion replenishment for hydroponic solutions (W. J. Cho et al., 2017; D.-H. Jung et al., 2019; D. H. Jung et al., 2015; H. J. Kim et al., 2013).

In the previous studies, two types of dosing algorithms were representatively

applied to automatically calculate the amounts of stock nutrient solutions to be supplied based on the measured ion concentrations. One system used a simplex algorithm with a set of given constraints to determine the injection volumes of stock solutions simultaneously (G De Rijck & Schrevens, 1994; Gieling et al., 2005; D. H. Jung et al., 2015). However, this approach was often impossible to find a final solution of the calculation due to the presence of the coupled ions in the fertilizers, thereby leading to the deviated concentrations from the target values and there was no consideration of the important nutrient ions such as P and Mg.

Another dosing algorithm was based on the sequential calculation based on the pre-determined priority of the ions (W. J. Cho et al., 2017; D.-H. Jung et al., 2019). It employed six fertilizers to mitigate the problem of decoupled replenishment among nutrients and manage the P and Mg ions by applying linear concentration ratios related to NO_3 and Ca ions, respectively. However, the system could not flexibly respond to the low changes of NO_3 and Ca, so the P and Mg ions were gradually diminished. Also, micronutrients including Fe, Zn, Cu, etc., were not considered. It is thus important to develop an improved fertilizer dosing algorithm that can maintain the individual ion concentrations at the required levels while minimizing the accumulation or deficiency of the ions which are not measurable.

The main purpose of this study was to develop an ion-specific dosing algorithm that can conduct efficient dosing operations by determining the proper amount of fertilizers while minimizing the coupled injection of the nutrient ions. The specific objectives were (1) to build a decision tree model based closed control method with the NO_3, K, and Ca ISEs for the sequential decision of the operation time for each individual fertilizer and (2) to evaluate the effectiveness of the developed algorithm by applying the algorithm to an automated nutrient management system and conducting validation tests.

MATERIALS AND METHODS

DECISION TREE-BASED DOSING ALGORITHM

In hydroponics, all essential nutrients are supplied as nutrient solutions made by dissolving fertilizers in water. Fertilizer salts can be dissolved as more than two ions, the relative proportion of fertilizers should be considered. The use of various fertilizers would be helpful to flexibly control the individual ion concentrations, but there are several practical issues. For example, the supply of Ca ions cannot be decoupled from the NO_3, because there is no other available fertilizer salt (Resh, 2016). In addition, add-up of the fertilizers would require more space of tanks and increase the complexity of the calculation and system operation. Therefore, a total of seven fertilizers consisting of $Ca(NO_3)_2 \cdot 4H_2O$, KH_2PO_4, $NH_4H_2PO_4$, KNO_3, NH_4NO_3, $MgSO_4 \cdot 7H_2O$, and K_2SO_4 were selected as the stock solutions to have at least two salts for each ion besides the Ca and Mg. Then, the priority of the ions was determined based on the universal nutrient solution calculation method, i.e., $Ca > P = K > NO_3 > NH_4$ (Sonneveld et al., 1997).

In order to calculate the proper mass of the fertilizer salts based on the given ion concentrations and the priority, a decision tree was used. The decision tree method is a machine-learning method for constructing a series of dichotomous classifications (Namazkhan et al., 2020). The decision tree algorithm makes tree-shaped diagrams with a number of branches with decision and leaf nodes. Each decision node has a predictor variable to obtain a more proper answer for the given variable, and the leaf node shows the final optimized result under the framework of the decision tree model. The decision tree-based dosing algorithm consists of three parts. The first part is the calculation of the amounts of major ions considering the current nutrient solution volume, the target nutrient solution volume, and the ion compositions in water (eq. 5.1). The SO_4 is not considered because it is not harmful to crops (Sonneveld et al., 1997).

$$N_{Ca} = T_{Ca} \times V_{target} - D_{Ca} \times V_{current} - W_{Ca} \times (V_{target} - V_{current})$$

$$N_K = T_K \times V_{target} - D_K \times V_{current} - W_K \times (V_{target} - V_{current})$$

$$N_{NO3} = T_{NO3} \times V_{target} - D_{NO3} \times V_{current} - W_{NO3} \times (V_{target} - V_{current})$$

$$N_{NH4} = R_{N-N} \times N_{NO3} - W_{NH4} \times (V_{target} - V_{current})$$

$$N_{Mg} = T_{Mg} \times V_{target} - C_{Mg} \times V_{current} - W_{Mg} \times (V_{target} - V_{current}), \text{ or } R_{Ca-Mg} \times N_{Ca} - W_{Mg} \times (V_{target} - V_{current})$$

$$N_P = T_P \times V_{target} - C_P \times V_{current} - W_P \times (V_{target} - V_{current}), \text{ or } R_{N-P} \times N_{NO3} - W_P \times (V_{target} - V_{current}) \quad (5.1)$$

where

N_x = amounts of ions (x = Ca, K, NO_3, NH_4, Mg, or P) to be replenished (mg)

T_x = target concentrations of ions (x = Ca, K, NO_3, NH_4, Mg, or P)

D_y = concentrations of ions (y = Ca, K, or NO_3) determined by ISEs ($mg \cdot L^{-1}$)

W_x = concentrations of ions (x = Ca, K, NO_3, NH_4, Mg, or P) in water determined by standard analyzers ($mg \cdot L^{-1}$)

V_{target} = target volume of the nutrient solution in the mixing tank (L)

$V_{current}$ = current volume of the nutrient solution in the mixing tank (L)

C_z = concentrations of ions (z = Mg or P) determined by the standard instruments

R_{N-N}, R_{Ca-Mg}, R_{N-P} = absorption ratios of NO_3 to NH_4, Ca to Mg, and NO_3 to P

In this study, the absorption ratio of 0.029 was used for NO_3-NH_4 based on the previous study (D Savvas et al., 2006; Sonneveld et al., 1997). The relationships between P and NO_3 ions and between Mg and Ca ions could be set as 0.0108:1 and 0.5882:1, respectively.

The next part is the decision tree-based calculation of the required amounts of fertilizer salts while minimizing the over injection. Fig. 5.1 shows the calculation steps of the decision tree-based approach. There are two trees in the algorithm.

One is to calculate the proper mass of the $Mg(SO_4)_2 \cdot 7H_2O$. There is only one salt for replenishing the Mg, and the injection of the $Mg(SO_4)_2 \cdot 7H_2O$ does not affect

the other nodes, so the tree is operated independently (Fig. 5.1a).

Another tree is for calculating the amounts of the other salts, i.e., $Ca(NO_3)_2 \cdot 4H_2O$, KH_2PO_4, $NH_4H_2PO_4$, KNO_3, NH_4NO_3, and K_2SO_4. The salts in the second tree are interconnected with each other, so the tree categorizes the salts according to the determined priority. Then, the calculation of the amounts of the salts is achieved sequentially. For example, if the NH_4 was required to be replenished, the amount of the $NH_4H_2PO_4$ would be calculated based on the needed mass of the NH_4. The next node then assesses the effect of the calculated amount of the $NH_4H_2PO_4$ in H_2PO_4. If there was no over-dose of H_2PO_4, the $NH_4H_2PO_4$ would be injected as the calculation. If not, the amount of the $NH_4H_2PO_4$ to be supplied would be re-calculated based on the required amount of the H_2PO_4, because the priority of the P is higher than the NH_4. In this case, the second final amount of the $NH_4H_2PO_4$ would be supplied rather than the first final amount of the $NH_4H_2PO_4$. In the same manner, the amounts of the other salts could be calculated by the decision tree-based approach (Fig. 5.1b).

After the amounts of the salts to be supplied were determined, the running time of the pump corresponding to each fertilizer salt was obtained by eq. 5.2.

$$P_x = \frac{M_x}{C_x \times D_x} \quad (5.2)$$

where

x = $Ca(NO_3)_2 \cdot 4H_2O$, KH_2PO_4, $NH_4H_2PO_4$, KNO_3, NH_4NO_3, $MgSO_4 \cdot 7H_2O$, or K_2SO_4

P_x = running time of metering pump for stock solution of fertilizer salt, x (s)

M_x = mass amount of stock solution of fertilizer salt, x (mg)

C_x = concentration of stock solution of fertilizer salt, x ($mg \cdot L^{-1}$)

D_x = discharge volume of metering pump for seven stock solutions of fertilizer salts ($L \cdot s^{-1}$)

The final part of the dosing algorithm is for the micronutrients and water replenishment. Currently, there are few commercially available ionophores for

micronutrient ions, so the replenishment of the micronutrients is carried out by injecting the micronutrients proportional to the difference between the target volume and the current volume of the nutrient solution (eq. 5.3).

$$P_m = \frac{C_m \times (V_{target} - V_{current})}{D_m} \quad (5.3)$$

where

P_m = running time of metering pump for concentrated solution of micronutrients (s)

C_m = multiple of concentrated solution of micronutrients to the final working concentration (dimensionless)

D_m = discharge volume of metering pump for concentrated solution of micronutrients ($L \cdot s^{-1}$)

Then, the volume of water to add could be obtained by subtracting the total volumes of the stock solutions and the concentrated micronutrient solution from the difference between the target volume and the current volume of the nutrient solution (eq. 5.4).

$$P_w = \frac{V_{target} - V_{current} - \sum V_{stock\ solution\ for\ x} - V_m}{D_w} \quad (5.4)$$

where

x = $Ca(NO_3)_2 \cdot 4H_2O$, KH_2PO_4, $NH_4H_2PO_4$, KNO_3, NH_4NO_3, $MgSO_4 \cdot 7H_2O$, or K_2SO_4

P_w = running time of metering pump for water (s)

$V_{stock\ solution\ for\ x}$ = volume of stock solution of fertilizer salt, x to add (L)

V_w = volume of concentrated solution of micronutrients to add

D_w = discharge volume of metering pump for water ($L \cdot s^{-1}$)

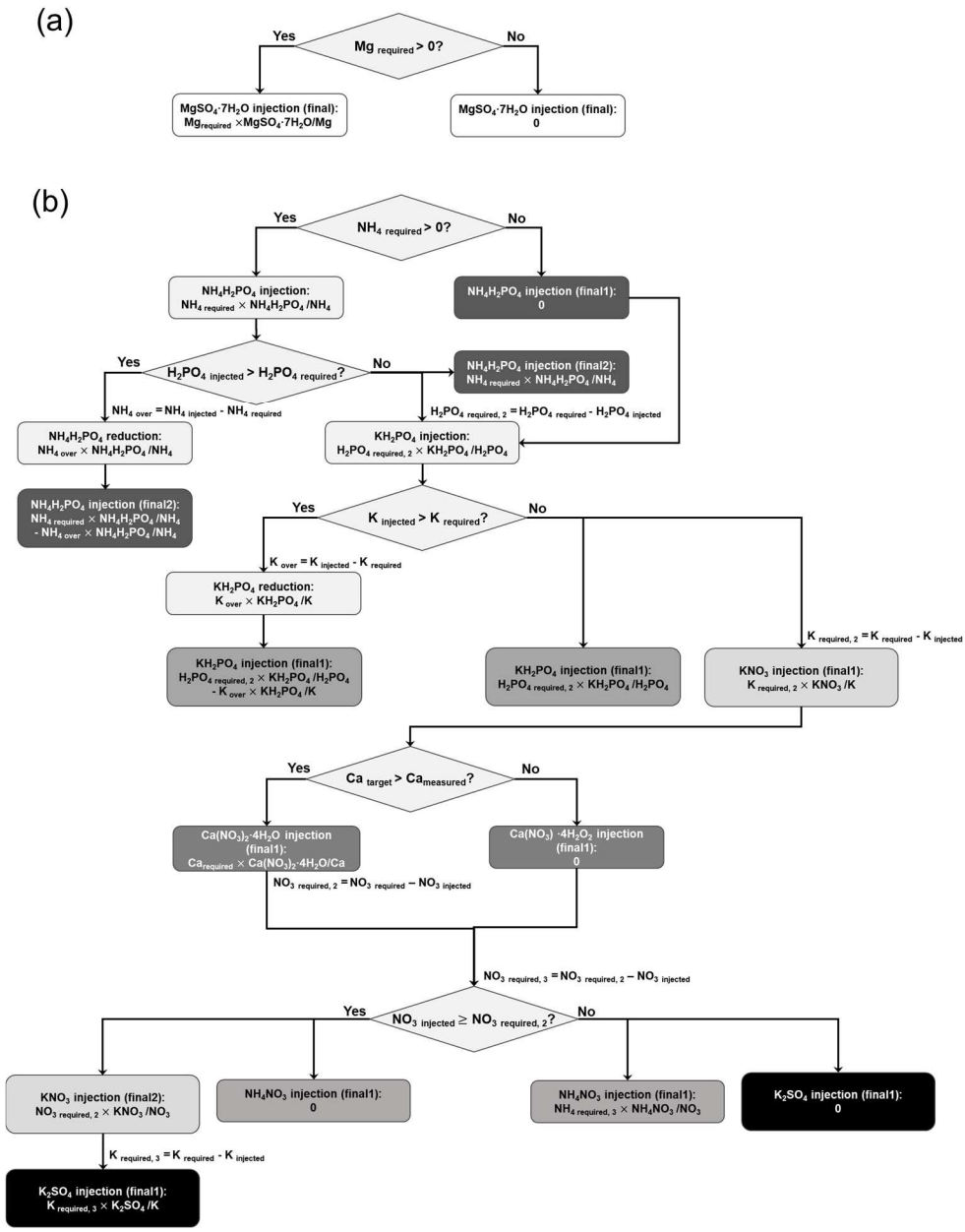

Fig. 5.1. Decision tree model for calculating the amounts of the fertilizer salts to be replenished, for $Mg(SO_4)_2 \cdot 7H_2O$ (a) and other salts (b). The $X_{injected}$ (X: NH_4, H_2PO_4, K, or NO_3) represents the injected amount of the ion by the previously injected salt. The node including 'final' indicates the leaf node, and the higher number behind the 'final' means the result would be a more appropriate amount of the salt.

DEVELOPMENT OF AN ION-SPECIFIC NUTRIENT MANAGEMENT SYSTEM

The ion-specific nutrient management system should have the capability of automatically measuring the ion concentrations of the nutrient solution, replenishing the nutrient solution considering the ion balance, and supplying the managed nutrient solution to the growing bed. In this study, the ion-specific nutrient management system was constructed for the NFT growing bed described in Chapter 3.

Fig. 5.2 shows an overview of the developed ion-specific nutrient management system and the specifications of the system are listed in Table 5.1. Relating to solutions used by the system, a nutrient mixing tank and twelve reservoirs for the seven stock solutions, one micronutrient stock solution, one pH control solution, water, and the two-point normalization solutions were imposed (Fig. 5.2a). For the two-point normalization, two mixed solutions containing NO_3, K, and Ca ions at two different concentrations, i.e., 100 and 1,000 $mg \cdot L^{-1}$, 30 and 300 $mg \cdot L^{-1}$, and 26 and 260 $mg \cdot L^{-1}$, respectively, were prepared based on the composition of the modified Hoagland's hydroponic nutrient solution to minimize the background effects from the real hydroponic solutions (W.-J. Cho et al., 2019; Hoagland & Arnon, 1950). The ion concentrations of the prepared stock solutions, pH control solution, and the two-point normalization solutions are displayed in A4.

To check the volume of the nutrient solution tank, a reflective ultrasonic water-level transmitter (EchoPod UG01, Flowline, Inc., CA, USA) was installed on the mixing tank (Fig. 5.2a).

For the two-point normalization, sampling, drainage, and the stock solutions, peristaltic pumps were employed due to the advantages such as sanitized transport of the fluid, self-priming operation, absence of backflow, and high repeatability (Klespitz & Kovács, 2014). The flow rate of the peristaltic pump determines the minimum injection volume, which is important because it is directly related to the accuracy of the replenishment. Therefore, the flow rates of the pumps for stock

solutions and water were determined to have the relative error from the minimum injection volume less than 0.1%, considering the concentrations of the stock solutions were prepared as 20,000 $mg \cdot L^{-1}$, and the multiple of the concentrated minor elements solution was 200. Furthermore, novoprene tubing, which is resistant to chemicals, was employed for the injection pumps (SR10/50, ASF THOMAS, Puchheim, Germany) for fertilizer salts (i.e., $Ca(NO_3)_2 \cdot 4H_2O$, KH_2PO_4, $NH_4H_2PO_4$, KNO_3, NH_4NO_3, $MgSO_4 \cdot 7H_2O$, and K_2SO_4), micronutrients, and acid, considering their high concentrations. Similarly, PharMed BPT tubing was applied to the pumps for the two-point normalization solutions. Drainage, sampling, and water pumps used silicone tubing because there were relatively low concentrations of ions.

For the quantification of NO_3 and K ions, ISEs using two different polyvinyl chloride (PVC)-based ion-selective membranes were fabricated according to the chemical compositions and procedures reported in the previous studies (W. J. Cho et al., 2017; D. H. Jung et al., 2015; H. J. Kim et al., 2013) (Chapter 4). For the Ca ions, a commercially available Ca ISE (Orion 9320BN, Thermo Fisher, MA, USA) was used. Finally, an array of ISEs composed of three ISEs for NO_3, three ISEs for K, two ISEs for Ca, and one reference electrode was installed to a sample chamber to measure the ion concentrations of nutrient solutions. A double-junction electrode (Orion 900200, Thermo Fisher, MA, USA) was used as the reference electrode. To minimize the residual solutions after the drainage, which could induce errors in measurements, the bottom of the sensor array chamber was designed to have a slope of 15° for more clear drainage (Fig. 5.2c).

An isolation circuit board (NI SCC-AI13, National Instruments, TX, USA) was used to buffer the impedance of each electrode, and the buffered signals were collected by a data acquisition board (NI PCI-6221, National Instruments, TX, USA). Also, an in-line EC probe (HI7635, Sistemes Electrònics Progrés S. A., Lleida, Spain), a pH probe (HI1001, Hanna instruments, RI, USA), and a

transmitter (TK4S, Autonics, Busan, South Korea) with a PT100 were employed for the EC, pH, and solution temperature measurements, respectively (Figs. 5.2a and 5.2d).

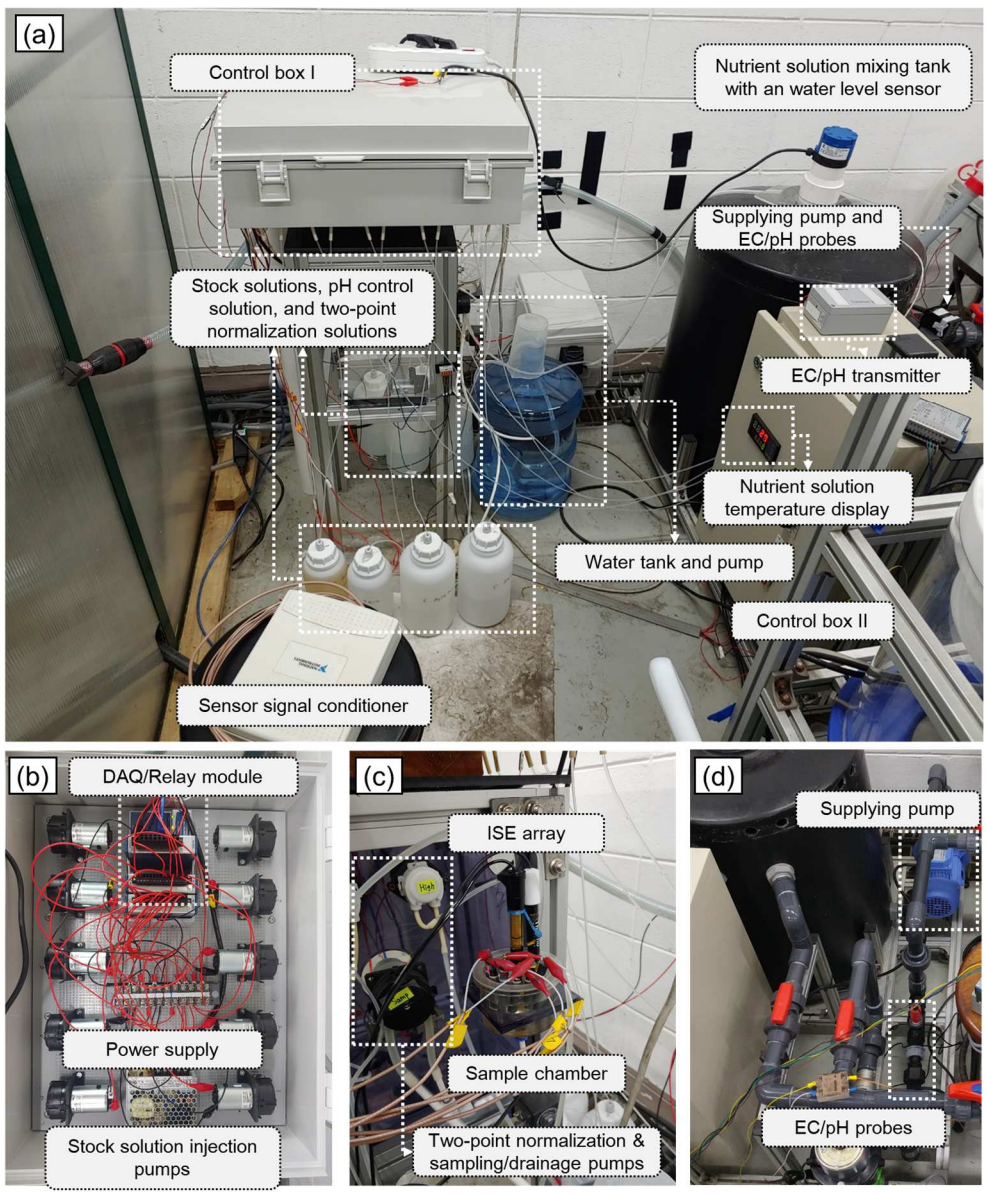

Fig. 5.2. Views of the ion-specific nutrient management system: (a) overview of the constructed ion-specific nutrient management system; (b) internal view of the control box I; (c) Sample chamber and sensor array of the system; (d) Supplying pump and pipe with an in-line EC probe and a pH probe

Table 5.1. Specifications of components of the Ion-specific management system

Component	Specification	Manufacturer/Model
Sample chamber	A chamber of Poly(methyl methacrylate): 100 mL	Megascience (Seoul, South Korea), Sensor chamber
Sensor array	K ISE Measuring range: 3-700 $mg \cdot L^{-1}$ Detection limit: 3 Response time: ~50s NO_3 ISE Measuring range: 3-1600 $mg \cdot L^{-1}$ Detection limit: 3 Response time: ~50s Ca ISE Measuring range: 3-700 $mg \cdot L^{-1}$ Detection limit: 3 Response time: ~50s Reference electrode: Double-junction	K, NO_3: Laboratory-made Ca: Thermo Fisher Scientific (MA, USA), 9320BN Reference: Thermo Fisher Scientific (MA, USA), 900200
EC probe	Flow-thru EC monitoring Automatic temperature compensation: 0-50 °C EC reading range: 0-20.0 $dS \cdot m^{-1}$ Max. pressure: 5.1 $kgf \cdot cm^{2}$	Sistemes Electrònics Progrés S. A. (Lleida, Spain), HI7635
pH probe	Flow-thru pH monitoring pH reading range: 0-14.0 pH Max. pressure: 6.1 $kgf \cdot cm^{-2}$	Hanna instruments (RI, USA), HI1001
EC/pH transmitter	pH/EC output range: 4-20 mA Power: 12 VDC	Sistemes Electrònics Progrés S. A. (Lleida, Spain), pH/CE transmitter
Temperature sensor	Transmitter with a PT100 probe Temperature range: -50-150 °C Output range: 4-20 mA Power: 220 VAC	Autonics (Busan, South Korea), TK4S
Two-point normalization pumps	Peristaltic pump Flow rate: 0.037 $L \cdot min^{-1}$ Tubing material: PharMed BPT Inner tubing diameter: 1.5 mm Power: 24 VDC	ASF THOMAS (Puchheim, Germany), SR10/30
Sampling & drainage pumps	Peristaltic pump Flow rate: 0.22 $L \cdot min^{-1}$ Tubing material: Silicon Inner tubing diameter: 1.6 mm Power: 24 VDC	ASF THOMAS (Puchheim, Germany), SR10/50
Stock solution pumps	Peristaltic pump Flow rate: 0.1 $L \cdot min^{-1}$ Tubing material: Novoprene Inner tubing diameter: 1.6 mm Power: 24 VDC	ASF THOMAS (Puchheim, Germany), SR10/50

Table 5.1. (Continued)

Component	Specification	Manufacturer/Model
Water replenishment pump	Peristaltic pump Flow rate: 0.525 L·min^{-1} Tubing material: Silicon Inner tubing diameter: 4.8 mm Power: 24 VDC	BOXER (Ottobeuren, Germany), QQ15
Nutrient solution supplying pump	Centrifugal pump Flow rate: 33.3 L·min^{-1} Maximum pressure height: 10.19 kgf·cm^{-2} Power: 3PH 380 VAC	Hwarang System Co., Ltd. (Incheon, South Korea), PP50Y
Main control system	CPU: 3.4 GHz (i7 4770, Intel) Memory: DDR3 8gb OS: Window 7 Main program: LabVIEW (v2015, National Instruments, TX, USA)	Hewlett-Packard (CA, USA), EliteDesk 800 G1 TWR
Solution tanks	Two-point normalization solutions (5 L for each)	Korea First Safety (Incheon, South Korea), 5L HDPE (high density polyethylene) tank
	Stock solutions (2 L for each)	Korea First Safety (Incheon, South Korea), 2L HDPE (high density polyethylene) water tank
	Nutrient solution mixing tank (Max. 100 L)	Bestplastic (Gyeonggi-do, South Korea), 100L PE (polyethylene) water tank
Water-level sensor	Reflective Ultrasonic Level Transmitters Measurement range: 0.038-1.5 m Automatic temperature compensation: -40-80 °C Signal output range: 4-20 mA Power: 24 VDC	Flowline, Inc. (CA, USA), EchoPod UG01
Data acquisition board	A/D converter for EC, pH, water temperature, and water level sensors Input channel: 16 bit analog input 8 ch. Input range: ± 20 mA Sampling rate: 200 kS·s^{-1}	National Instrument (TX, USA), NI-9203
Data acquisition board	A/D converter for ISE signals Input channel: 16 bit analog input Sampling rate: 250 kS·s^{-1}	National Instrument (TX, USA), PCI-6221
Signal conditioner	Isolated analog input board for ISEs Input range: ± 10 V Gain: 1	National Instrument (TX, USA), SCC-AI13
Relay	Solid state relay Input voltage range: 0~60 VDC Output voltage range: 0~60 VDC Channel: 8 ch.	National Instrument (TX, USA), NI-9485

IMPLEMENTATION OF ION-SPECIFIC NUTRIENT MANAGEMENT WITH CLOSED-LOOP CONTROL

Fig. 5.3 shows the sequence of ion-specific nutrient management. When the preset time was reached, the system conducted the ion-specific measurement using the sensor array with the two-point normalization. For the two-point normalization, two known standard solutions of low and high concentrations were injected into the sample chamber and measured by the ISE array sequentially. Then, each ISE was standardized based on the calibration equations for NO_3, K, or Ca reported in the previous study (D. H. Jung et al., 2015). After the measurements of the two-point normalization solutions, the nutrient solution was automatically sampled and transported to the chamber. The first nutrient solution sample was used to rinse the chamber to remove any residue of the previously injected solution. The second nutrient solution was measured by the ISE array and the NO_3, K, and Ca concentrations were estimated based on the two-point normalization method. Once the nutrient solution measurement sequence was finished, the two-point normalization solution of low concentration was pumped into the chamber for conditioning of the ISEs.

In order to avoid the unnecessary replenishment, the estimated NO_3, K, and Ca concentrations and the volume of the nutrient solution were judged based on the low limits that could be determined by the user. The adjustment of the excess nutrient ions in nutrient solutions is only possible if the nutrient solution is discarded or diluted by water, but it inevitably induces waste of water and nutrient. In addition, overflow of the nutrient solution could be occurred by an excessive replenishment. Therefore, the judgement on the replenishment was constructed to be triggered only by the deficiency of the measurable ions (i.e., Ca, K, and NO_3) and the current volume of the nutrient solution.

If the replenishment was triggered, the amounts of stock solutions and water to be replenished and the running times of the pumps were calculated according to the

decision tree-based dosing algorithm. Finally, the nutrient and water replenishment were conducted by operating the pumps based on the determined running times.

The proposed decision tree-based dosing algorithm is a proportional model, assuming the responses of the pumps and the mixing process in the nutrient solution would be linear. However, there would be some errors in the pump operations or concentrations of the stock solutions, so it was necessary to apply a closed-loop control scheme to the ion-specific nutrient management for more accurate replenishment. In general, the ion sensing by the ISEs takes more than 10 minutes due to the rinsing, sampling, drainage, two-point normalization, and stabilizing times for the measurements (D.-W. Kim et al., 2017). Therefore, it is difficult to apply the instantaneous feedback control to the pump operations corresponding to the ion concentrations. Alternatively, an evaluation of the management was conducted after the replenishment to achieve the closed-loop control.

The overall operation of the system was controlled by a personal computer with a program based on LabVIEW (v2015, National Instruments, TX, USA) (A5).

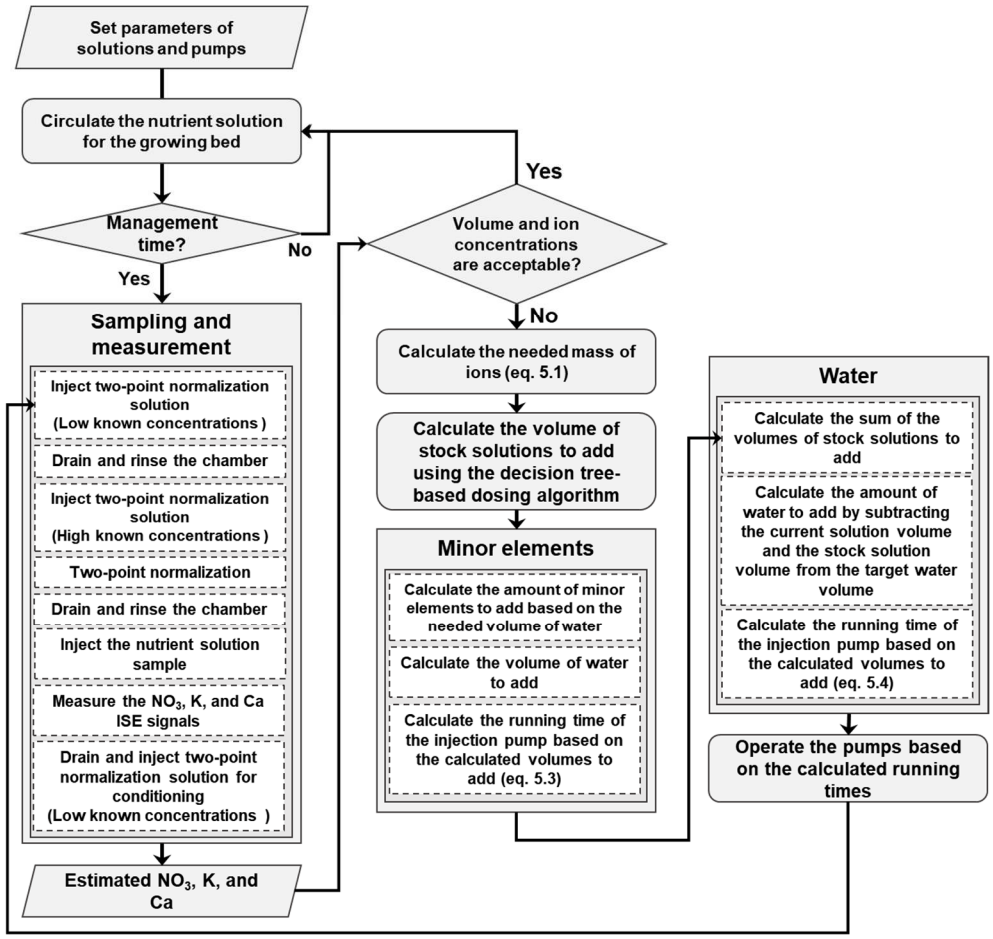

Fig. 5.3. Flow of the ion-specific nutrient management operation with the closed-loop control

SYSTEM VALIDATION TESTS

The performance of the system was validated through a stepwise management test. Specifically, the test began with a mixture of the modified Hoagland's hydroponic nutrient solution (Hoagland & Arnon, 1950). Then, the system conducted a serial of nutrient managements according to the given target concentrations of NO_3, K, and Ca, with the increasing levels of the target nutrient solution volume. The target concentrations were randomly determined with three levels of 80, 100, and 120% for the standard concentrations. The desired values for the stepwise management test are summarized in Table 5.2. After each replenishment, the nutrient solution was sampled and analyzed by a commercial

soil and water quality analysis center (NICEM, Seoul, South Korea) to determine actual concentrations using standard analyzers, i.e., ion chromatography for NO_3 and ICP spectrophotometry for K and Ca measurements. Then, the performance of the replenishment sequence was evaluated by comparing the target and actual concentrations determined by standard methods.

The automated ion-specific nutrient management was performed with the lower limits of 20% and 10% to the ion concentrations and the nutrient solution volume, respectively, for the closed-loop control. The two-point normalization solutions were prepared to have NO_3, K, and Ca ions at two different concentrations (100 and 1,000 $mg \cdot L^{-1}$, 30 and 300 $mg \cdot L^{-1}$, 24 and 240 $mg \cdot L^{-1}$, respectively) with the same background components as the nutrient solution.

To evaluate the performance of the proposed dosing algorithm, simulated calculations for the ion concentrations during the stepwise test were conducted based on the conventional simplex matrix method (Gieling et al., 2005; D. H. Jung et al., 2015)

Table 5.2. Target values of hydroponic solutions to be supplied in the stepwise test

Step	Target ion concentration ($mg \cdot L^{-1}$)			Target water volume (L)
	Ca	NO_3	K	
Initial	80	434	117	10
1st	80	347.2	93.6	15
2nd	96	347.2	117	20
3rd	64	434	140.4	25
4th	80	434	93.6	30
5th	96	520.8	140.4	40

The variation of the Ca concentration in the stepwise test was lower than that of NO_3 or K concentration so the response of the system to the Ca was investigated with more detail as follows.

1) A new nutrient solution was prepared using the used nutrient solution of Hoagland's composition.

2) 6L of water was supplied to the mixing tank to verify the system could detect

the decrease of the ion concentrations.

3) 5L of water was supplied again.

4) After the water replenishment, the target levels of water and Ca were set as the 65 L and 110 $mg \cdot L^{-1}$, respectively, then the system conducted the replenishment.

5) The system evaluated the status of the replenished solution.

6) The target volume and Ca concentration were revised as 66 L and 130 $mg \cdot L^{-1}$, respectively, then the system conducted the replenishment.

7) After the replenishment, the system evaluated the resulting solution.

During the validation, the allowable error percentages were set as 5% and 2.5% for the Ca concentration and the solution volume, respectively.

RESULTS AND DISCUSSION

FIVE-STEPWISE REPLENISHMENT TEST

For the given target concentrations of the five-steps, the system conducted the replenishment based on the developed dosing algorithm, and the NO_3, K, and Ca ions in the resulting solutions were measured by the system and the standard analyzers (Fig. 5.4).

From the Ca concentration, there was an over-injection in the 3rd step, thereby inducing the 13.6% higher resulting concentration in the 4th step (Fig. 5.4a). It would be due to the underestimation in the 3rd step. However, the Ca concentration measured by the system in the 4th step was comparable to the actual concentration, so the Ca concentration accurately followed the target concentration in the 5th step.

Although the K concentration was higher than the target value in the 4th step, it was due to the effect of the high K concentration in the previous step (Fig. 5.4b). The K concentration and the volume measured by the system in the 3rd step were 155.7 $mg \cdot L^{-1}$ and 22.52 L, which could make the K concentration of the solution as 116.88 $mg \cdot L^{-1}$ at the target volume of the 4th step without the K injection. In actual, the K concentration measured by the system was 113.8 $mg \cdot L^{-1}$, which was almost same as the expected concentration. The underestimated K concentration by 11% was appeared in the 5th step, but the closed-loop control was not conducted because

it was within the constraint of 20%.

Besides the above cases, the resulting NO_3 concentrations and the nutrient solution volumes were well followed the target values (Figs. 5.4c and 5.4d). Overall, the Ca, K, and NO_3 concentrations and volume of the nutrient solution were controlled with the average relative errors of 10.6 ±8.0%, 7.9 ±2.1%, 8.0 ±11.0%, and 4.2 ±3.7%, respectively, for the stepwise test.

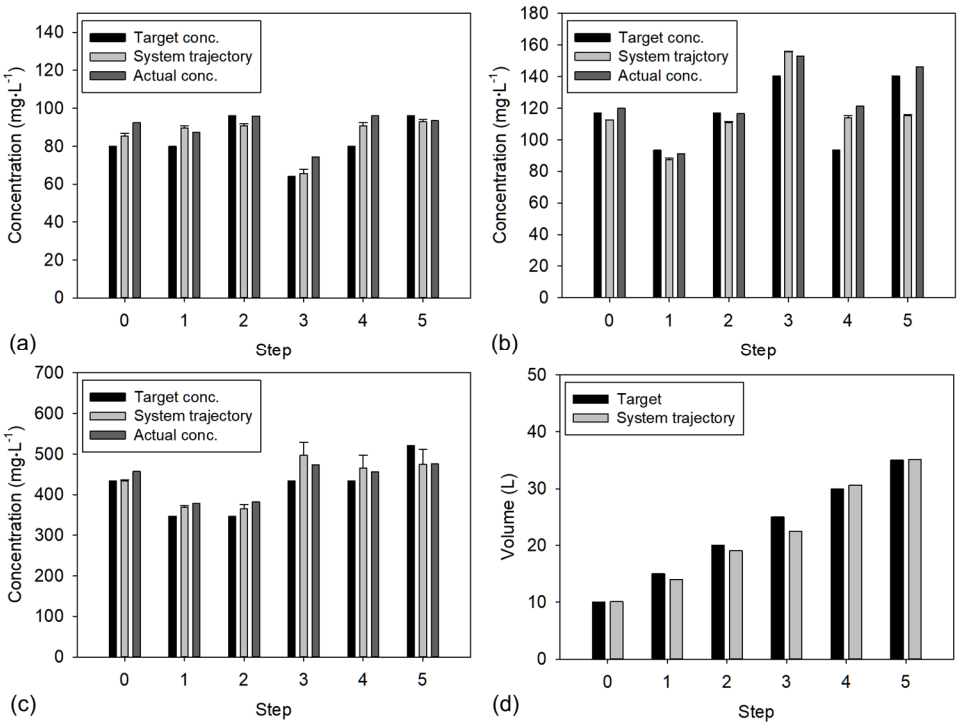

Fig. 5.4. Changes in ion concentrations and nutrient solution volume for the stepwise test: (a) Ca; (b) K; (c) NO_3; (d) Nutrient solution volume. Error bars denote the standard deviation of the multiple ISEs for NO_3, K, and Ca.

Based on the time log of the fertilizer pumps and the measured ion concentrations, the amounts of the fertilizer salts to add determined by the decision-tree method and the simplex method were obtained and compared (Table 5.3). The required volumes of the concentrated solution for minor elements were same because it was determined according to the water volume to add. The determined amounts of $Ca(NO_3)_2 \cdot 4H_2O$ and $MgSO_4 \cdot 7H_2O$ were also same for the simplex method and the decision-tree method. However, the required amounts of

KH_2PO_4, $NH_4H_2PO_4$, KNO_3, NH_4NO_3, and K_2SO_4 were differently calculated according to the dosing algorithms. Specifically, although the use of KNO_3 in the simplex method was less than the decision-tree method, the simplex method determined to use the KH_2PO_4, $NH_4H_2PO_4$, NH_4NO_3, and K_2SO_4 salts more than the decision-tree method. As the result, the total amounts of the fertilizer salts to add were higher in the simplex method than the decision-tree method.

In actual, the dosing amounts calculated from the simplex method could have negative values to make an exact solution for the given target concentrations. However, it is impossible to conduct the negative dosing for the specific ion because the pump cannot remove the nutrient salt individually. Therefore, the operation times for the pumps were just displayed as 0. However, the other salts including the same ions with the nutrient salts had the negative dosing amounts should have large amounts for the replenishment to compensate for the negative amounts of ions. Although the simplex method could be modified to calculate the approximated solution consisting of the positive numbers, it would require more complex calculation and processing times. On the other hand, the decision-tree method was operated to minimize the over-injection by the compromise of the injection mass based on the preset nutrient priority.

Fig. 5.5 shows the resulting amounts of NO_3, K, and Ca ions to add determined by the simplex method and the decision-tree method in comparison with the actual required ion mass. The calculated amounts of the Ca ion were same with the required amounts, showing both methods could make the exact solution (Fig. 5.5a). Although the over-injections of the NO_3 ions were observed in both methods due to the coupling of the NO_3 with the Ca, the amounts were slightly higher in the simplex method (Fig. 5.5b). It might be due to the effect of the negative numbers from the exact solutions by the simplex method as mentioned above. It was more obviously shown in K, showing the decision-tree method would be more feasible than the original simplex method (Fig. 5.5c)

The ion concentration measurements by the system using the ISEs showed the feasibility by the comparison of the ion concentrations determined by the system and the standard analyzers (Fig. 5.6). In terms of RMSE, the accuracies of the ISE array measurements were 29.5, 10.1, and 6.1 $mg \cdot L^{-1}$ for NO_3, K, and Ca,

respectively.

The results proved the system based on the developed dosing algorithm could effectively control the individual ion concentrations by calculating the optimal injection volumes of the seven kinds of fertilizer salts for the given target ion concentrations.

Table 5.3. Amounts of the fertilizer salts to add determined by the simplex method and the decision-tree method for the five-stepwise test

Step	Simplex method								Decision-tree method							
	Injected salts (mg)							Minor (ml)	Injected salts (mg)							Minor (ml)
	$Ca(NO_3)_2 \cdot 4H_2O$	KH_2PO_4	$NH_4H_2PO_4$	KNO_3	NH_4NO_3	$MgSO_4 \cdot 7H_2O$	K_2SO_4		$Ca(NO_3)_2 \cdot 4H_2O$	KH_2PO_4	$NH_4H_2PO_4$	KNO_3	NH_4NO_3	$MgSO_4 \cdot 7H_2O$	K_2SO_4	
1st	1983	0	223.8	0	0	1618.4	853.2	24.4	1983	81.8	152.5	0	0	1618.4	541.5	24.4
2nd	3946.7	0	337.5	0	0	557.1	2928.4	30.15	3946.7	99.9	207.9	0	0	557.1	2428.8	30.15
3rd	0	1626.5	0	4565.6	1611.6	842.8	0	29.7	0	0	21.3	4778.8	1142.8	842.8	0	29.7
4th	5443.2	0	699.1	0	0	1971.8	1353.1	37.4	5443.2	89.2	339.7	0	0	1971.8	0	37.4
5th	3412.9	901.2	0	2482.5	870.7	1066.7	474.2	21.9	3412.9	0	252	3582.3	0	1066.7	103.1	21.9
Total*	14785.8	2527.7	1260.4	7048.1	2482.3	6056.4	5608.9	143.55	14785.8	270.9	973.4	8361.1	1142.8	6056.4	3073.4	143.55
Total**	39769.6							143.55	34663.8							143.55

* Total amounts for each fertilizer salts

** Total amounts for all fertilizer salts

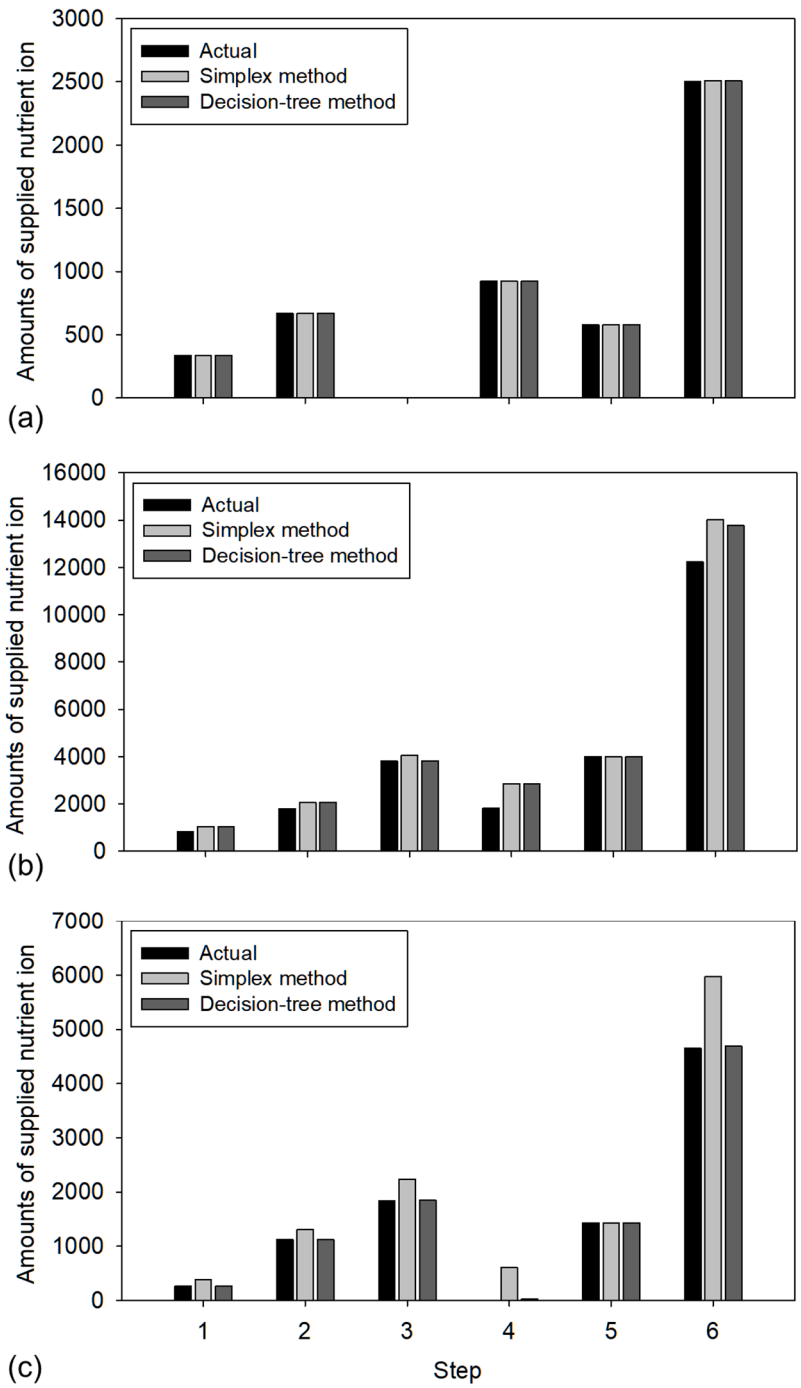

Fig. 5.5. Amounts of the three nutrient ions required for the five-stepwise replenishment: (a) Ca; (b) NO_3; (c) K

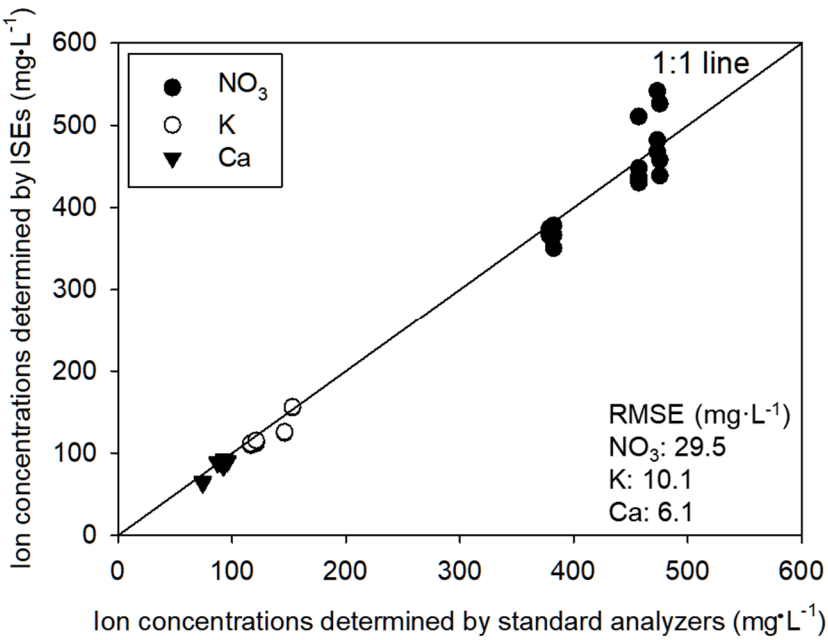

Fig. 5.6. Comparison of ion concentrations in the resulting solutions of the stepwise test predicted by standard analysis and ISEs

REPLENISHMENT TEST FOCUSED ON THE CA

Fig. 5.8 shows the NO_3, K, and Ca concentrations and the volume of the nutrient solution were changed according to the sequences. Obviously, the volume of the nutrient solution was increased corresponding to the water supplement and the replenishment sequences (Fig. 5.7a). Specifically, the volume levels of the nutrient solution were within the allowable error ranges, but the replenishments were conducted to follow the given target levels of Ca in sequences of 4 and 6.

The system noticed the changes in the ion concentrations induced by the water supplement (Figs. 5.7b, 5.7c, and 5.7d). Although the K measurement made an overestimation in sequence 3, the trends of the NO_3, K, and Ca concentrations were almost similar to the actual concentrations determined by the standard analyzers.

One of the noticeable points was the effect of the closed-loop control in sequence 4. The system conducted a replenishment for the target Ca level of 110 $mg \cdot L^{-1}$, but the first resulting solution showed 98.8 $mg \cdot L^{-1}$ of Ca concentration. The error was 10.2%, which was higher than the constraint level of 2.5%. As the

result, a closed-loop control was triggered and an additional replenishment was conducted in sequence 4 and fulfilled more accurate Ca management by reducing the relative error as 1.5%. The relative error of the volume was also reduced from -1.5% to -0.6%, though both were within the constraint of 5%. After the replenishment, the target volume and Ca concentration were revised as 66 L and 130 $mg \cdot L^{-1}$, respectively (Sequence 5).

In sequence 6, the system just checked the status of the current nutrient solution, so the measured concentrations and the nutrient solution volume must have been the same conditions in sequence 5.

Finally, the system conducted the replenishment for the given targets of 66 L and 130 $mg \cdot L^{-1}$ Ca, and the volume and Ca concentration of the resulting solution were measured as 65.8 L and 135.5 $mg \cdot L^{-1}$ of Ca. The errors of the measured volume and Ca concentrations were -0.3% and 4.2% for the target levels, respectively, so the closed-loop control was not triggered.

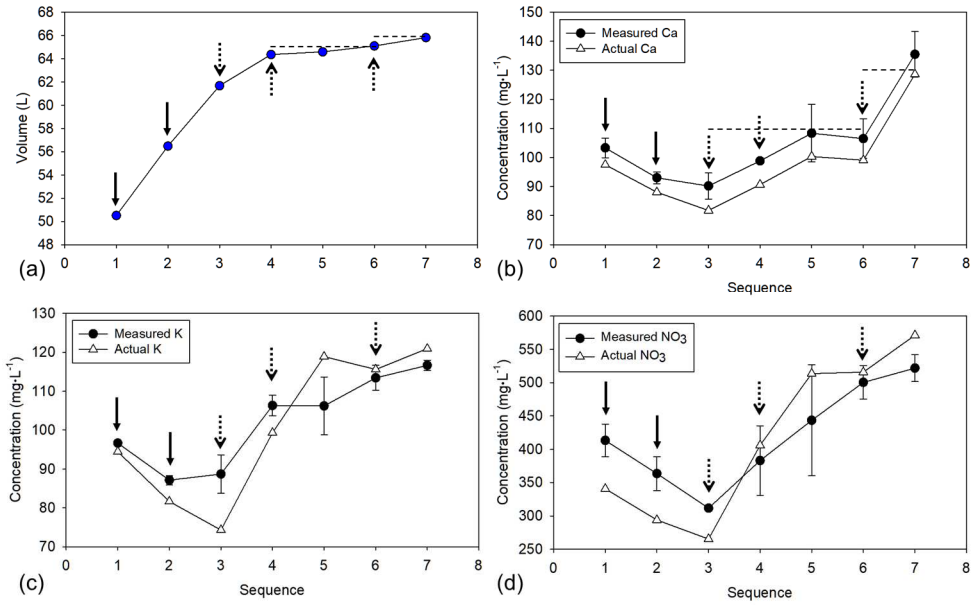

Fig. 5.7. Changes in ion concentrations and nutrient solution volume for the Ca focused replenishment test. Dash line means the target values for the sequences. Line arrow and dotted line arrow indicate the water supplement and the replenishment, respectively. Error bars denote the standard deviation of the multiple ISEs for NO_3, K, and Ca.

CONCLUSIONS

In this study, a decision tree-based dosing algorithm for closed-loop control of the hydroponic solution was developed and applied to an automated ion-specific nutrient management system with an array of NO_3, K, and Ca ISEs. The performance of the dosing algorithm was evaluated based on the five stepwise test and the Ca focused replenishment test.

In the five-stepwise test, the varied concentrations of NO_3, K, and Ca which were corresponding to the 80, 100, and 120% of the standard Hoagland's solution were randomly selected as the target concentrations while the target volume of the nutrient solution was increased. The results proved the system was able to formulate the nutrient solution within a set of given constraints that concern the individual ions using the decision-tree method. Specifically, The system controlled the ion concentrations in the nutrient solution with the average relative errors of

10.6 ±8.0%, 7.9 ±2.1%, 8.0 ±11.0%, and 4.2 ±3.7%, respectively, for the Ca, K, and NO_3 concentrations and volume of the nutrient solution. Moreover, during the test, the ISE array measurements showed the RMSEs of 29.5, 10.1, and 6.1 for NO_3, K, and Ca, respectively, indicating the measurements by the system would be feasible.

The replenishment test focusing on the Ca concentration showed the system was able to catch the variations in ion concentrations and the nutrient solution volume and actively cope with the changes to achieve the given target values. From the results, the system observed the decrease and increase of the ion concentrations according to the water supplement or nutrient salt replenishment. Specifically, when the managed Ca concentration was not reached to the ranges of the allowable level of the given target concentration 110 $mg \cdot L^{-1}$, i.e., 104.5-115.5 $mg \cdot L^{-1}$ the closed-loop control was conducted and the satisfactory result was achieved (108.3 $mg \cdot L^{-1}$). It showed the effectiveness of closed-loop control in nutrient solution replenishment.

* Note: Dae-Hyun Jung and Chan-Woo Jeon shared their knowledge to design the decision tree-based dosing algorithm. The research was financially supported by the Rural Development Administration, Republic of Korea (PJ01385203201901). I would like to express my sincere gratitude to their support.

CHAPTER 6. ION-SPECIFIC AND CROP GROWTH SENSING BASED NUTRIENT SOLUTION MANAGEMENT SYSTEM FOR CLOSED HYDROPONICS

ABSTRACT

Precision nutrient solution management in closed hydroponics is an important task to secure sustainable water and nutrient uses. However, the difficulty in assessing the water needs of the plants due to the varied plant growth and the ion balance in recycled nutrient solution hinder the establishment of the precision hydroponic nutrient solution management. In this study, a hydroponic nutrient solution management system that could variably supply the nutrient solution based on the plant-growth information while managing the ion balance of the nutrient solution was developed. In application test with the lettuces growing in the nutrient film technique, the developed system reduced the nutrient solution supply by 57.4% in comparison with the timer-based fertigation strategy, while meeting the actual daily water consumption of the plants with an error of 7.3%, when the lettuces were saturated. In addition, the promoted increasing rate of the leaf area showed the plant-based fertigation could provide higher productivity than the timer-based fertigation. During the cultivation period, the system maintained the target concentrations of 436, 117, and 80 $mg \cdot L^{-1}$ with the RMSEs of 50.6, 12.5, and 33.3 $mg \cdot L^{-1}$ for NO_3, K, and Ca ions, respectively. Although the Ca concentration higher than the target value could not be recovered by the system, the overdose of the Ca in the nutrient solution was prevented. In addition, the system showed the feasibility of the closed-loop control to accurately replenish the deficient ions, showing the daily example that the relative errors of -19, -9.9, 40.6, and -3.6% were reduced as the 4.2, 9.4, 10.1, and -0.02% for the NO_3, K, and Ca concentrations and the nutrient solution volume, respectively. The low CVs of 7.0%, 9.9%, 4.7%, 4.6%, and 17.5% for the actual NO_3, K, Ca, Mg, and P

concentrations in the nutrient solution supported the feasibility of the system in maintaining the ion balance.

INTRODUCTION

In hydroponics, fertigation (i.e., irrigation combined with fertilization) is one of the most important factors that are closely related to the crop yield and quality (Incrocci et al., 2017; P Agung Putra & Henry Yuliando, 2015). Fundamentally, fertigation is the only way for supplying the water and nutrients to plants in soilless cultivation, so it is the key factor directly related to the water and nutrient use efficiencies. Furthermore, the efficient fertigation has become more important in closed soilless cultivation because the inefficient fertigation could lead to the discharge of the reused nutrient solution, thereby inducing the environmental pollution and waste of the resources such as nutrients and water (Ahn & Son, 2019; Matthew Bamsey et al., 2012; D. H. Jung et al., 2015).

For these reasons, precision nutrient solution management, which is a technique that provides water and nutrients based on the needs of the plant, has been emerged and widely investigated in the last years (Matthew Bamsey et al., 2012; García et al., 2020; Mafuta et al., 2013; F. F. Montesano et al., 2018; Sambo et al., 2019; Smith & Baillie, 2009). Currently, there are two challenging issues for precision hydroponics: ion imbalance of the recycled nutrient solution and fertigation control based on the response of plants.

Imbalance of nutrient ions in the recycled nutrient solutions is usually occurred by the replenishment based on the electrical conductivity (EC) of the solutions, which could not provide information on the concentrations of individual ions despite the varied uptakes of the growing plants for the individual ions (Matthew Bamsey et al., 2012; Gieling et al., 2005; Zheng, 2017). Similarly, the inefficient fertigation scheduling comes from the limitations of the current sensor technology. In actual, a lack of the non-destructive, accurate, and rapid monitoring techniques

for the crop growth makes it difficult to estimate the water needs of the plants (Jiang et al., 2018; Nikolaos Katsoulas et al., 2016; Kirk et al., 2009; Sigrimis et al., 2001).

The overall goal of this research was to develop a precision nutrient solution management system that can effectively replenish the fertilizer solutions to maintain target concentrations of macronutrients based on the measurement and control of individual macronutrients while variably controlling the fertigation interval based on the plant growth by measuring the canopy cover (CC) of growing plants. Specific objectives were to (1) integrate the on-the-go crop monitoring system for the canopy cover assessment with the ion-specific nutrient measurement and replenishment system to develop a precision hydroponic system and (2) investigate the performance of the integrated system in the ion balance management and water use efficiency for the closed hydroponic lettuce cultivation.

MATERIALS AND METHODS

SYSTEM INTEGRATION

The precision nutrient solution management could be conducted by a combination of two main subsystems. One is the on-the-go crop monitoring system with the environmental sensors developed in Chapter 3, and another is the ion-specific nutrient management system developed in Chapter 5. The schematic diagram of the integrated system is shown in Fig. 6.1.

The overall process for the observations or controls of the system was programmed using LabVIEW (v2015, National Instruments, TX, USA) besides the image monitoring and processing for the CC. The image monitoring and processing were conducted based on Python 3.7.3 program with several third-party libraries (A1). After the CC measurement, the obtained CC was transferred to the LabVIEW program through a TCP/IP network. The process flow of the integrated precision nutrient solution management system is shown in Fig. 6.2. The LabVIEW program

is displayed in A5.

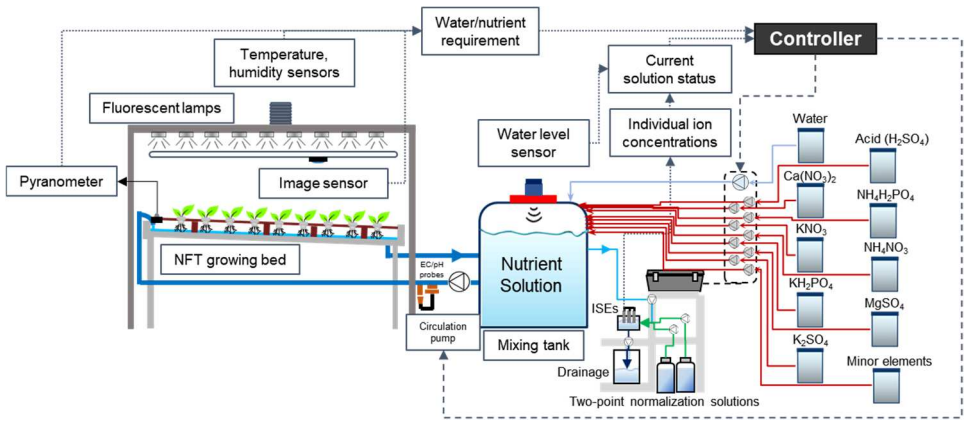

Fig. 6.1. Schematic diagram of the precision nutrient solution management system for closed hydroponics

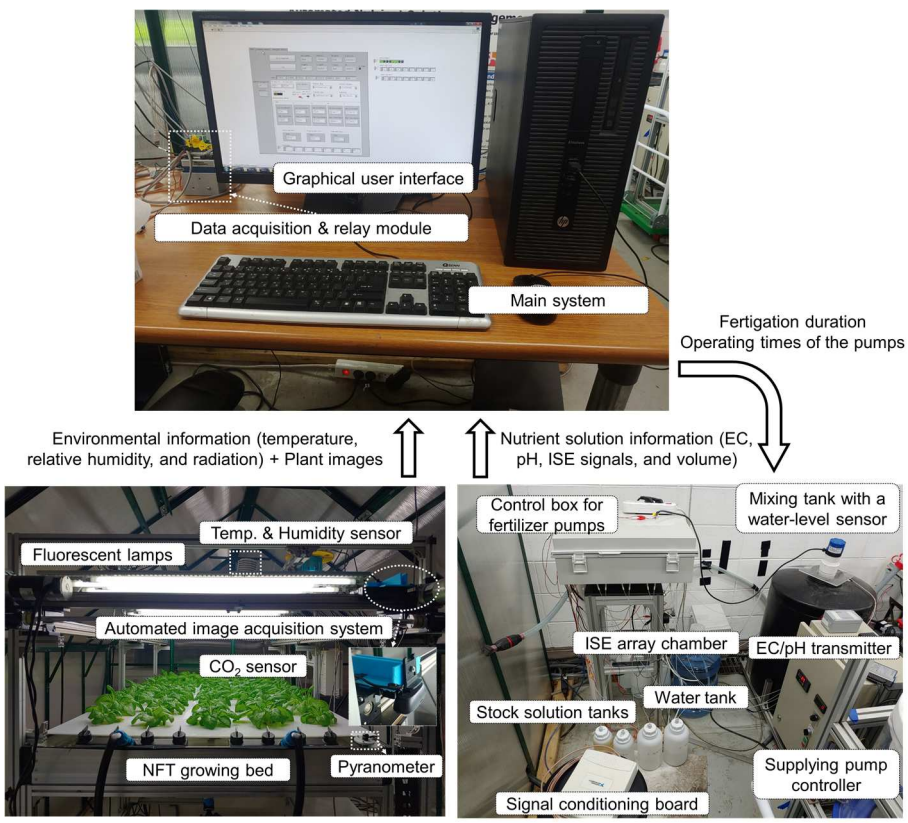

Fig. 6.2. Views of the precision nutrient solution management system with data flow

A user interface (UI) of the program was designed with three parts. At the main display, the starting time of the ion-specific management, system operation status, the standard concentrations of the two-point normalization solutions, the types of the ISEs connected to the data acquisition board, and the recently measured nutrient solution status including the concentrations of NO_3, K, and Ca, temperature, EC, and pH (Fig. 6.3a).

The second display tab shows the measured volume of the nutrient solution, constraints of the solution volume and ion concentrations for the closed-loop control, the types of fertilizer salts (i.e., $Ca(NO_3)_2 \cdot 4H_2O$, KH_2PO_4, $NH_4H_2PO_4$, KNO_3, NH_4NO_3, $MgSO_4 \cdot 7H_2O$, K_2SO_4, and minor stock solutions) for the pumps, the volume rates of the pumps for fertilizer stock solutions, water, and pH control solution, concentrations of the stock solutions, the target ion concentrations of NO_3, K, Ca, Mg, and P, the target nutrient solution volume, ratios of NO_3 to P and Mg to Ca for the proportional injections, the operation times of the pumps calculated from the dosing algorithm, and the diagnostic index based on the sensor sensitivity for the ISEs (Fig. 6.3b).

The final tap provides the setting of the number of growing plants, the fraction of drain, and the fertigation duration for the growing bed calculated based on the plant-growth information (Fig. 6.3c).

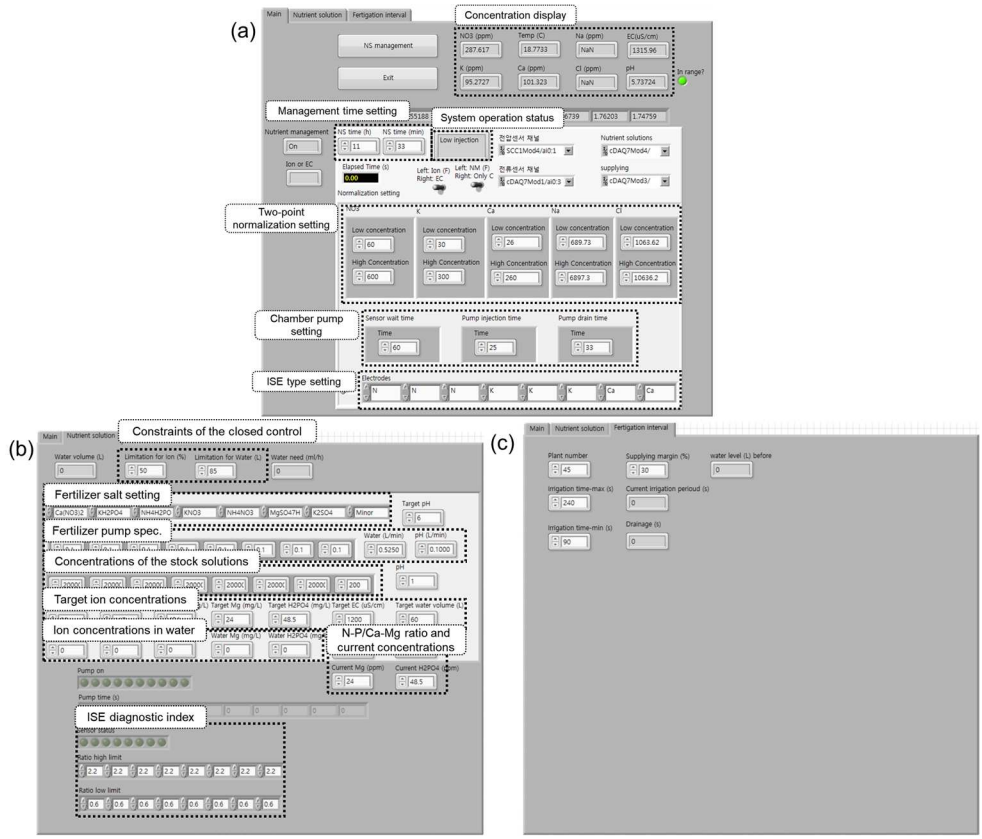

Fig. 6.3. User interface of the precision nutrient solution management system: (a) main display with the ion concentrations and the ISE settings; (b) stock solutions and pumps settings; (c) fertigation settings

IMPLEMENTATION OF THE PRECISION NUTRIENT SOLUTION MANAGEMENT SYSTEM

Fig. 6.4 shows the overall flow of the precision nutrient solution management system. The flow consisted of five separate operations, i.e., crop monitoring, aerial environment monitoring, nutrient solution circulation, nutrient solution measurement, and nutrient replenishment.

In the crop monitoring sequence, the RGB camera position was initialized to precisely move to the determined positions for the image acquisition when a preset time was reached. Then, the RGB images of the growing plants were obtained by the moving camera, and the pixels of the images were converted to the excess green (ExG). Then, the plant area was segmented based on the Otsu threshold and

the ratio of the plant pixels to the whole pixels was calculated as the CC. After the images acquisition was over, the aggregated CC values of the images were divided by the number of the images to calculate the average CC of the growing plants.

The aerial environment (i.e., temperature, relative humidity, and radiation) of the growing bed was monitored to predict the transpiration rate of the growing plants. Every 10 minutes, the average air temperature and relative humidity monitored during the time were updated and used to calculate the vapor pressure deficit (VPD). Then, the VPD and the average CC obtained from the crop monitoring sequence were applied to the transpiration rate estimation model based on the modified Penman-Monteith equation (Baille et al., 1994; J. W. Lee et al., 2013). In this study, the parameters for the lettuces determined in Chapter 3 were used.

Although the estimated E_t from the model could be assumed as the water need of the plant, several steps for the conversion of the estimated crop water need to the fertigation volume were required because the root zone of the growing plants was relatively small in comparison with the entire bed and the water uptake could be affected by the environmental conditions or the compositions of the nutrient solutions (M. Gallardo et al., 2013; Schwarz & Kuchenbuch, 1993). In this study, the complicated interactions in the plant water uptake were simplified as follows.

1) The root zone area of the growing lettuce was assumed same as the hole area and consistent during the cultivation.
2) The supplied nutrient solution was assumed to be uniformly distributed for the growing bed.
3) The root zone water potential was assumed as constant during the cultivation, so the ratio of the water uptake for the fertigation would be parameterized by a simple linear model as the previous study (Feddes, 1982; Herkelrath et al., 1977). The effects of the nutrient ion compositions or the ion concentrations were not considered.

In addition, the final fertigation volume should be higher than the volume

estimated based on the crop water need to clear out the contamination and to maintain favorable conditions in the root environment (F. Montesano et al., 2016; Rodríguez et al., 2015; Sigrimis et al., 2001). Finally, the fertigation volume to be supplied according to the estimated crop water need was defined as the following equation (eq. 6.1). The density of the nutrient solution was almost 1 $g \cdot ml^{-1}$, so the unit of the E_t could be assumed as 1 $ml \cdot h^{-1}$.

$$\text{Fertigation volume rate } (L \cdot 10\ min^{-1}) = \frac{E_t \times \frac{10}{60} \times \frac{1}{1000}}{\alpha \times \left(\frac{\pi \times d^2}{4} \div total\ bed\ area \right) \times (1-f)} \quad (6.1)$$

where α is the root water uptake coefficient for the supplied nutrient solution, d is the diameter of the growing hole, and *f* is the leaching fraction for the fertigation. In this study, α was calculated as 0.00034 by measuring the nutrient solution consumption for the fertigation during the cultivation conducted in Chapter 3. The leaching fraction (*f)* was determined as 0.25, which is suggested by Rodríguez et al. (2015).

Then, the fertigation duration was determined by dividing the pump flow rate ($ml \cdot s^{-1}$) into the estimated fertigation volume (eq. 6.2). The pump rate indicates the volume increasing rate under the holes of the growing bed when the pump is operated.

$$\text{Fertigation duration } (s \cdot 10\ min^{-1}) = \frac{Fertigation\ volume\ rate\ (L \cdot 10\ min^{-1})}{Pump\ flow\ rate\ (L \cdot s^{-1})} \quad (6.2)$$

Based on the resulting time, the fertigation system operated the fertigation pump for the determined fertigation duration. After the fertigation time had been elapsed, the system stopped the pump and waited until the update of the environmental parameters (eq. 6.3).

$$\text{Waiting time } (s \cdot 10\ min^{-1}) = 600 - fertigation\ duration \quad (6.3)$$

The nutrient solution measurement and replenishment were conducted in serial. Specifically, the nutrient solution measurement included the two-point normalization. As reported in previous studies (D. H. Jung et al., 2015; H. J. Kim et al., 2013), the two-point normalization method, consisting of a sensitivity

adjustment followed by an offset adjustment, was used to standardize the responses of multiple electrodes for each ion so that the calibration equations for each ISE developed in a previous study (D. H. Jung et al., 2015) could be applied across all electrodes of a given type. Details of the procedures and a description of the two-point normalization were provided in previous studies (D. H. Jung et al., 2015; H. J. Kim et al., 2013).

Two mixed solutions containing NO_3, K, and Ca ions at two different concentrations (100 and 1,000 $mg \cdot L^{-1}$, 30 and 300 $mg \cdot L^{-1}$, 24 and 240 $mg \cdot L^{-1}$, respectively) were used as known standard solutions of low and high concentrations to determine the slope and offset values. The concentration ranges for the NO_3, K, and Ca ions were chosen to encompass the typical concentration ranges used in hydroponic solutions in South Korea. Using this approach, any drift in the ISE signal was intermittently determined using the two normalization solutions, and the drift effect was compensated when the ISE measurement was made. After the measurement, the two-point normalization solution of the low concentrations was injected into the chamber to protect the leaching of the ions from the membranes after the sample measurement sequence was completed.

The replenishment sequence was started when the ion concentrations and the volume of the nutrient solution were lower than the preset constraints. If the status of the nutrient solution was not reached to the allowable levels of ion concentrations and volume, the decision tree-based ion-specific dosing algorithm was computed to calculate the required volumes of the fertilizer salts and determine the operating times of the fertilizer pumps and water pump for replenishment. After the replenishment, the nutrient solution measurement sequence was conducted again to evaluate the resulting solution for the closed-loop control, as described in Chapter 5.

While the nutrient solution measurement and replenishment sequences were operated, the circulation of the nutrient solution for the growing bed was stopped to

remove any effects on the measurements.

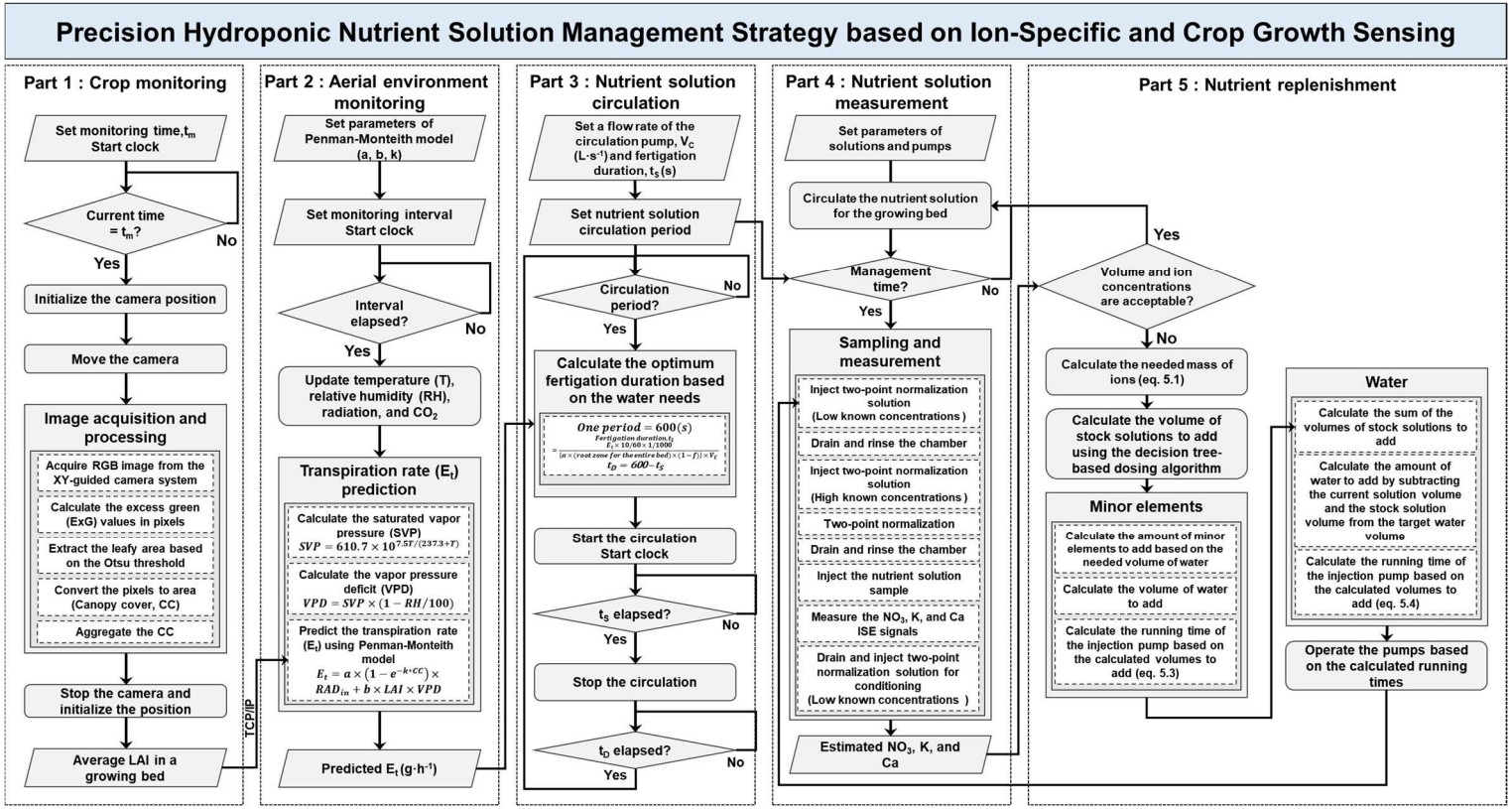

Fig. 6.4. Flowchart of the proposed precision nutrient solution management system operations

APPLICATION OF THE PRECISION NUTRIENT SOLUTION MANAGEMENT SYSTEM TO CLOSED LETTUCE SOILLESS CULTIVATION

To evaluate the performance of the system, 45 lettuces were transplanted to the experimental growth chamber where the system was applied. The lighting period was introduced as a 12h light/12h dark alternation and the crop-growth monitoring was conducted once a day, at the beginning time of lighting (i.e., 12:10 AM). The measurement and the replenishment of the recycled nutrient solution were conducted once a day, at 10:00 AM. The experiment was carried out until the CC of the lettuces were saturated. For the closed-loop control, the lower limits of 15% and 64.5L to the ion concentrations and the nutrient solution volume were applied, respectively.

For the comparison, additional cultivation was conducted based on the EC-based replenishment according to the conventional nutrient replenishment equation (eq. 6.4) (D Savvas & Manos, 1999).

$$V_T C_T = V_C C_C + V_W C_W + V_S C_S, V_T = V_C - V_W - V_S \qquad (6.4)$$

where V_T (L) is the target volume for the nutrient solution, C_T (mEq·L^{-1}) is the target total equivalent concentration, V_C is the current volume, C_C (mEq·L^{-1}) is the total equivalent concentration in the current nutrient solution, V_W (L) is the amount of tap water input to the mixing tank, C_w (mEq·L^{-1}) is the total equivalent concentration in tap water, V_S (L) is the amount of stock solution input to the mixing tank, and C_S (mEq·L^{-1}) is the total equivalent concentration of the stock solution. In this study, the total equivalent concentration was converted to EC based on the third-order relationship between EC and the total equivalent concentration of nutrient solution presented by Barradas et al. (2018).

For the two cultivation periods, subsamples of the hydroponic solutions were manually taken and sent to a standard chemical testing laboratory (NICEM, Seoul, South Korea) to determine their actual concentrations using standard methods, i.e., ion chromatography (ICS-5000, Thermo Scientific, MA, USA) for NO_3 and

inductively coupled plasma (ICP) spectrophotometry (iCAP 7400, Thermo Scientific, MA, USA) for K, Ca, Mg, and P. The actual concentrations were used to validate the performance of the ion balance maintenance by the system.

The performance of the ion balance maintenance was evaluated based on the coefficient of variation (CV) of the concentrations of Ca, K, NO_3, Mg, and P during the experimental period (eq. 6.5).

$$\mathrm{CV} = \frac{SD}{\bar{x}} \times 100, SD = \sqrt{\frac{\sum_i^N (x_i - \bar{x})^2}{N-1}} \qquad (6.5)$$

where $\bar{x}$ is the average concentration for each ion, SD is the standard deviation of the sample measurements, N is the number of sample measurement by the standard methods, and x_i is the actual concentration for each ion.

RESULTS AND DISCUSSION

EVALUATION OF THE PLANT GROWTH-BASED FERTIGATION IN THE CLOSED LETTUCE CULTIVATION

Fig. 6.5 shows the monitored environmental conditions and plant-growth information during the lettuce cultivation. The behavior of the air temperature was almost similar to the radiation, indicating the fluorescent lamps would generate heat (Figs. 6.5a and 6.5e). Also, it can be observed that the estimated transpiration rate and fertigation volume were small when the CC of the growing lettuces was small (Figs. 6.5f, 6.5g, and 6.5h). From the CC data, the growth of the lettuces could be observed until DAT 17 (Fig. 7.5f). However, after DAT 17, the CC value was almost steady, indicating the lettuces would be saturated and waited for the harvest.

The fertigation volumes from DAT 17 to DAT 20 were varied during the day-time despite the almost same CC, which would be affected by the radiation and the VPD (Figs. 6.5d, 6.5e, and 6.5h). It means the proposed fertigation system could cope with the varying lighting conditions by distinguishing the day and night and

considering the ambient conditions.

To validate the effectiveness of the plant growth-based fertigation, the daily fertigation volume for the last day of the experimental period (DAT 21) was compared with the volume simulated from the timer-based fertigation of 3 min on/7 min off cycle (Fig. 6.6). In the case of the timer-based fertigation, the fertigation volume would be consistent and the over-fertigation occurred during the period (Fig. 6.6a). On the contrary, the plant-based fertigation variably supplied the nutrient solution during the day, significantly reducing the cumulative water use (Fig. 6.7b). The results indicate the timer-based fertigation cannot respond to the changes in the weather conditions, which would cause the over- or under-fertigation. In addition, the daily cumulative fertigation volume, which is directly related to the water use efficiency of the fertigation, shows the plant-based fertigation would use much lower nutrient solution than the timer-based fertigation (Fig. 6.6b).

In actual, the effective fertigation volume of the developed system, which was obtained by multiplying the root water uptake coefficient for the supplied nutrient solution, was 2.06 L, but the simulated fertigation volume of the timer-based fertigation method was 4.84 L for DAT 21. It means the developed system could reduce the 57.4% of the nutrient solution in comparison with the timer-based fertigation. Although the timer-based control could reduce the supplied nutrient solution by adjusting the fertigation on/off cycle, it is inevitable the under-fertigation or over-fertigation would be inevitable during the overall growing period due to the varying crop water requirements. In addition, the reduction of the nutrient solution in the tank during the DAT 21 was 1.92 L, which would be regarded as the actual water consumption for growing the plants. Compared to the value, there was only 7.3% of error in the estimated water consumption from the plant-based fertigation, showing the proposed method was well followed the actual water need of the plants. Table 6.1 summarizes the expected water consumptions

by the growing lettuces determined from the plant-based fertigation, the timer-based fertigation, and the water-level sensor for the DAT 21.

The average CCs during the experimental period are displayed with the average CCs of the lettuces cultivated by the timer-based fertigation in Chapter 3 to compare the performance of the system on the growth (Fig. 6.7). The CC of the plant-based fertigation was saturated in DAT 17. However, the CC of the timer-based fertigation was saturated in DAT 23, indicating the growth rate of the timer-based fertigation was lower than the plant-based fertigation despite the over fertigation. It might indicate that the fertigation volume meeting the plant demand would be more effective in crop productivity, as reported in the previous study (Liu & Xu, 2018).

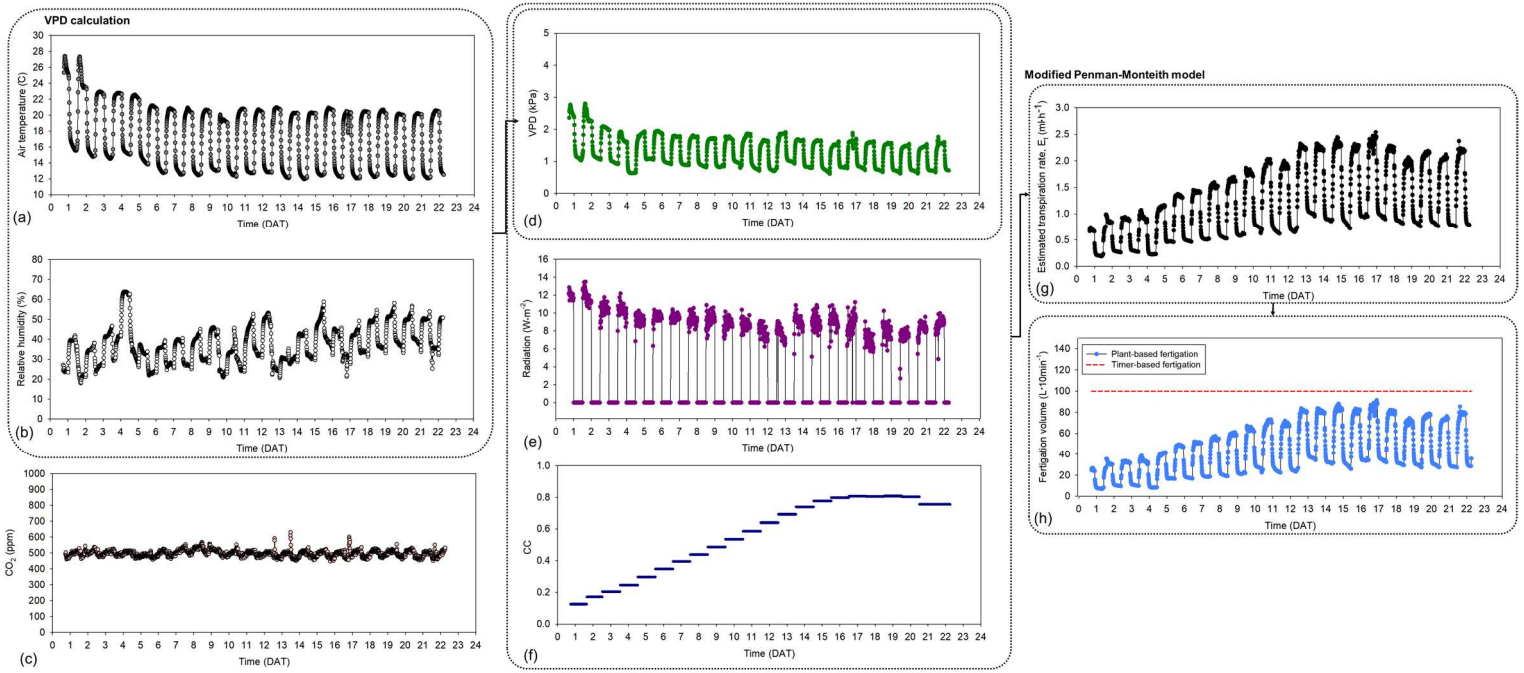

Fig. 6.5. Environmental conditions and the plant-growth information monitored by the system during the lettuce cultivation: (a) air temperature; (b) relative humidity; (c) CO_2 concentration; (d) VPD calculated from the temperature and relative humidity; (e) radiation; (f) CC; (g) estimated transpiration rate; (h) the determined fertigation volume

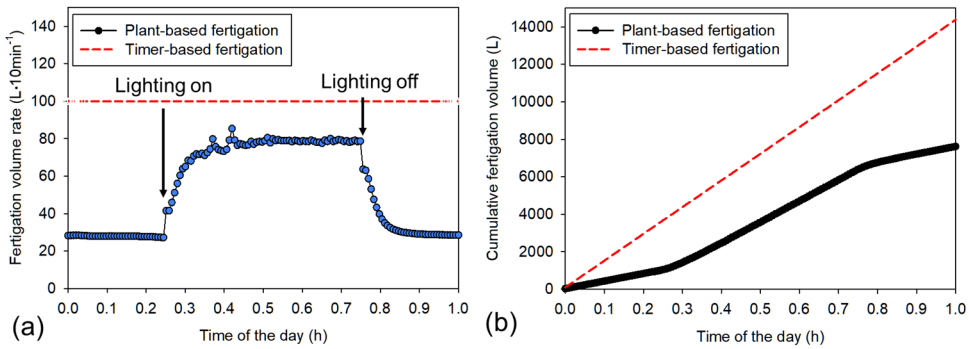

Fig. 6.6. Comparison of the plant-based fertigation proposed in this study and the conventional timer-based fertigation (simulation) during the DAT 21 in terms of the fertigation volume (a) and the cumulative fertigation volume (b)

Table 6.1. The expected uptake volumes according to the plant-based fertigation, the timer-based fertigation, and the actual consumption for the DAT 21

Method	Plant-based fertigation	Timer-based fertigation	Actual consumption
Volume (L)	2.06	4.84	1.92
Accuracy error (%)	7.3	152.1	-

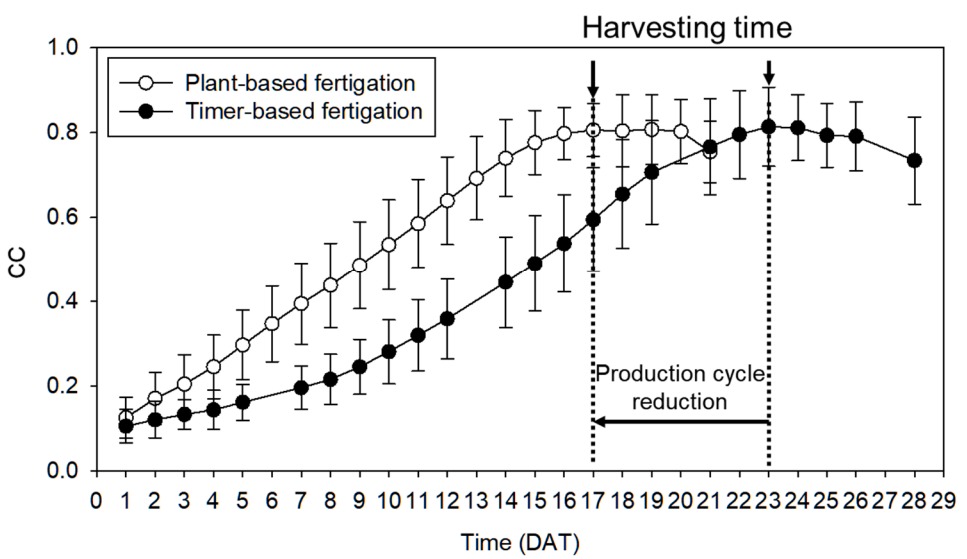

Fig. 6.7. Comparison of the average CCs from the plant-based fertigation and the timer-based fertigation. Error bars denote the standard deviation of the analyzed frames. Arrows indicate the CC saturation time.

EVALUATION OF THE ION-SPECIFIC MANAGEMENT IN THE CLOSED LETTUCE CULTIVATION

Fig. 6.8 shows changes in the ion concentrations measured with the ISE array of the system for NO_3, K, and Ca (Fig. 6.8a), the amounts of six nutrient ions replenished (Fig. 6.8b), and the volume of hydroponic solution contained in the mixing tank (Fig. 6.8c) during the growing period.

On the first day, about 60 L of the hydroponic solution was prepared manually, and the remaining volume for the target volume of 65 L was replenished automatically by the system. After the replenishment, the concentrations of Ca and NO_3 were slightly over the target concentrations. In addition, the Ca concentration in the nutrient solution was higher than the target value in most cases (Fig. 6.8a). Possible causes for the high Ca concentration of the nutrient solution might be the over-injection of the $Ca(NO_3)_2 \cdot 4H_2O$ salt and the Ca in water used for replenishment. In actual, the concentration of the $Ca(NO_3)_2 \cdot 4H_2O$ stock solution was higher than the expected (A4). As the result, the RMSEs of NO_3, K, and Ca were 50.6, 12.5, and 33.3 $mg \cdot L^{-1}$, respectively, for the target concentrations, showing the RMSE of Ca was relatively high considering the target concentration of 80 $mg \cdot L^{-1}$. The result showed the limitation of the dosing algorithm that could not conduct the dilution.

However, the system could reduce the unnecessary injection of the fertilizer salts. In actual, the fertilizer salts were almost not injected for DAT of 2~5, 10, 16, 18, and 19 because the system calculated the contents of the ions in the solution would be sufficient to achieve the target values after the water replenishment. Besides, the system showed it could effectively replenish the nutrient solution for each deficient nutrient based on the measurement of individual nutrient concentrations. Specifically, four days of the study period (i.e., DAT 3, 5, 15, and 17) when the closed-loop control was operated showed that the system could manage the nutrient solution more accurately.

As an example, Fig. 6.9 shows the daily result of the ion-specific nutrient management for DAT 15. In control step 1, the system measured the ion concentrations in the nutrient solution and the relative errors of NO_3, K, and Ca concentrations and volume were -15.9, -6.5, 45.9, and -3.6%, respectively, which were less than the lower limits of the NO_3 and nutrient solution volume. Therefore, the system calculated the mass of each ion and water to rehabilitate the nutrient solution as the target condition (Fig. 6.9a). Then, the injection pumps were operated to supply the calculated amounts of nutrient ions and water to the mixing tank (Figs. 6.9b and 6.9c).

After the replenishment, the system rechecked the ion concentrations of the resulting solution (step 2). In step 2, the ion concentrations were well managed within the lower limits, but the relative error of the nutrient solution volume was still larger than the limit of 64.5L (-0.77%) for the closed-loop control (Fig. 6.9c). Therefore, an additional replenishment was triggered. Finally, the measured relative errors of NO_3, K, and Ca concentrations and volume in step 3 were 4.2, 9.4, 10.1, and -0.02%, respectively, so the replenishment was stopped. The changes of the NO_3, K, and Ca concentrations and nutrient solution volume according to the closed-loop controls are summarized in Table 6.2.

As a result of the ion-specific management by the system, the average concentrations of NO_3, K, and Ca were 445.6, 116.6, and 108.9 $mg \cdot L^{-1}$, respectively, which were comparable to the target concentrations.

Fig. 6.10 shows changes in EMFs obtained with two-point normalization solutions (the high and low concentrations for NO_3 (Fig. 6.10a), K (Fig. 6.10b), and Ca (Fig. 6.10c), respectively) during the experimental period. As shown in the figures, the EMFs were varied over time, but the differences between the low and high concentration solutions, i.e., sensitivities, were nearly constant. The results mean the two-point normalization would be effective to improve the accuracy of the measurements by compensating for the drifting behaviors over time.

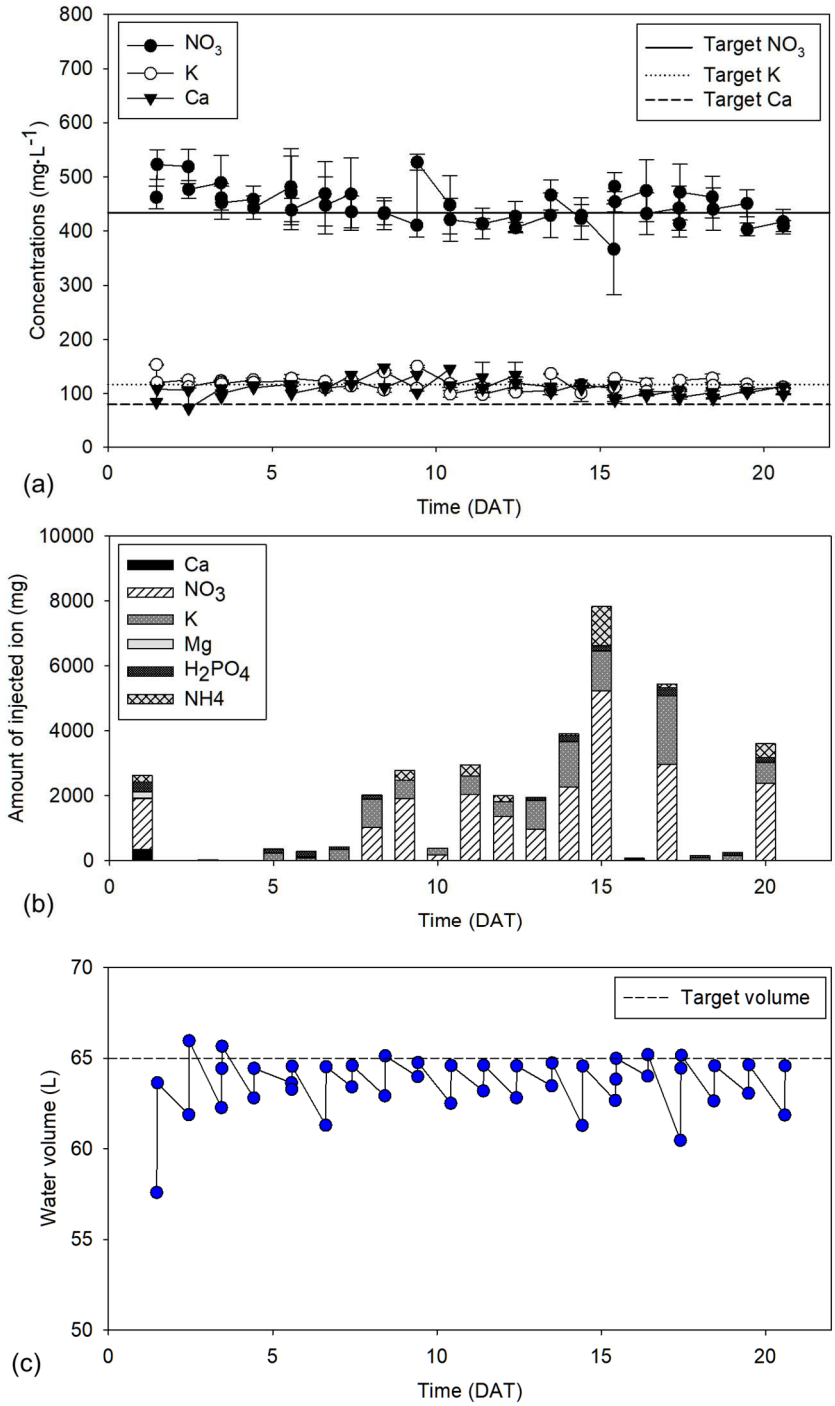

Fig. 6.8. Changes in ion concentrations measured by the system (a), the calculated injection mass of the individual ions from the stock solutions (b), and the volume of the nutrient solution (c) during the 20-day lettuce growing period

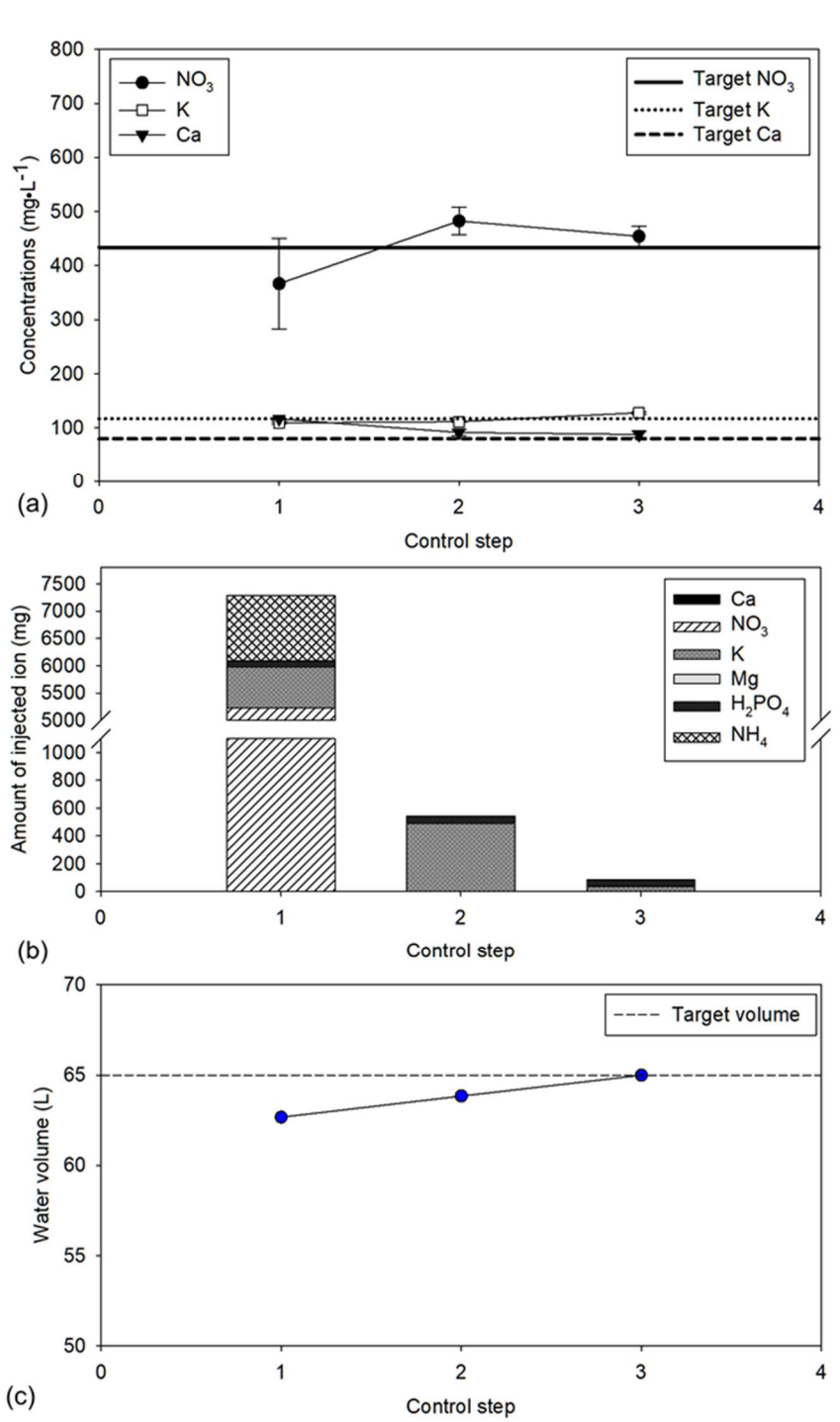

Fig. 6.9. Changes in ion concentrations measured by the system (a), the calculated injection mass of the individual ions from the stock solutions (b), and the volume of the nutrient solution (c) during a day of DAT 15

Table 6.2. Changes in the ion concentrations and the nutrient solution volume measured by the system for the closed-loop control

DAT	Control step	Concentrations of the ions ($mg \cdot L^{-1}$)*			Nutrient solution volume (L)*
		NO_3	K	Ca	
3	1	489.3 (12.2%)	124.1 (6.1%)	109.6 (37.0%)	62.3 (-4.2%)
	2	461.4 (5.8%)	121.2 (3.6%)	93.6 (17.0%)	64.4 (-0.9%)
	3	452.4 (3.8%)	118.1 (1.0%)	100.53 (25.7%)	65.7 (1.0%)
5	1	481.8 (10.5%)	124.0 (5.9%)	117.6 (47.0%)	63.6 (-2.1%)
	2	471.1 (8.1%)	116.7 (-0.3%)	109.4 (36.8%)	63.3 (-2.6%)
	3	438.9 (0.7%)	128.4 (9.8%)	100.1 (25.2%)	64.6 (-0.7%)
15	1	366.7 (-15.9%)	109.4 (-6.5%)	116.7 (45.9%)	62.67 (-3.6%)
	2	482.7 (10.7%)	111.5 (-4.7%)	91.5 (14.4%)	63.83 (-1.8%)
	3	454.4 (4.2%)	128.0 (9.4%)	88.1 (10.1%)	64.99 (-0.02%)
17	1	442.7 (1.5%)	103.9 (-11.2%)	106.6 (33.2%)	60.5 (-7.0%)
	2	414.1 (-5.0%)	105.8 (-9.6%)	91.6 (14.5%)	64.4 (-0.9%)
	3	472.0 (8.3%)	124.6 (6.5%)	93.1 (16.4%)	65.2 (0.2%)
Target value		436	117	80	65
Lower limit		370.6 (-15%)	99.5 (-15%)	68 (-15%)	64.5 (-0.77%)

* The percentage in parenthesis indicate the relative error to the target value.

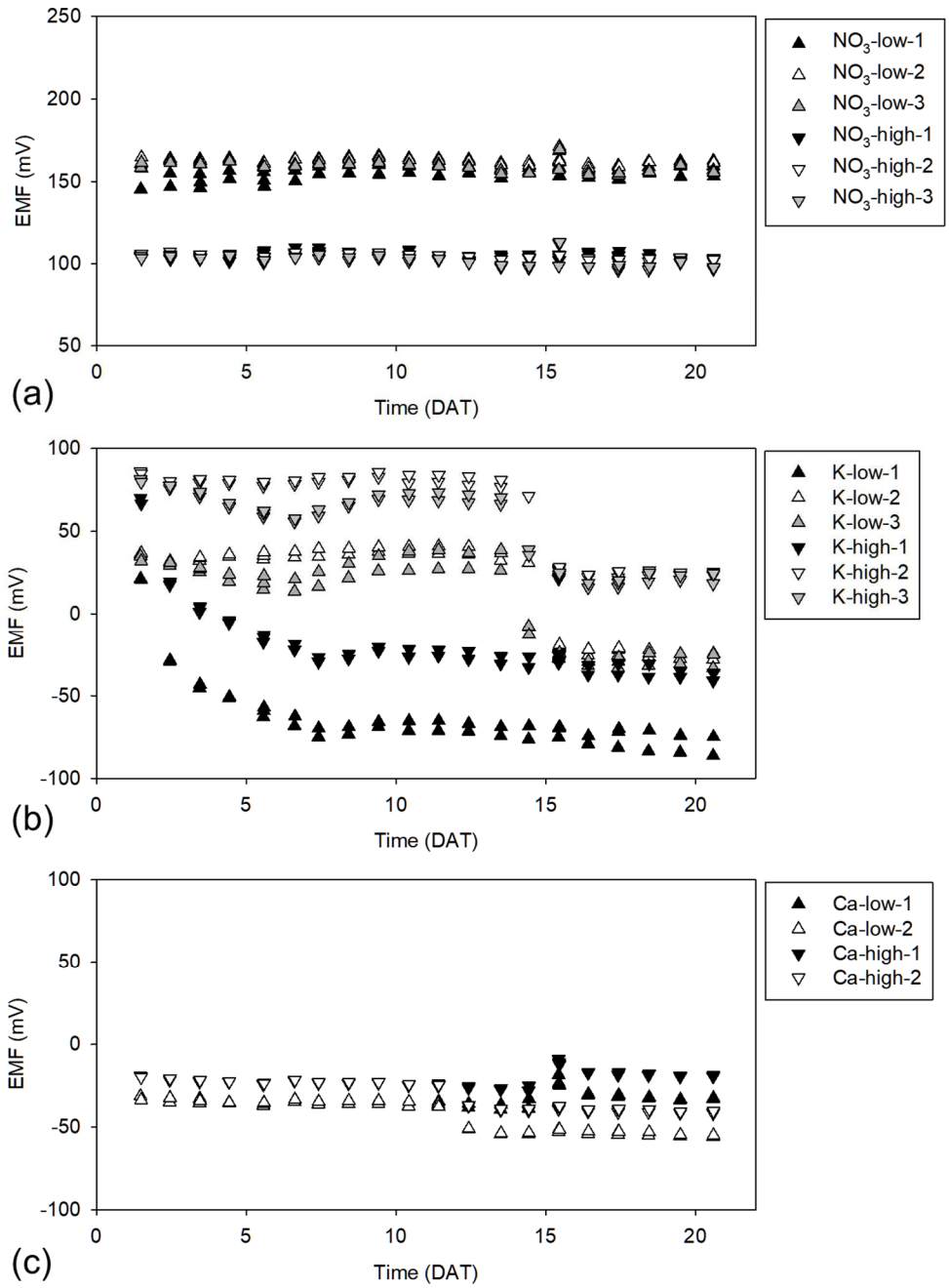

Fig. 6.10. EMF responses for the two-point normalization solutions during the experimental period: (a) the responses of three NO_3 ISEs; (b) the responses of three K ISEs; the responses of two Ca ISEs. 'Low' and 'High' in legends indicate the EMF values from the low and high concentrations of two-point normalization solutions.

Fig. 6.11 shows the trend of the ion balance based on the actual ion concentrations of NO_3, K, Ca, Mg, and P present in the hydroponic solutions managed by the EC-based replenishment and the ion-specific replenishment. During the cultivation, the EC-based replenishment showed the CVs of 6.9%, 4.9%, 23.7%, 8.6%, and 8.3% for NO_3, K, Ca, Mg, and P concentrations, respectively. In the case of the ion-specific replenishment, the CVs of NO_3, K, Ca, Mg, and P concentrations were 4.9%, 1.4%, 3.2%, 5.2%, and 14.9%, respectively. Although the CV of the P from the ion-specific replenishment was slightly higher than the EC-based replenishment, the P ratio was the smallest among the five nutrient ions so the CV could be increased by the small changes. On the other hand, the CV of the K ratio, which was the second-largest ratio among the five nutrient ions, showed a higher value in the EC-based replenishment. The comparative results of the EC-based replenishment and the ion-specific replenishment for the CVs of the five macronutrient ions in the nutrient solutions are summarized in Table 6.3.

Specifically, the Mg and P concentrations, which were controlled based on the linear relationships in the ion-specific replenishment, were managed as 29.9 ±1.4 $mg \cdot L^{-1}$and 10.2 ±1.8 $mg \cdot L^{-1}$, respectively, showing they were maintained at constant levels comparable to the conventional EC-based replenishment (Mg: 31.6 ±2.2 $mg \cdot L^{-1}$ and P: 13.1 ±0.7 $mg \cdot L^{-1}$) (Fig. 6.12).

The EC and pH of the nutrient solution were more varied in the ion-specific management, showing the CVs of 5.9% and 5.4% with the average values of 1.32 $dS \cdot m^{-1}$ and pH 5.7, respectively, while the CVs of the EC and pH managed by the EC-based replenishment were 1.1% and 2.7% with the average values of 1.393 $dS \cdot m^{-1}$ and pH 6.9, respectively (Figs. 6.13a and 6.13b). The result showed the conventional EC-based replenishment could maintain the EC of the nutrient solution successfully. However, the accumulation of the SO_4 obviously was not considered in the EC-based replenishment (Fig. 6.13c), thereby inducing the ion

imbalance as reported in the previous studies (M. T. Ko et al., 2013; Sambo et al., 2019; Zekki et al., 1996).

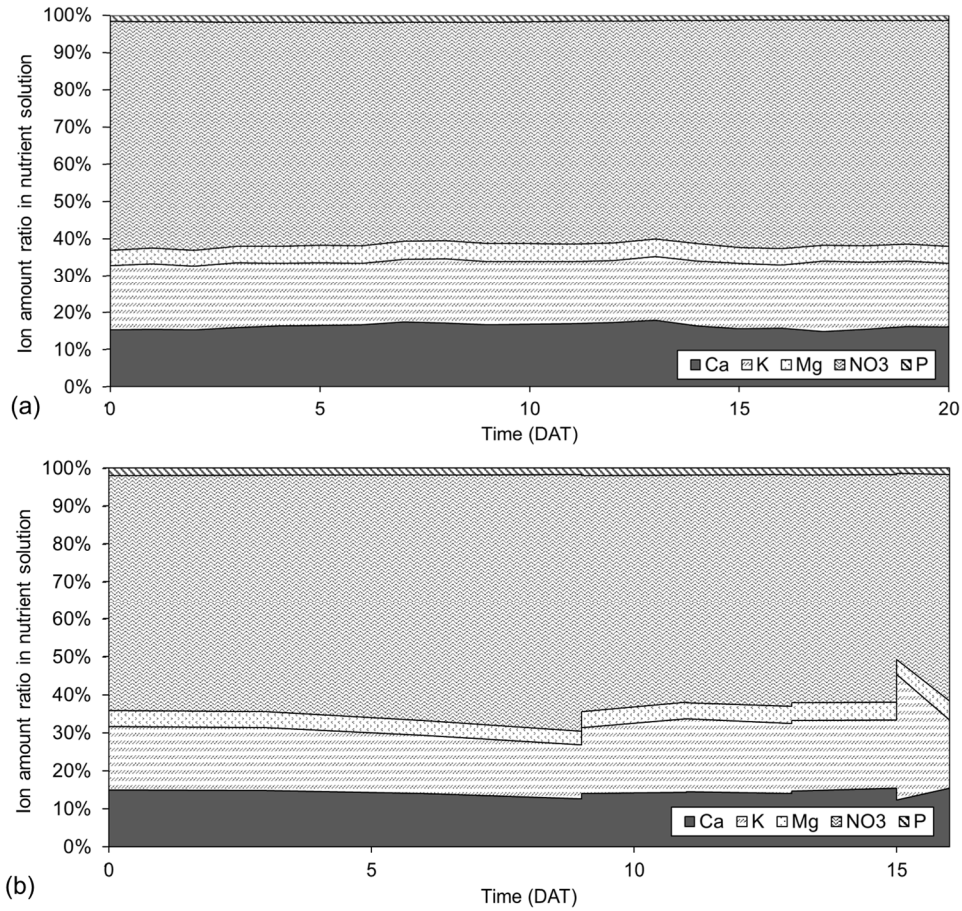

Fig. 6.11. Changes in ion ratios in the nutrient solutions managed by (a) the ion-specific replenishment and (b) the EC-based replenishment

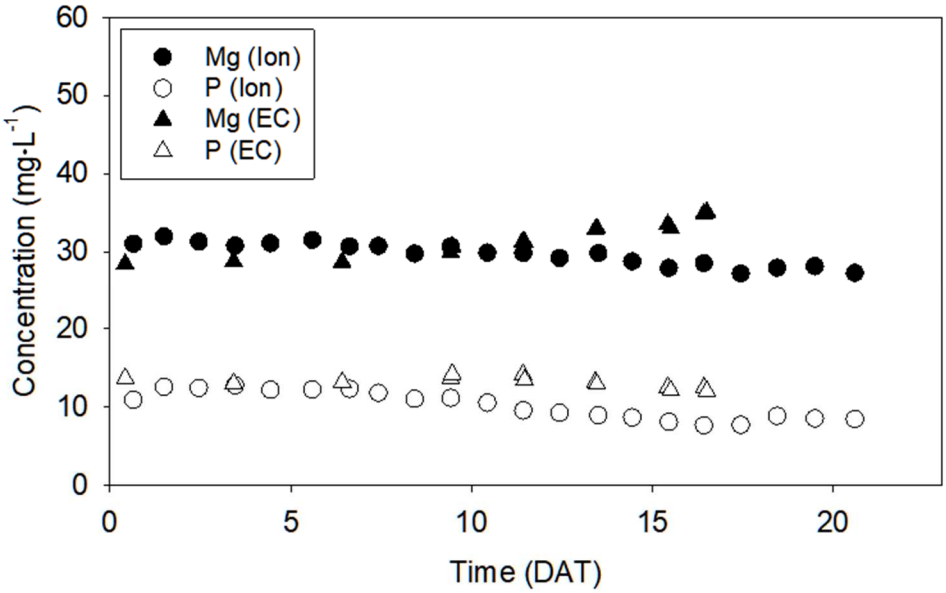

Fig. 6.12. Changes in Mg and P concentrations under the ion-specific replenishment and the EC-based replenishment

Table 6.3. Comparison of the nutrient ion balances in the nutrient solutions managed by the EC-based replenishment and the ion-specific replenishment*

Nutrient ion	Ca		NO_3		K		Mg		P	
	EC	Ion	EC	Ion	EC	Ion	EC	Ion	EC	Ion
Initial ratio (%)	15.0	15.2	62.1	61.6	16.7	17.6	4.2	4.2	2.0	1.5
Average ratio (%)	14.4	16.2	60.8	60.1	18.6	17.5	4.3	4.6	1.8	1.6
Maintenance (CV, %)	6.9	4.9	6.6	1.4^{++}	23.7	3.2^{++}	8.6	5.2^{+}	8.3	14.9

* Statistical differences were calculated by using Student's paired t-test ($^{+}P<0.05$: $^{++}P<0.01$)

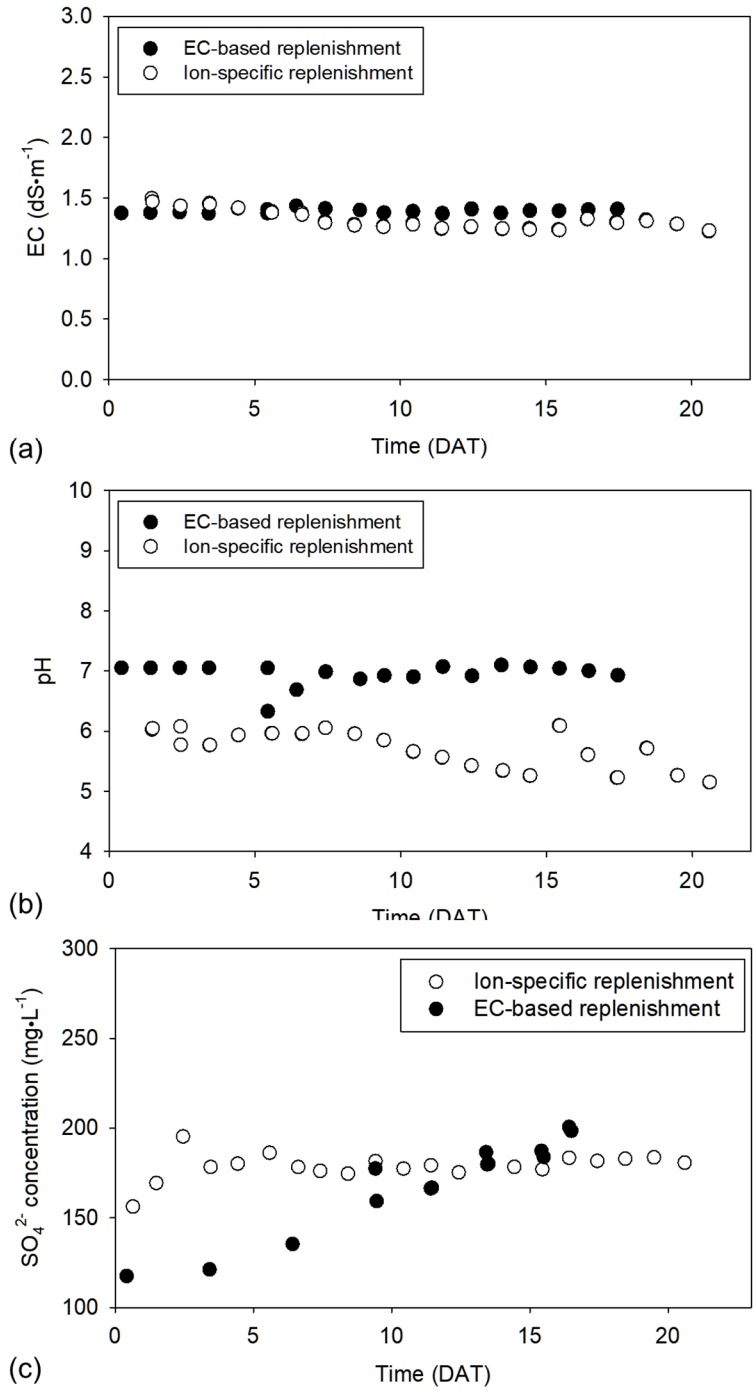

Fig. 6.13. Changes in (a) EC and (b) pH monitored by the system and (c) SO_4 concentration under the ion-specific replenishment and the EC-based replenishment

CONCLUSIONS

In this study, a precision nutrient solution management system that could both variably control the fertigation volume based on the ambient condition and the plant-growth information and correct each deficient nutrient ion based on the measurement of individual nutrient concentrations was developed and the performance of the system was evaluated by the application test in closed lettuce soilless cultivation.

Regarding the fertigation duration, the developed system succeeded in controlling the fertigation time according to the varied ambient conditions of the VPD and the radiation as well as the growth of the lettuces. In the intensive investigation of the DAT 21, the system proved the supplied nutrient solution volume could be reduced by 57.4% in comparison with the timer-based fertigation strategy, showing an error of 7.3% in estimating the daily water consumption of the plants. In addition, the reduced growing period for the CC saturation implied the plant-based fertigation could provide more yields than the timer-based fertigation by shortening the growing period.

The individual ion concentrations in nutrient solution were well maintained based on the measured ion concentrations using an array of ISEs in conjunction with a newly developed decision tree-based nutrient dosing algorithm for growing lettuces in closed hydroponic systems. Although the Ca concentration higher than the target value showed the limitation of the system in dilution of the solution, the system minimized the overdose of the Ca in the nutrient solution and proved it was able to accurately replenish the deficient ions through the closed-loop control loop. In particular, the trend and the CVs of the ion balances obtained from the nutrient solutions showed that the developed system was able to maintain the five ion balances more constantly than the conventional EC-based replenishment while recycling the nutrient solution over the growing period despite the absence of the Mg and P sensors.

* Note: Yoon-Hong Yi provided technical assistance for lettuce cultivation. The research was financially supported by the Rural Development Administration, Republic of Korea (PJ01385203201901). I would like to express my sincere gratitude to their support.

CHAPTER 7. CONCLUSIONS

CONCLUSIONS OF THE STUDY

In this study, a precision nutrient solution management system that can variably control the fertigation duration according to the crop water needs based on the canopy cover and replenish the deficient ions and water for the recycled nutrient solution based on a sensor array of NO_3, K, and Ca ion-selective electrodes (ISEs) was developed. Conclusions based on the results are:

1) An on-the-go crop monitoring system was constructed and proved that it could collect the images of the growing lettuces over the entire growing bed and compute the canopy cover (CC) with the accuracy of 98.5 ±1.7% during the vegetative growth period. Furthermore, the transpiration rates of the growing lettuces were successfully characterized based on the modified Penman-Monteith equation. Specifically, the modified Penman-Monteith equation was calibrated using the automatically updated CC, radiation, air temperature, and relative humidity and showed strong predictability for the transpiration rate, which had a highly linear relationship for the directly measured transpiration rates, showing a slope of 0.91, coefficient of determination (R^2) >0.9, and standard error of the regression (SER) of <0.51. The results proved the on-the-go crop monitoring system would enable the simple and fast assessment of the water needs of the growing lettuces.
2) Three types of signal processing methods, i.e., two-point normalization (TPN), artificial neural network (ANN), and a hybrid method combining the TPN and the ANN, were evaluated for the predictability of the NO_3, K, and Ca ISEs in hydroponic solution. The hybrid method showed the best accuracy in measuring ion concentrations in hydroponic solutions, but the vulnerability to the sensor malfunction may induce errors in nutrient solution monitoring and replenishment that require the long-term use of the ISEs.

Therefore, the two-point normalization-based compensation was selected as the applicable method for ion-specific monitoring and replenishment.

3) A decision tree-based approach for calculating the required fertilizer salts to replenish the recycled hydroponic solutions while minimizing the accumulation or deficiency of the ions was developed and validated. The successful formulation of the nutrient solution for the given target ion concentrations and the nutrient solution volume in the two-validation tests supported the proposed dosing algorithm could efficiently determine the fertilizer salts to be replenished. Furthermore, the closed-loop control showed it could allow more accurate ion-specific management.
4) A precision nutrient solution management that variably controls the fertigation volume based on the crop water needs and replenishes the deficient nutrients based on the individual ion concentrations was applied for the NFT-based lettuce cultivation using the on-the-go crop image monitoring system and the ion-specific nutrient management system. The application test showed the capability of variably controlling the fertigation volumes based on the varied canopy cover and the environmental conditions. Specifically, the estimated fertigation volume calculated from the estimated crop water need was comparable to the actual water consumption, indicating the appropriate volume of the nutrient solution would be supplied to the growing lettuces. Furthermore, the nutrient ion balance in the nutrient solution was maintained by the system over the lettuce growing period, showing the less CVs in ion concentrations of NO_3, K, Ca, and Mg than the EC-based replenishment. The system could variably supply the nutrient solution according to the crop water need and prolong the lifespan of the recycled nutrient solution, thereby allowing more efficient water and nutrient use in closed hydroponics.

Although the general objectives of the study were accomplished, the proposed plant-based fertigation strategy was established based on the 2D canopy cover-based crop water need estimation. Therefore, it would be only feasible for shoots or leafy vegetables in the vegetative growth stage, which have relatively low heights and complexity in water and nutrient uptakes. On the other hand, the ion-specific monitoring and replenishment can be used for any mixing tank, so it would be feasible for most closed hydroponic methods such as DFT, NFT, drip system, or aeroponics. The comparison of the conventional system and the developed system is summarized in Table 8.1.

Table 7.1. Comparison of the conventional system and the developed system

Category	Limitations of the conventional systems	Strength of the developed system in this study	Applicable system	On-going issues
Nutrient solution management	● Lack of information about the individual ion concentration and balance ● Impossible to correct the deficiency of each ion ● Short nutrient solution lifespan due to ion imbalance	● NO_3, K, Ca monitoring ● Correction of each deficiency of NO_3, K, Ca while managing Mg, P, and Minor elements ● Increased nutrient solution lifespan	● NFT (nutrient film technique) ● Aeroponics ● DFT (deep flow technique) ● Ebb and flow ● Drip system	● Need of the mixing tank (Batch-tank) ● Complicated system (increased number of stock solution tanks and sensors) ● Limited ion sensing (Mg, P) ● No active control for the over-concentrated ions
Fertigation scheduling	● No considerations for the varied plant water uptake ● Indirect relationship to the plant responses ● Lack of consideration for the spatial variability in plant growth	● Variable fertigation according to the canopy cover and the environmental conditions ● On-the-go monitoring for entire growing crops	● Transplant production system ● Plant factories or greenhouses growing the leafy vegetables with short heights	● No consideration for the complex interactions of the growing stage, root growth, ion compositions in nutrient and water uptakes by crops ● Spatial limitation (Increase of processing time and hardware for the spacious bed, need of installation space) ● Lack of information about the varied crop nutrient need

SUGGESTIONS FOR FUTURE STUDY

Based on the results obtained from this study, future studies are recommended as follows:

1) The water needs of plants are varied according to the growth stages or the plant species. However, the CC is insufficient to provide the crop water needs varied with the growth stages or the specific plant species. Further researches on remote sensing and image processing techniques for other effective parameters that can allow more accurate and precise crop water need estimation for the varying growth stages and species are necessary for more efficient water uses in hydroponics.
2) The simplifications in the conversion of the estimated transpiration rate to the fertigation volume would induce errors in fertigation. In addition, the experimental hydroponic system used in this study was conducted without water-holding substrates. Therefore, further investigations are needed for the application of the system to the other cultivation methods, specifically in the substrate culture method, which is mainly used for the fruit vegetables or the transplant production systems because the varied water holding capacity of the substrates or the water transfer efficiency should be considered in the conversion of the crop water needs to the fertigation duration.
3) To develop robust, and highly selective ion sensors for Mg and P is needed to cope with the varying plant uptakes according to the environmental conditions, plant species, or plant growth stages, thereby allowing more efficient and accurate replenishment for the closed hydroponic solutions.
4) In this study, only crop water need was considered in fertigation due to the difficulty in assessing the nutrient uptakes of plants. Further studies on the adaptive management of ion concentrations in nutrient solution according to the growth stages are needed to achieve more improved nutrient use efficiency and crop yields. A possible approach might be to use the

relationship between the transpiration and the nutrient uptake, thereby controlling the target ion concentrations in hydroponic nutrient solutions (Houshmandfar et al., 2018).

LIST OF REFERENCES

Abioye, E. A., Abidin, M. S. Z., Mahmud, M. S. A., Buyamin, S., Ishak, M. H. I., Rahman, M. K. I. A., . . . Ramli, M. S. A. (2020). A review on monitoring and advanced control strategies for precision irrigation. *Computers and Electronics in Agriculture, 173*, 105441. doi:https://doi.org/10.1016/j.compag.2020.105441

Abtew, W., & Melesse, A. (2013). Vapor pressure calculation methods *Evaporation and evapotranspiration* (pp. 53-62): Springer.

Ahn, T. I., Shin, J. W., & Son, J. E. (2010). Analysis of changes in ion concentration with time and drainage ratio under EC-based nutrient control in closed-loop soilless culture for sweet pepper plants (Capsicum annum L. 'Boogie'). *Journal of Bio-Environment Control, 19*(4), 298-304.

Ahn, T. I., & Son, J. E. (2019). Theoretical and Experimental Analysis of Nutrient Variations in Electrical Conductivity-Based Closed-Loop Soilless Culture Systems by Nutrient Replenishment Method. *Agronomy, 9*(10), 649.

Allen, R. G., Pereira, L. S., Raes, D., & Smith, M. (1998). Crop evapotranspiration-Guidelines for computing crop water requirements-FAO Irrigation and drainage paper 56. *Fao, Rome, 300*(9), D05109.

Baek, S., Jeon, E., Park, K. S., Yeo, K.-H., & Lee, J. (2018). Monitoring of Water Transportation in Plant Stem With Microneedle Sap Flow Sensor. *Journal of Microelectromechanical Systems, 27*(3), 440-447.

Bailey, B. J., Haggett, B. G. D., Hunter, A., Albery, W. J., & Svanberg, L. R. (1988). Monitoring Nutrient Film Solutions Using Ion-Selective Electrodes. *Journal of Agricultural Engineering Research, 40*(2), 129-142. doi:Doi 10.1016/0021-8634(88)90110-2

Baille, M., Baille, A., & Laury, J. C. (1994). A simplified model for predicting evapotranspiration rate of nine ornamental species vs. climate factors and leaf area. *Scientia Horticulturae, 59*(3-4), 217-232.

Bamsey, M., Graham, T., Thompson, C., Berinstain, A., Scott, A., & Dixon, M. (2012). Ion-specific nutrient management in closed systems: the necessity for ion-selective sensors in terrestrial and space-based agriculture and water management systems. *Sensors (Basel), 12*(10), 13349-13392. doi:10.3390/s121013349

Bamsey, M., Graham, T., Thompson, C., Berinstain, A., Scott, A., & Dixon, M. (2012). Ion-specific nutrient management in closed systems: the necessity for ion-selective sensors in terrestrial and space-based agriculture and water management systems. *Sensors, 12*(10), 13349-13392.

Barbosa, G. L., Gadelha, F. D. A., Kublik, N., Proctor, A., Reichelm, L., Weissinger, E., . . . Halden, R. U. (2015a). Comparison of land, water, and energy requirements of lettuce grown using hydroponic vs. conventional agricultural methods. *International journal of environmental research and public health, 12*(6), 6879-6891.

Barbosa, G. L., Gadelha, F. D. A., Kublik, N., Proctor, A., Reichelm, L., Weissinger, E., . . . Halden, R. U. (2015b). Comparison of Land, Water, and Energy Requirements of Lettuce Grown Using Hydroponic vs. Conventional Agricultural Methods. *International journal of environmental research and public health, 12*(6), 6879-6891. doi:10.3390/ijerph120606879

Baret, M., Massart, D., Fabry, P., Conesa, F., Eichner, C., & Menardo, C. (2000). Application of neural network calibrations to an halide ISE array. *Talanta, 51*(5), 863-877. doi:https://doi.org/10.1016/s0039-9140(99)00334-3

Barradas, J. M., Dida, B., Matula, S., & Dolezal, F. (2018). A model to formulate nutritive solutions for fertigation with customized electrical conductivity and nutrient ratios.

Irrigation Science, 36(3), 133-142.
Bonachela, S., González, A. M., & Fernández, M. D. (2006). Irrigation scheduling of plastic greenhouse vegetable crops based on historical weather data. *Irrigation Science, 25*(1), 53.
Bratov, A., Abramova, N., & Ipatov, A. (2010). Recent trends in potentiometric sensor arrays—A review. *Analytica Chimica Acta, 678*(2), 149-159. doi:https://doi.org/10.1016/j.aca.2010.08.035
Córcoles, J. I., Ortega, J. F., Hernández, D., & Moreno, M. A. (2013). Estimation of leaf area index in onion (Allium cepa L.) using an unmanned aerial vehicle. *Biosystems engineering, 115*(1), 31-42.
Caceres, R., Pol, E., Narvaez, L., Puerta, A., & Marfa, O. (2017). Web app for real-time monitoring of the performance of constructed wetlands treating horticultural leachates. *Agricultural water management, 183*, 177-185. doi:10.1016/j.agwat.2016.09.004
Chai, H., Chen, X., Cai, Y., & Zhao, J. (2019). Artificial Neural Network Modeling for Predicting Wood Moisture Content in High Frequency Vacuum Drying Process. *Forests, 10*(1), 16. doi:https://doi.org/10.3390/f10010016
Chauhan, Y. S., Wright, G. C., Holzworth, D., Rachaputi, R. C., & Payero, J. O. (2013). AQUAMAN: a web-based decision support system for irrigation scheduling in peanuts. *Irrigation Science, 31*(3), 271-283.
Chen, W.-T., Yeh, Y.-H. F., Liu, T.-Y., & Lin, T.-T. (2016). An Automated and Continuous Plant Weight Measurement System for Plant Factory. *Frontiers in plant science, 7*, 392.
Cho, W.-J., Kim, D.-W., Jung, D. H., Cho, S. S., & Kim, H.-J. (2016). An automated water nitrate monitoring system based on ion-selective electrodes. *Journal of Biosystems Engineering, 41*(2), 75-84.
Cho, W.-J., Kim, H.-J., Jung, D.-H., Han, H.-J., & Cho, Y.-Y. (2019). Hybrid Signal-Processing Method Based on Neural Network for Prediction of NO3, K, Ca, and Mg Ions in Hydroponic Solutions Using an Array of Ion-Selective Electrodes. *Sensors, 19*(24), 5508.
Cho, W.-J., Kim, H.-J., Jung, D.-H., Kim, D.-W., Ahn, T. I., & Son, J.-E. (2018). On-site ion monitoring system for precision hydroponic nutrient management. *Computers and Electronics in Agriculture, 146*, 51-58. doi:https://doi.org/10.1016/j.compag.2018.01.019
Cho, W. J., Kim, H. J., Jung, D. H., Kang, C. I., Choi, G. L., & Son, J. E. (2017). An Embedded System for Automated Hydroponic Nutrient Solution Management. *Transactions of the ASABE, 60*(4), 1083-1096. doi:https://doi.org/10.13031/trans.12163
Cloutier, G. R., Dixon, M. A., & Arnold, K. E. (1997). *Evaluation of sensor technologies for automated control of nutrient solutions in life support systems using higher plants.* Paper presented at the Proceedings of the sixth European symposium on space environmental control systems, Noordwijk, the Netherlands.
De Rijck, G., & Schrevens, E. (1994). *Application of mixture-theory for the optimisation of the composition of the nutrient solution.* Paper presented at the International Symposium on Growing Media & Plant Nutrition in Horticulture 401.
De Rijck, G., & Schrevens, E. (1997). pH Influenced by the elemental composition of nutrient solutions. *Journal of plant nutrition, 20*(7-8), 911-923. doi:10.1080/01904169709365305
Del Amor, F. M., Cuadra-Crespo, P., Walker, D. J., Cámara, J. M., & Madrid, R. (2010). Effect of foliar application of antitranspirant on photosynthesis and water relations of pepper plants under different levels of CO2 and water stress. *Journal of plant physiology, 167*(15), 1232-1238.

Domingues, D. S., Takahashi, H. W., Camara, C. A. P., & Nixdorf, S. L. (2012). Automated system developed to control pH and concentration of nutrient solution evaluated in hydroponic lettuce production. *Computers and Electronics in Agriculture, 84*, 53-61. doi:https://doi.org/10.1016/j.compag.2012.02.006

Dorneanu, S. A., Coman, V., Popescu, I. C., & Fabry, P. (2005). Computer-controlled system for ISEs automatic calibration. *Sensors and Actuators B-Chemical, 105*(2), 521-531. doi:10.1016/j.snb.2004.07.014

Elvanidi, A., Katsoulas, N., Augoustaki, D., Loulou, I., & Kittas, C. (2018). Crop reflectance measurements for nitrogen deficiency detection in a soilless tomato crop. *Biosystems engineering, 176*, 1-11.

Escarabajal-Henarejos, D., Molina-Martínez, J., Fernández-Pacheco, D., Cavas-Martínez, F., & García-Mateos, G. (2015). Digital photography applied to irrigation management of Little Gem lettuce. *Agricultural water management, 151*, 148-157.

Feddes, R. A. (1982). *Simulation of field water use and crop yield*: Pudoc.

Fernández-Pacheco, D. G., Escarabajal-Henarejos, D., Ruiz-Canales, A., Conesa, J., & Molina-Martínez, J. M. (2014). A digital image-processing-based method for determining the crop coefficient of lettuce crops in the southeast of Spain. *Biosystems engineering, 117*, 23-34.

Fernández-Pacheco, D. G., Escarabajal-Henarejos, D., Ruiz-Canales, A., Conesa, J., & Molina-Martínez, J. M. (2014). A digital image-processing-based method for determining the crop coefficient of lettuce crops in the southeast of Spain. *Biosystems engineering, 117*, 23-34. doi:https://doi.org/10.1016/j.biosystemseng.2013.07.014

Freeman, J. A., & Skapura, D. M. (1991). *Neural networks: algorithms, applications, and programming techniques*: Addison Wesley Longman Publishing Co., Inc.

Gallardo, J., Alegret, S., Munoz, R., Leija, L., Hernandez, P. R., & Del Valle, M. (2005). Use of an Electronic Tongue Based on All-Solid-State Potentiometric Sensors for the Quantitation of Alkaline Ions. *Electroanalysis: An International Journal Devoted to Fundamental and Practical Aspects of Electroanalysis, 17*(4), 348-355. doi:https://doi.org/10.1002/elan.200303097

Gallardo, M., Thompson, R. B., & Fernández, M. D. (2013). Water requirements and irrigation management in Mediterranean greenhouses: the case of the southeast coast of Spain. *Good Agricultural Practices for greenhouse vegetable crops*, 109.

García-Mateos, G., Hernández-Hernández, J., Escarabajal-Henarejos, D., Jaén-Terrones, S., & Molina-Martínez, J. (2015). Study and comparison of color models for automatic image analysis in irrigation management applications. *Agricultural water management, 151*, 158-166.

García, L., Parra, L., Jimenez, J. M., Lloret, J., & Lorenz, P. (2020). IoT-Based Smart Irrigation Systems: An Overview on the Recent Trends on Sensors and IoT Systems for Irrigation in Precision Agriculture. *Sensors, 20*(4), 1042.

Gieling, T. H., van Straten, G., Janssen, H. J. J., & Wouters, H. (2005). ISE and chemfet sensors in greenhouse cultivation. *Sensors and Actuators B-Chemical, 105*(1), 74-80. doi:https://doi.org/10.1016/j.snb.2004.02.045

Gitelson, A. A., Viña, A., Arkebauer, T. J., Rundquist, D. C., Keydan, G., & Leavitt, B. (2003). Remote estimation of leaf area index and green leaf biomass in maize canopies. *Geophysical research letters, 30*(5).

González-Esquiva, J., Oates, M. J., García-Mateos, G., Moros-Valle, B., Molina-Martínez, J. M., & Ruiz-Canales, A. (2017). Development of a visual monitoring system for water balance estimation of horticultural crops using low cost cameras. *Computers and Electronics in Agriculture, 141*, 15-26.

Gutierrez, M., Alegret, S., Caceres, R., Casadesus, J., Marfa, O., & del Valle, M. (2007). Application of a potentiometric electronic tongue to fertigation strategy in

greenhouse cultivation. *Computers and Electronics in Agriculture*, *57*(1), 12-22. doi:https://doi.org/10.1016/j.compag.2007.01.012

Gutierrez, M., Alegret, S., Caceres, R., Casadesus, J., Marfa, O., & del Valle, M. (2008). Nutrient solution monitoring in greenhouse cultivation employing a potentiometric electronic tongue. *J Agric Food Chem*, *56*(6), 1810-1817. doi:https://doi.org/10.1021/jf073438s

Hara, K., Saito, D., & Shouno, H. (2015). *Analysis of function of rectified linear unit used in deep learning.* Paper presented at the 2015 International Joint Conference on Neural Networks (IJCNN).

He, D., Matsuura, Y., Kozai, T., & Ting, K. (2003). A binocular stereovision system for transplant growth variables analysis. *Applied Engineering in Agriculture*, *19*(5), 611.

Heinen, M., & Harmanny, K. (1991). *Evaluation of the performance of ion-selective electrodes in an automated NFT system.* Paper presented at the I International Workshop on Sensors in Horticulture 304.

Herkelrath, W., Miller, E., & Gardner, W. (1977). Water uptake by plants: II. The root contact model. *Soil Science Society of America Journal*, *41*(6), 1039-1043.

Hoagland, D. R., & Arnon, D. I. (1950). The water-culture method for growing plants without soil. *Circular. California agricultural experiment station*, *347*(2nd edit).

Houshmandfar, A., Fitzgerald, G. J., O'Leary, G., Tausz-Posch, S., Fletcher, A., & Tausz, M. (2018). The relationship between transpiration and nutrient uptake in wheat changes under elevated atmospheric CO2. *Physiologia plantarum*, *163*(4), 516-529.

Hu, Y., Wang, L., Xiang, L., Wu, Q., & Jiang, H. (2018). Automatic Non-Destructive Growth Measurement of Leafy Vegetables Based on Kinect. *Sensors*, *18*(3), 806.

Incrocci, L., Massa, D., & Pardossi, A. (2017). New trends in the fertigation management of irrigated vegetable crops. *Horticulturae*, *3*(2), 37.

Jiang, J.-s., Kim, H.-J., & Cho, W.-J. (2018). On-the-go image processing system for spatial mapping of lettuce fresh weight in plant factory. *IFAC-PapersOnLine*, *51*(17), 130-134.

Jones, H. G. (2004). Irrigation scheduling: advantages and pitfalls of plant-based methods. *Journal of experimental botany*, *55*(407), 2427-2436.

Joo, H.-J., & Jeong, H.-Y. (2017). Growth analysis system for IT-based plant factory. *Multimedia Tools and Applications*, *76*(17), 17785-17799.

Jung, D.-H., Kim, H.-J., Cho, W.-J., Park, S. H., & Yang, S.-H. (2019). Validation testing of an ion-specific sensing and control system for precision hydroponic macronutrient management. *Computers and Electronics in Agriculture*, *156*, 660-668.

Jung, D. H., Kim, H. J., Choi, G. L., Ahn, T. I., Son, J. E., & Sudduth, K. A. (2015). Automated Lettuce Nutrient Solution Management Using an Array of Ion-Selective Electrodes. *Transactions of the ASABE*, *58*(5), 1309-1319. doi:https://doi.org/10.13031/trans.58.11228

Kacira, M., & Ling, P. (2001). Design and development of an automated and Non–contact sensing system for continuous monitoring of plant health and growth. *Transactions of the ASAE*, *44*(4), 989.

Kamimura, R. (2016). *Solving the Vanishing Information Problem with Repeated Potential Mutual Information Maximization*, Cham.

Katsoulas, N., Elvanidi, A., Ferentinos, K. P., Kacira, M., Bartzanas, T., & Kittas, C. (2016). Crop reflectance monitoring as a tool for water stress detection in greenhouses: A review. *Biosystems engineering*, *151*, 374-398.

Katsoulas, N., Savvas, D., Kitta, E., Bartzanas, T., & Kittas, C. (2015). Extension and evaluation of a model for automatic drainage solution management in tomato crops grown in semi-closed hydroponic systems. *Computers and Electronics in*

Agriculture, 113, 61-71. doi:https://doi.org/10.1016/j.compag.2015.01.014
Kim, D.-W., Jung, D.-H., Cho, W.-J., Sim, K.-C., & Kim, H.-J. (2017). On-site water nitrate monitoring system based on automatic sampling and direct measurement with ion-selective electrodes. *Journal of Biosystems Engineering, 42*(4), 350-357.
Kim, D.-W., Yun, H. S., Jeong, S.-J., Kwon, Y.-S., Kim, S.-G., Lee, W. S., & Kim, H.-J. (2018). Modeling and testing of growth status for Chinese cabbage and white radish with UAV-based RGB imagery. *Remote Sensing, 10*(4), 563.
Kim, H.-J., Hummel, J. W., Sudduth, K. A., & Birrell, S. J. (2007). Evaluation of phosphate ion-selective membranes and cobalt-based electrodes for soil nutrient sensing. *Transactions of the ASABE, 50*(2), 415-425.
Kim, H. J., Kim, D. W., Kim, W. K., Cho, W. J., & Kang, C. I. (2017). PVC membrane-based portable ion analyzer for hydroponic and water monitoring. *Computers and Electronics in Agriculture, 140*, 374-385. doi:10.1016/j.compag.2017.06.015
Kim, H. J., Kim, W. K., Roh, M. Y., Kang, C. I., Park, J. M., & Sudduth, K. A. (2013). Automated sensing of hydroponic macronutrients using a computer-controlled system with an array of ion-selective electrodes. *Computers and Electronics in Agriculture, 93*, 46-54. doi:https://doi.org/10.1016/j.compag.2013.01.011
Kirk, K., Andersen, H. J., Thomsen, A. G., Jørgensen, J. R., & Jørgensen, R. N. (2009). Estimation of leaf area index in cereal crops using red–green images. *Biosystems engineering, 104*(3), 308-317. doi:https://doi.org/10.1016/j.biosystemseng.2009.07.001
Kläring, H.-P. (2001). Strategies to control water and nutrient supplies to greenhouse crops. A review.
Klespitz, J., & Kovács, L. (2014). *Peristaltic pumps—A review on working and control possibilities.* Paper presented at the 2014 IEEE 12th International Symposium on Applied Machine Intelligence and Informatics (SAMI).
Ko, M. T., Ahn, T. I., Shin, J. H., & Son, J. E. (2014). Effects of renewal pattern of recycled nutrient solution on the ion balance in nutrient solutions and root media and the growth and ion uptake of paprika (Capsicum annuum L.) in closed soilless cultures. *Korean Journal of Horticultural Science & Technology, 32*(4), 463-472.
Ko, M. T., Ahn, T. I., & Son, J. E. (2013). Comparisons of Ion Balance, Fruit Yield, Water, and Fertilizer Use Efficiencies in Open and Closed Soilless Culture of Paprika (Capsicum annuum L.). *Korean Journal of Horticultural Science & Technology, 31*(4), 423-428. doi:https://doi.org/10.7235/hort.2013.13028
Kozai, T., Tsukagoshi, S., & Sakaguchi, S. (2018). Toward Nutrient Solution Composition Control in Hydroponic System *Smart Plant Factory* (pp. 395-403): Springer.
Lati, R. N., Filin, S., & Eizenberg, H. (2013). Estimating plant growth parameters using an energy minimization-based stereovision model. *Computers and Electronics in Agriculture, 98*, 260-271.
Lee, J. W., Eom, J. N., Kang, W. H., Shin, J. H., & Son, J. E. (2013). Prediction of transpiration rate of lettuces (Lactuca sativa L.) in plant factory by Penman-Monteith model. *Protected Horticulture and Plant Factory, 22*(2), 182-187.
Lee, J. Y., Rahman, A., Azam, H., Kim, H. S., & Kwon, M. J. (2017). Characterizing nutrient uptake kinetics for efficient crop production during Solanum lycopersicum var. cerasiforme Alef. growth in a closed indoor hydroponic system. *PloS one, 12*(5), e0177041.
Li, L., Zhang, Q., & Huang, D. (2014). A review of imaging techniques for plant phenotyping. *Sensors, 14*(11), 20078-20111.
Liu, Z., & Xu, Q. (2018). An Automatic Irrigation Control System for Soilless Culture of Lettuce. *Water, 10*(11), 1692.
Lomako, S., Astapovich, R., Nozdrin-Plotnitskaya, O., Pavlova, T., Lei, S., Nazarov, V., . . . Egorov, V. (2006). Sulfate-selective electrode and its application for sulfate

determination in aqueous solutions. *Analytica Chimica Acta, 562*(2), 216-222.
Lorente, D., Aleixos, N., Gómez-Sanchis, J., Cubero, S., García-Navarrete, O. L., & Blasco, J. (2012). Recent advances and applications of hyperspectral imaging for fruit and vegetable quality assessment. *Food and Bioprocess Technology, 5*(4), 1121-1142.
Mafuta, M., Zennaro, M., Bagula, A., Ault, G., Gombachika, H., & Chadza, T. (2013). Successful deployment of a wireless sensor network for precision agriculture in Malawi. *International Journal of Distributed Sensor Networks, 9*(5), 150703.
Maucieri, C., Nicoletto, C., Os, E. v., Anseeuw, D., Havermaet, R. V., & Junge, R. (2019). Hydroponic Technologies. In S. Goddek, A. Joyce, B. Kotzen, & G. M. Burnell (Eds.), *Aquaponics Food Production Systems: Combined Aquaculture and Hydroponic Production Technologies for the Future* (pp. 77-110). Cham: Springer International Publishing.
Meric, M., Tuzel, I., Tuzel, Y., & Oztekin, G. (2011). Effects of nutrition systems and irrigation programs on tomato in soilless culture. *Agricultural water management, 99*(1), 19-25. doi:https://doi.org/10.1016/j.agwat.2011.08.004
Mimendia, A., Gutiérrez, J. M., Leija, L., Hernández, P. R., Favari, L., Muñoz, R., & del Valle, M. (2010). A review of the use of the potentiometric electronic tongue in the monitoring of environmental systems. *Environmental Modelling & Software, 25*(9), 1023-1030. doi:https://doi.org/10.1016/j.envsoft.2009.12.003
Montesano, F., Van Iersel, M., & Parente, A. (2016). Timer versus moisture sensor-based irrigation control of soilless lettuce: Effects on yield, quality and water use efficiency. *Horticultural Science, 43*(2), 67-75.
Montesano, F. F., Van Iersel, M. W., Boari, F., Cantore, V., D'Amato, G., & Parente, A. (2018). Sensor-based irrigation management of soilless basil using a new smart irrigation system: Effects of set-point on plant physiological responses and crop performance. *Agricultural water management, 203*, 20-29.
Morimoto, T., Hatou, K., & Hashimoto, Y. (1996). Intelligent control for a plant production system. *Control Engineering Practice, 4*(6), 773-784.
Mueller, A. V., & Hemond, H. F. (2013). Extended artificial neural networks: Incorporation of a priori chemical knowledge enables use of ion selective electrodes for in-situ measurement of ions at environmentally relevant levels. *Talanta, 117*, 112-118. doi:https://doi.org/10.1016/j.talanta.2013.08.045
Mueller, A. V., & Hemond, H. F. (2016). Statistical generation of training sets for measuring NO 3−, NH 4+ and major ions in natural waters using an ion selective electrode array. *Environmental Science: Processes & Impacts, 18*(5), 590-599. doi:https://doi.org/10.1039/c6em00043f
Nair, V., & Hinton, G. E. (2010). *Rectified linear units improve restricted boltzmann machines.* Paper presented at the Proceedings of the 27th international conference on machine learning (ICML-10).
Namazkhan, M., Albers, C., & Steg, L. (2020). A decision tree method for explaining household gas consumption: The role of building characteristics, socio-demographic variables, psychological factors and household behaviour. *Renewable and Sustainable Energy Reviews, 119*, 109542.
Nemali, K. S., Montesano, F., Dove, S. K., & van Iersel, M. W. (2007). Calibration and performance of moisture sensors in soilless substrates: ECH2O and Theta probes. *Scientia Horticulturae, 112*(2), 227-234.
Nguyen, H. D. D., Pan, V., Pham, C., Valdez, R., Doan, K., & Nansen, C. (2020). Night-based hyperspectral imaging to study association of horticultural crop leaf reflectance and nutrient status. *Computers and Electronics in Agriculture, 173*, 105458.
Ni, W., Nørgaard, L., & Mørup, M. (2014). Non-linear calibration models for near infrared spectroscopy. *Analytica Chimica Acta, 813*, 1-14.

doi:https://doi.org/10.1016/j.aca.2013.12.002
Nikolaou, G., Neocleous, D., Katsoulas, N., & Kittas, C. (2019). Irrigation of Greenhouse Crops. *Horticulturae, 5*(1), 7.
Nobel, P., Forseth, I., & Long, S. (1993). Canopy structure and light interception *Photosynthesis and production in a changing environment* (pp. 79-90): Springer.
Noh, E.-H., Jun, H.-J., & Son, J.-E. (2011). Growth Characteristics and Nutrient Uptake of Kalanchoe Plants (Kalanchoe blossfeldiana'Marlene') at Different Light Intensities and Nutrient Strengths in Ebb and Flow Subirrigation Systems. *Korean Journal of Horticultural Science and Technology, 29*(3), 187-194.
Osroosh, Y., Peters, R. T., Campbell, C. S., & Zhang, Q. (2016). Comparison of irrigation automation algorithms for drip-irrigated apple trees. *Computers and Electronics in Agriculture, 128*, 87-99. doi:https://doi.org/10.1016/j.compag.2016.08.013
Otsu, N. (1979). A threshold selection method from gray-level histograms. *IEEE transactions on systems, man, and cybernetics, 9*(1), 62-66.
Pardossi, A., Incrocci, L., Incrocci, G., Malorgio, F., Battista, P., Bacci, L., . . . Balendonck, J. (2009). Root zone sensors for irrigation management in intensive agriculture. *Sensors, 9*(4), 2809-2835.
Prenger, J., Ling, P., Hansen, R., & Keener, H. (2005). Plant response-based irrigation control system in a greenhouse: system evaluation. *Transactions of the ASAE, 48*(3), 1175-1183.
Putra, P. A., & Yuliando, H. (2015). Soilless Culture System to Support Water Use Efficiency and Product Quality: A Review. *Agriculture and Agricultural Science Procedia, 3*, 283-288. doi:https://doi.org/10.1016/j.aaspro.2015.01.054
Putra, P. A., & Yuliando, H. (2015). Soilless culture system to support water use efficiency and product quality: a review. *Agriculture and Agricultural Science Procedia, 3*(1), 283-288.
Raviv, M., Lieth, J. H., & Bar-Tal, A. (2019). *Soilless culture: Theory and practice: Theory and practice*: Elsevier.
Resh, H. M. (2016). *Hydroponic food production: a definitive guidebook for the advanced home gardener and the commercial hydroponic grower*: CRC Press.
Riehle, D., Reiser, D., & Griepentrog, H. W. (2020). Robust index-based semantic plant/background segmentation for RGB-images. *Computers and Electronics in Agriculture, 169*, 105201.
Rius-Ruiz, F. X., Andrade, F. J., Riu, J., & Rius, F. X. (2014). Computer-operated analytical platform for the determination of nutrients in hydroponic systems. *Food chemistry, 147*, 92-97. doi:https://doi.org/10.1016/j.foodchem.2013.09.114
Rius-Ruiz, F. X., Andrade, F. J., Riu, J., & Rius, F. X. (2014). Computer-operated analytical platform for the determination of nutrients in hydroponic systems. *Food Chem, 147*, 92-97. doi:10.1016/j.foodchem.2013.09.114
Rodríguez, D., Reca, J., Martínez, J., & Urrestarazu, M. (2015). New adaptive hybrid-automatic irrigation control system for soilless culture. *Journal of Irrigation and Drainage Engineering, 141*(7), 04014083.
Romero, R., Muriel, J., García, I., & de la Peña, D. M. (2012). Research on automatic irrigation control: State of the art and recent results. *Agricultural water management, 114*, 59-66.
Ryder, E. J. (1999). *Lettuce, endive and chicory*: Cab International.
Saeys, W., Mouazen, A. M., & Ramon, H. (2005). Potential for onsite and online analysis of pig manure using visible and near infrared reflectance spectroscopy. *Biosystems engineering, 91*(4), 393-402. doi:https://doi.org/10.1016/j.biosystemseng.2005.05.001
Sambo, P., Nicoletto, C., Giro, A., Pii, Y., Valentinuzzi, F., Mimmo, T., . . . Astolfi, S. (2019). Hydroponic solutions for soilless production systems: Issues and

opportunities in a smart agriculture perspective. *Frontiers in plant science, 10*.
Saurina, J., López-Aviles, E., Le Moal, A., & Hernández-Cassou, S. (2002). Determination of calcium and total hardness in natural waters using a potentiometric sensor array. *Analytica Chimica Acta, 464*(1), 89-98. doi:https://doi.org/10.1016/s0003-2670(02)00474-9
Savvas, D. (2002). SW—Soil and Water: Automated Replenishment of Recycled Greenhouse Effluents with Individual Nutrients in Hydroponics by Means of Two Alternative Models. *Biosystems engineering, 83*(2), 225-236.
Savvas, D., & Gizas, G. (2002). Response of hydroponically grown gerbera to nutrient solution recycling and different nutrient cation ratios. *Scientia Horticulturae, 96*(1-4), 267-280. doi:https://doi.org/10.1016/s0304-4238(02)00054-7
Savvas, D., & Manos, G. (1999). Automated composition control of nutrient solution in closed soilless culture systems. *Journal of Agricultural Engineering Research, 73*(1), 29-33.
Savvas, D., Passam, H., Olympios, C., Nasi, E., Moustaka, E., Mantzos, N., & Barouchas, P. (2006). Effects of ammonium nitrogen on lettuce grown on pumice in a closed hydroponic system. *HortScience, 41*(7), 1667-1673.
Schippers, P. (1979). *Composition changes in the nutrient solution during the growth of plants in recirculating nutrient culture.* Paper presented at the Symposium on Research on Recirculating Water Culture 98.
Schwarz, D., & Kuchenbuch, R. (1993). *Water uptake by tomato plants grown in closed hydroponic systems dependent on the EC-level.* Paper presented at the International Symposium on Water Quality & Quantity-Greenhouse 458.
Seelig, H.-D., Stoner, R. J., & Linden, J. C. (2012). Irrigation control of cowpea plants using the measurement of leaf thickness under greenhouse conditions. *Irrigation Science, 30*(4), 247-257. doi:10.1007/s00271-011-0268-2
Sesma, J., Molina-Martínez, J., Cavas-Martínez, F., & Fernández-Pacheco, D. (2015). A mobile application to calculate optimum drip irrigation laterals. *Agricultural water management, 151*, 13-18.
Sigrimis, N., Arvanitis, K., Pasgianos, G., & Ferentinos, K. (2001). Hydroponics water management using adaptive scheduling with an on-line optimiser. *Computers and Electronics in Agriculture, 31*(1), 31-46.
Smith, R., & Baillie, J. (2009). *Defining precision irrigation: A new approach to irrigation management.* Paper presented at the Irrigation Australia 2009: Irrigation Australia Irrigation and Drainage Conference: Proceedings.
Son, J. E., Kim, H. J., & Ahn, T. I. (2020). Chapter 20 - Hydroponic systems. In T. Kozai, G. Niu, & M. Takagaki (Eds.), *Plant Factory (Second Edition)* (pp. 273-283): Academic Press.
Sonneveld, C., & Van den Bos, A. (1995). Effects of nutrient levels on growth and quality of radish (Raphanus sativus L.) grown on different substrates. *Journal of plant nutrition, 18*(3), 501-513.
Sonneveld, C., Voogt, W., & Spaans, L. (1997). *A universal algorithm for calculation of nutrient solutions.* Paper presented at the International Symposium on Growing Media and Hydroponics 481.
Steiner, A. A. (1961). A universal method for preparing nutrient solutions of a certain desired composition. *Plant and Soil, 15*(2), 134-154. doi:10.1007/bf01347224
Steiner, A. A. (1966). The influence of the chemical composition of a nutrient solution on the production of tomato plants. *Plant and Soil, 24*(3), 454-466. doi:10.1007/bf01374052
Stojanova, D., Panov, P., Gjorgjioski, V., Kobler, A., & Džeroski, S. (2010). Estimating vegetation height and canopy cover from remotely sensed data with machine learning. *Ecological Informatics, 5*(4), 256-266.

Story, D., & Kacira, M. (2015). Design and implementation of a computer vision-guided greenhouse crop diagnostics system. *Machine Vision and Applications, 26*(4), 495-506. doi:10.1007/s00138-015-0670-5

Sun, Y., Tong, C., He, S., Wang, K., & Chen, L. (2018). Identification of nitrogen, phosphorus, and potassium deficiencies based on temporal dynamics of leaf morphology and color. *Sustainability, 10*(3), 762.

Te, L., Cheng, L., Chih, L., & CHENG, C. (2011). A three-dimensional imaging approach for plant feature measurement using stereo vision. *Tarım Makinaları Bilimi Dergisi, 7*(2).

Terabayashi, S., Muramatsu, I., Tokutani, S., Ando, M., Kitagawa, E., Shigemori, T., . . . Fujime, Y. (2004). Relationship between the weekly nutrient uptake rate during fruiting stages and fruit weight of tomato (Lycopersicon esculentum Mill.) grown hydroponically. *Journal of the Japanese Society for Horticultural Science, 73*(4), 324-329.

Van Os, E. (1994). Engineering and environmental aspects of soilless growing systems. *Hydroponics and Transplant Production 396*, 25-32. doi:https://doi.org/10.17660/actahortic.1995.396.2

Vardar, G., Altıkatoğlu, M., Ortaç, D., & Cemek, M. (2015). Measuring calcium, potassium, and nitrate in plant nutrient solutions using ion-selective electrodes in hydroponic greenhouse of some vegetables. *Biotechnol Appl Biochem, 62*(5), 663-668. doi:https://doi.org/10.1002/bab.1317

Voogt, W., & Sonneveld, C. (1997). Nutrient Management in Closed Growing Systems for Greenhouse Production. In E. Goto, K. Kurata, M. Hayashi, & S. Sase (Eds.), *Plant Production in Closed Ecosystems: The International Symposium on Plant Production in Closed Ecosystems held in Narita, Japan, August 26–29, 1996* (pp. 83-102). Dordrecht: Springer Netherlands.

Voogt, W., & Sonneveld, C. (1997). Nutrient management in closed growing systems for greenhouse production *Plant production in closed ecosystems* (pp. 83-102): Springer.

Wang, L., Cheng, Y., Lamb, D., Lesniewski, P. J., Chen, Z., Megharaj, M., & Naidu, R. (2017). Novel recalibration methodologies for ion-selective electrode arrays in the multi-ion interference scenario. *Journal of Chemometrics, 31*(2), e2870. doi:https://doi.org/10.1002/cem.2870

Wiser, L., & Blom, T. J. (2016). The Effect of Nitrogen and Phosphorus Ratios and Electrical Conductivity on Plant Growth. *American Journal of Plant Sciences, 7*(12), 1590.

Woebbecke, D. M., Meyer, G. E., Von Bargen, K., & Mortensen, D. (1995). Color indices for weed identification under various soil, residue, and lighting conditions. *Transactions of the ASAE, 38*(1), 259-269.

Xu, K., Kitazumi, Y., Kano, K., & Shirai, O. (2020). Automatic Management of Nutrient Solution for Hydroponics-Construction of multi-ion stat. *Anal Sci*, 20A002. doi:10.2116/analsci.20A002

Yeh, Y.-H. F., Lai, T.-C., Liu, T.-Y., Liu, C.-C., Chung, W.-C., & Lin, T.-T. (2014). An automated growth measurement system for leafy vegetables. *Biosystems engineering, 117*, 43-50.

Yu, H., & Wilamowski, B. M. (2011). Levenberg-marquardt training. *Industrial electronics handbook, 5*(12), 1.

Yu, J., Mo, W., Huang, Y.-K., Ip, E., & Kilper, D. C. (2019). Model transfer of QoT prediction in optical networks based on artificial neural networks. *Journal of Optical Communications and Networking, 11*(10), C48-C57. doi:https://doi.org/10.1364/JOCN.11.000C48

Zekki, H., Gauthier, L., & Gosselin, A. (1996). Growth, productivity, and mineral

composition of hydroponically cultivated greenhouse tomatoes, with or without nutrient solution recycling. *Journal of the American Society for Horticultural Science*, *121*(6), 1082-1088. doi:https://doi.org/10.21273/jashs.121.6.1082

Zeng, C.-Z., Bie, Z.-L., & Yuan, B.-Z. (2009). Determination of optimum irrigation water amount for drip-irrigated muskmelon (Cucumis melo L.) in plastic greenhouse. *Agricultural water management*, *96*(4), 595-602.

Zheng, Y. (2017). *Current nutrient management practices and technologies used in North American greenhouse and nursery industries.* Paper presented at the International Symposium on New Technologies for Environment Control, Energy-Saving and Crop Production in Greenhouse and Plant 1227.

APPENDIX

A1. PYTHON CODE FOR CONTROLLING THE IMAGE MONITORING AND CC CALCULATION

```
import serial
import time
import cv2
import numpy as np
import os
import openpyxl
import datetime
import socket

sock = socket.socket(socket.AF_INET, socket.SOCK_STREAM)
sock.connect(('localhost', 6340))

baud = 115200
port = 'com11'
ser = serial.Serial(port,baud,timeout=0)

while True:
    now = time.localtime()
    h = now.tm_hour
    m = now.tm_min

    if h == 13 and m == 50: #CC update time
        wb = openpyxl.Workbook()
        sheet = wb.get_active_sheet()
        sheet.title='Surface of Crop'

        sheet.cell(row=1, column=1).value='crop pixel'
        sheet.cell(row=1, column=3).value='crop surface'
        sheet.cell(row=1, column=5).value='Leaf Area Index'

        crop = 0
        surface = 0
        CC = 0
        MODE = 0


        #Initial position
        position_x = 0
        position_y = 0
        #num_x = int(100 / (600/15)) + 1
        #num_y = int(200 / (480/15)) + 1
        num_x = int(100/35.2) + 1
        num_y = int(200/26.4) + 1
        num_total = num_x * num_y
        temp_x_go = 0

        position_x = 6210
        position_y = -10810
        Temp2Con_x = 'go_position1 = ' + str(position_x) + '\r\n' # x-axis
        Temp2Con_y = 'go_position3 = ' + str(position_y) + '\r\n' # y-axis
        ser.write(Temp2Con_x.encode())
        time.sleep(1.5)
        ser.write(Temp2Con_y.encode())
        time.sleep(1.5)

        cap_initial = cv2.VideoCapture(0)
        _, Check = cap_initial.read(0)
```

```
Check_image = Check[0:480, 0:640]

count_ = 0
for y in range(0,Threshold_array_check[1] - 1):
    for x in range(0,Threshold_array_check[0] - 1):
        pixel_ = thres_check[x, y]
        if pixel_ == 255:
            count_ += 1

position_x = 0
position_y = 0
Temp2Con_x = 'go_position1 = ' + str(position_x) + '\r\n'
Temp2Con_y = 'go_position3 = ' + str(position_y) + '\r\n'
ser.write(Temp2Con_x.encode())
time.sleep(1.5)
ser.write(Temp2Con_y.encode())
time.sleep(1.5)

position_x = 6610
position_y = -39210
num = 0

cap = cv2.VideoCapture(0)
for i in range(0,num_total + 1):

    print('i =' ,i)

    if i == 0:
        x = 0
        y = 0
    elif (i % num_y) == 0:
        x = 1
        y = 0
    elif (i % num_y) != 0:
        x = 0
        y = 1 * (-1)**(int(i/num_y))
    elif i == num_total:
        x = 0
        y = 0

    position_x = position_x + 17826 * x
    position_y = position_y - 26739 * y
    Temp2Con_x = 'go_position1 = ' + str(position_x) + '\r\n' #
    Temp2Con_y = 'go_position3 = ' + str(position_y) + '\r\n' #
    ser.write(Temp2Con_x.encode())
    time.sleep(1.5)
    ser.write(Temp2Con_y.encode())
    time.sleep(1.5)
'''
    _, org = cap.read(0)
    img = org[0:480, 0:640]
    rgb = cv2.cvtColor(img, cv2.COLOR_BGR2RGB)
    '''ExG conversion'''
    R, G, B = cv2.split(rgb)
    R=R/255
    G=G/255
    B=B/255
    r = R/(R+G+B)
    g = G/(R+G+B)
    b = B/(R+G+B)

    ExG = 2*g - r - b
    ExG=255*ExG
```

```
otsu_thr, otsu_mask = cv2.threshold(ExG, 0, 255, cv2.THRESH_BINARY_INV | cv2.THRESH_OTSU)

thres = cv2.inRange(ExG,,otsu_thr, 255)
            crop_only = cv2.bitwise_and(img,img, mask= thres)
            '''realtime image'''
                if i != 0:
                cv2.imshow("Org",img)
                cv2.imshow("crop",crop_only)
                cv2.imshow("threshold",thres)

                Threshold_array = thres.shape
                count = 0
                for y in range(0,Threshold_array[1]):
                   for x in range(0,Threshold_array[0]):
                      pixel = thres[x, y]
                      if pixel == 255:
                            count += 1
                crop = crop + count
                surface = (crop * (16/6405))
                CC = surface/(640*480*24)
                '''cmd'''
                print(count,"pixels are crop.")
                print("accumulate crop pixel = ", crop)
                print("accumulate crop surface = ", surface, "cm^2")
                print("accumulate CC = ", CC)

            key = cv2.waitKey(1500)
            num += 1
            if key == 27:
                break

    cap_initial.release()
    cap.release()
    cv2.destroyAllWindows()

    '''(0,0) return_end'''
    Temp2Con_x = 'go_position1 = ' + str(0) + '\r\n' #
    Temp2Con_y = 'go_position3 = ' + str(0) + '\r\n' #
    ser.write(Temp2Con_x.encode())
    time.sleep(1.5)
    ser.write(Temp2Con_y.encode())
    time.sleep(1.5)

    print("\n")
    CC = round(CC,4)
    print("Canopy cover =", CC)

    cc = str(CC)
    sock.send(cc.encode('utf-8')) #

    time.sleep(5)
```

A2. ION CONCENTRATIONS OF THE SOLUTIONS USED IN CHAPTER 4 (UNIT: MG·L^{-1})

Solution	NO_3	K	Ca	Mg
1	101.9	39.4	143.02	101.13
2	539.5	167.71	156.36	104.4
3	102.8	37.6	150.78	13.63
4	554.9	294	41.09	12.59
5	101.1	296.23	40.32	52.54
6	1001.4	165.31	40.32	103.01
7	1002.6	302.57	259.21	12.91
8	547.1	162.14	41.73	50.28
9	102.1	161.51	144.73	13.35
10	993.5	302	163.41	55.43
11	547.6	165.66	275.94	12.62
12	1001.8	161.76	162	12.59
13	918.7	39.69	284.85	58.22
14	538	308.16	165.55	101.51
15	104.4	168.4	277.67	61.68
16	531.2	37.01	163.91	58.99
17	1002	303.9	160.43	58.54
18	1000.3	36.02	41.9	100.14
19	101.4	298.82	39.45	60.72
20	101.4	304.69	265.15	12.68
21	555.3	39.24	286.71	58.73
22	1015.5	168.13	281.78	101.73
23	512.7	312.96	280.85	103.64
24	102	40.01	283.47	106.26
25	99.1	303.27	40.61	96.41
26	553.4	32.72	40.26	13.8
27	1052.7	31.8	41.03	12.84
Two-point normalization (Low)	109.1	32.7	37.8	13.5
Two-point normalization (High)	1007.8	303.9	256.7	113.1
Basil 1	425.9	143.2	75.6	9.8
Kale	385.7	196.8	61.8	30.3
Basil 2	432.2	260.9	69.8	38.3
Beet	405.2	13.4	190.7	25.8
Atractylodes japonica	513.9	310.5	0.9	31.1
Glehnia littoralis 1	121.9	77.5	0.3	20.3
Paprika	1025.5	427.2	210.4	56.6
Glehnia littoralis 2	450.8	111.5	84.3	25.2

A3. BLOCK DIAGRAMS OF THE LABVIEW PROGRAM USED IN CHAPTER 4

a) LabVIEW block diagram for the initialization of the system

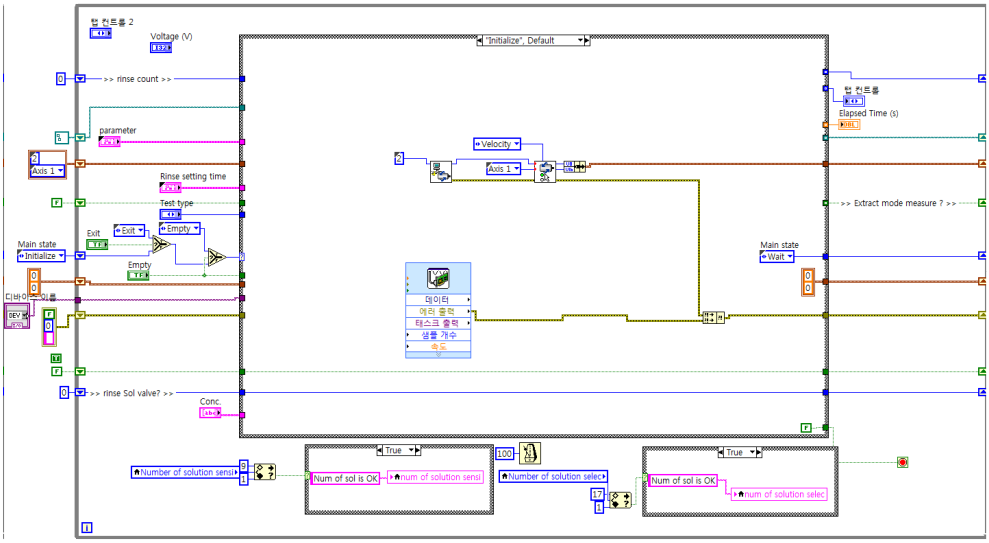

b) LabVIEW block diagram for waiting the selection of the test type

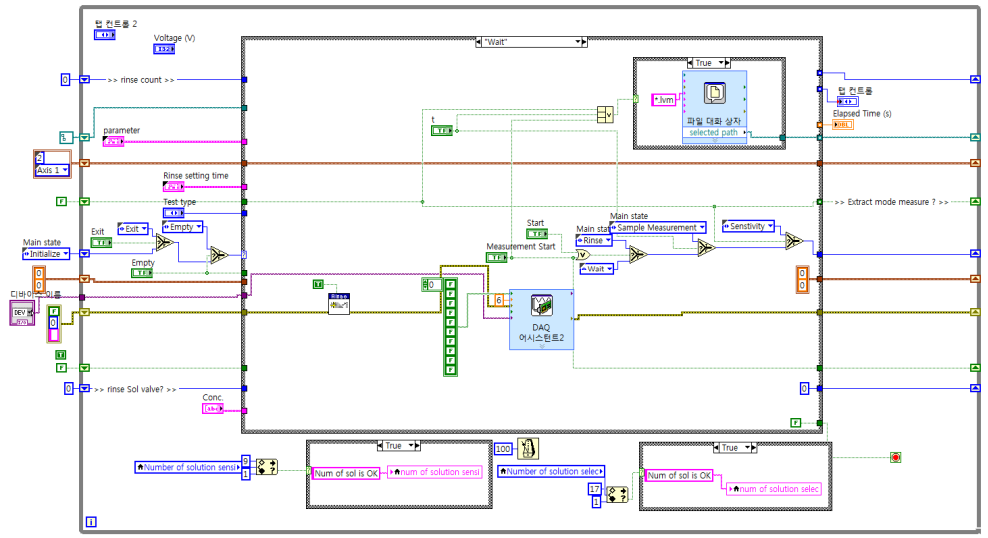

c) LabVIEW block diagram for the rinse sequence

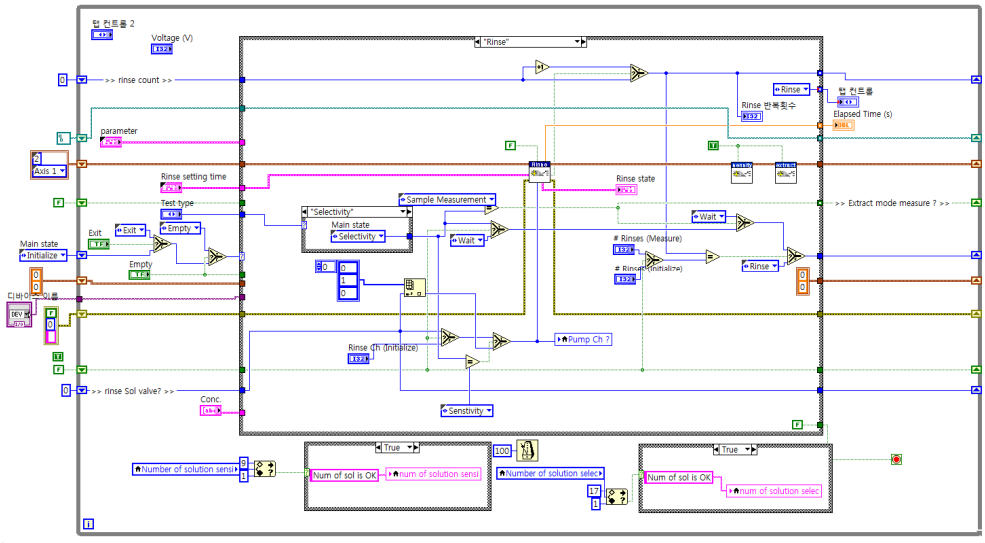

d) LabVIEW block diagram for the ISE sensitivity test sequence

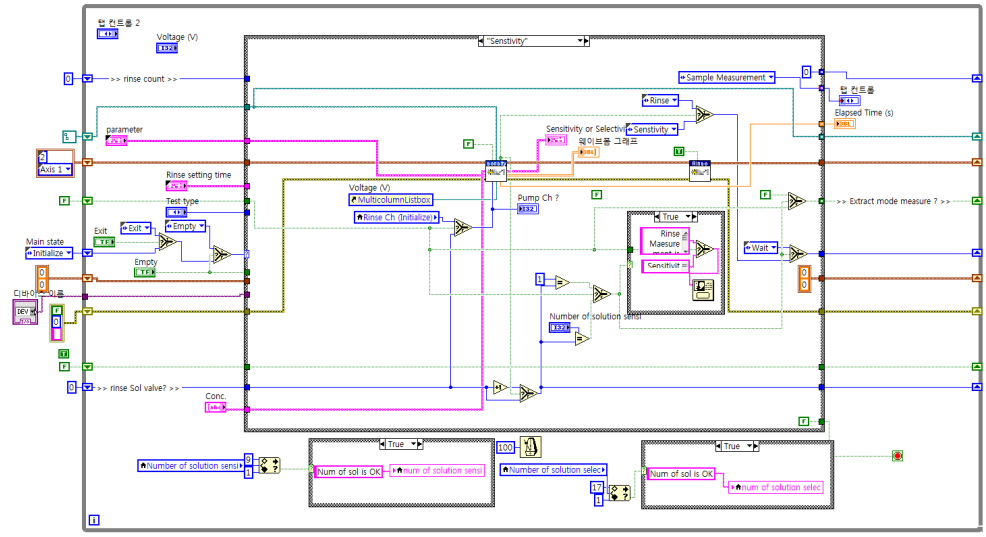

e) LabVIEW block diagram for the sample measurement test sequence

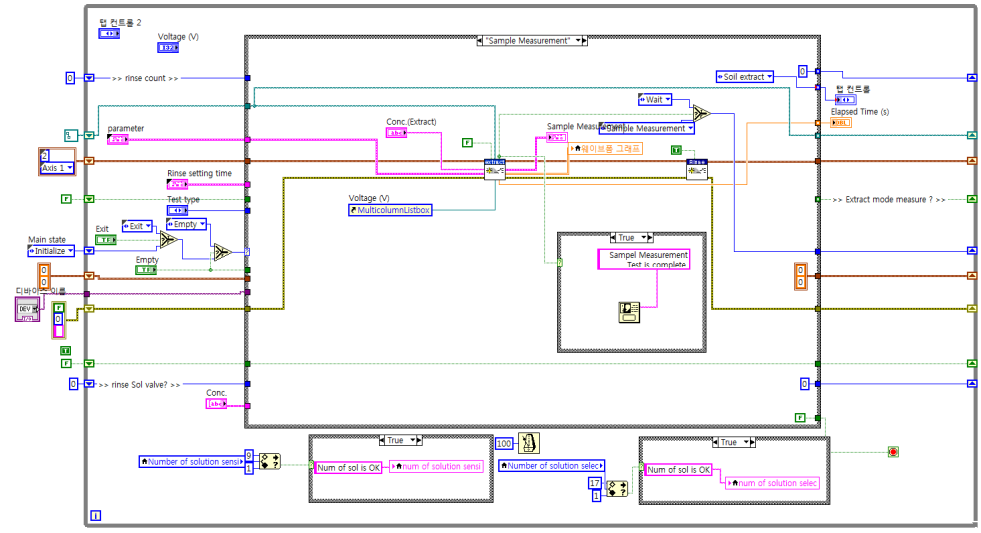

f) LabVIEW block diagram for the ISE selectivity test sequence

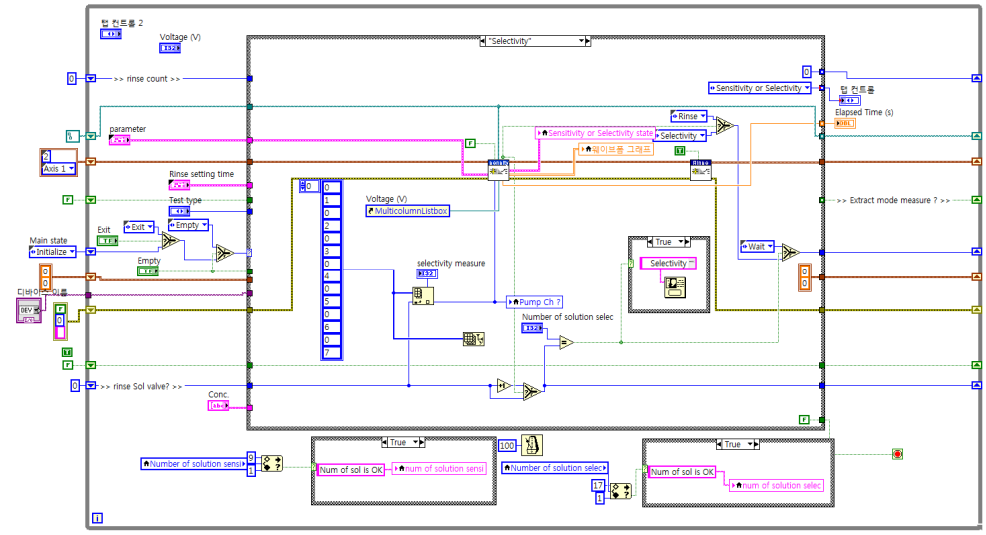

g) LabVIEW block diagram for the solution drainage sequence

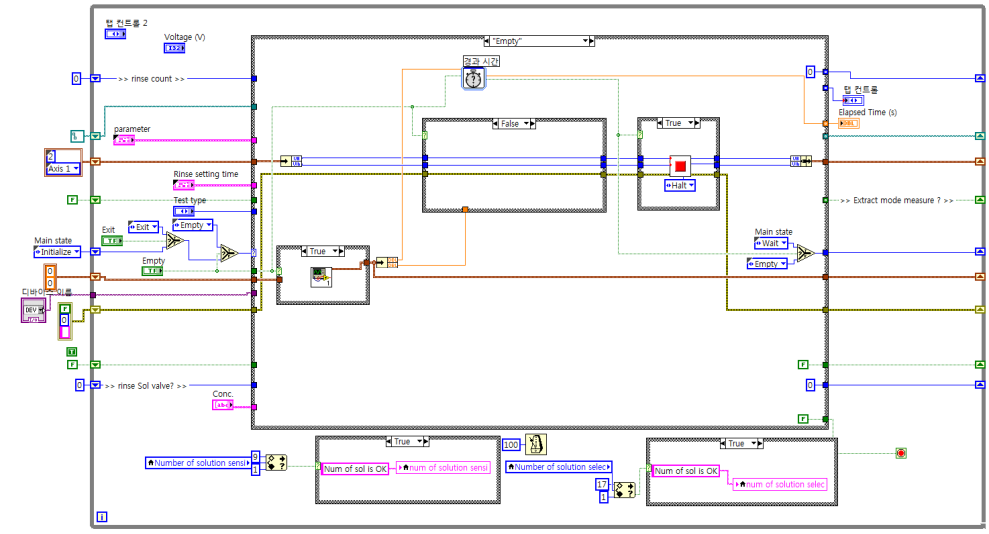

h) LabVIEW block diagram for the system exit

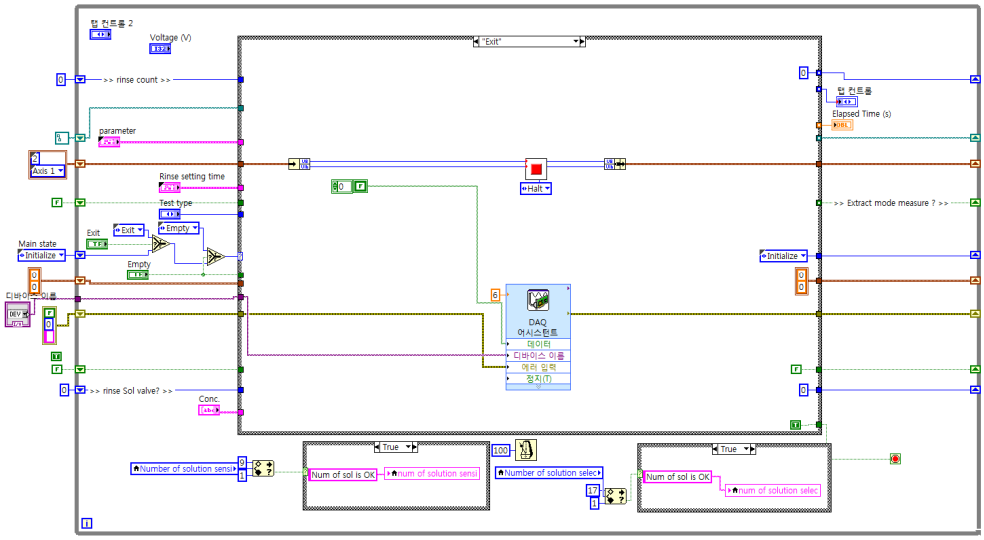

A4. ION CONCENTRATIONS OF THE SOLUTIONS USED IN CHAPTERS 5 AND 6 (UNIT: MG·L^{-1})

Solution	Concerned ion	Concentration (mg·L^{-1})
Two-point normalization solution (high)	Ca	248.03
	K	308.91
	NO_3	981.7
Two-point normalization solution (low)	Ca	28.37
	K	35.39
	NO_3	100.9
Stock solution 1 ($Ca(NO_3)_2{\cdot}4H_2O$)	Ca	3489.11
	NO_3	11243.6
Stock solution 2 (KH_2PO_4)	K	6450.5
	P	4149.582
Stock solution 3 ($NH_4H_2PO_4$)	NH_4	3340.28
	P	4732.319
Stock solution 4 (KNO_3)	K	7627.55
	NO_3	13564.3
Stock solution 5 (NH_4NO_3)	NH_4	4430.25
	NO_3	16608
Stock solution 6 ($MgSO_4{\cdot}7H_2O$)	Mg	2071.4
Stock solution 7 (K_2SO_4)	K	8857.83
pH control solution (H_2SO_4)	H	pH 2.0
Tap water	Ca	16.13-23.4
	K	2.66-3.51
	NO_3	5.9-9.2
	P	0.113-0.136
	Mg	3.24-4.77
	NH_4	Not detected
	SO_4	3.24-15.6

A5. BLOCK DIAGRAMS OF THE LABVIEW PROGRAM USED IN THE CHAPTERS 5 AND 6

a) LabVIEW block diagram for the environmental monitoring

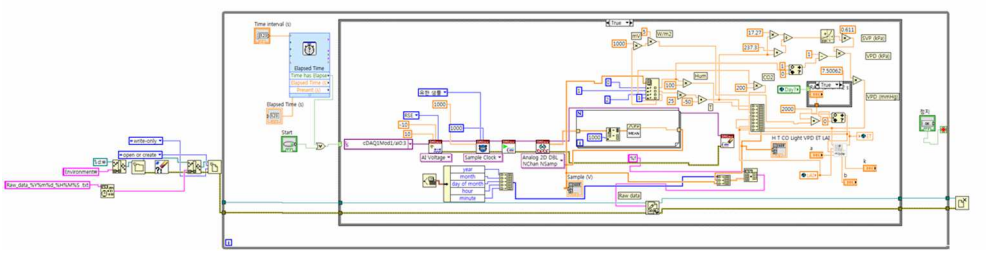

b) LabVIEW block diagram for the TCP/IP communication

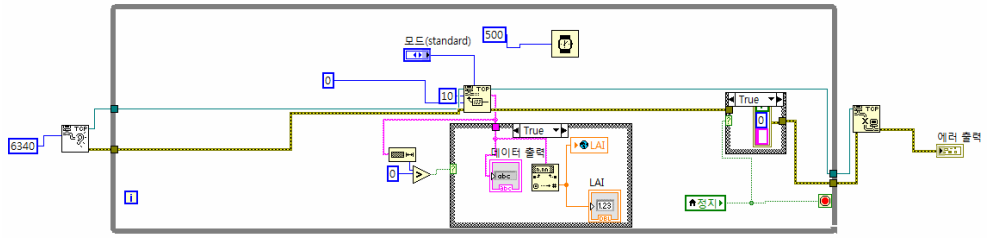

c) LabVIEW block diagram for the ion-specific management and fertigation

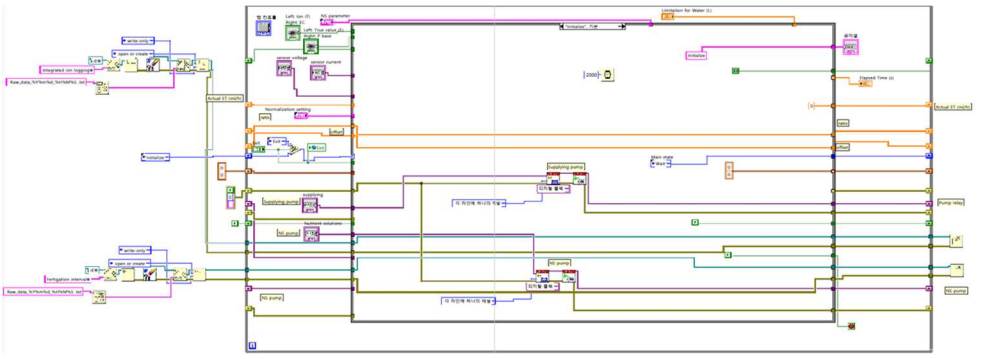

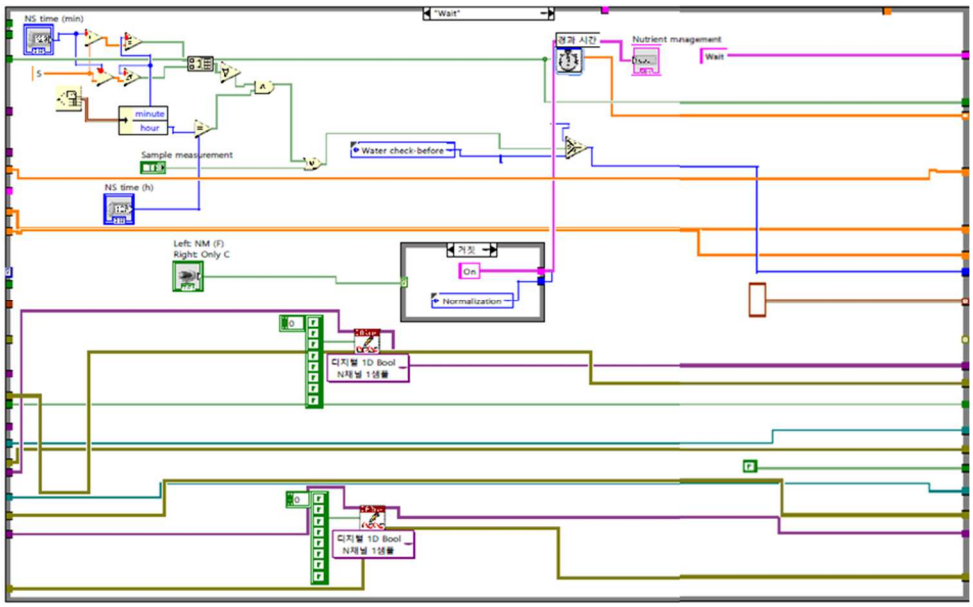
"Wait"
NS time (min)
minute
hour
Sample measurement
NS time (h)
Water check-before
경과 시간
Nutrient management
Wait
Left: NM (F)
Right: Only C
On
Normalization
디지털 1D Bool
N채널 1샘플

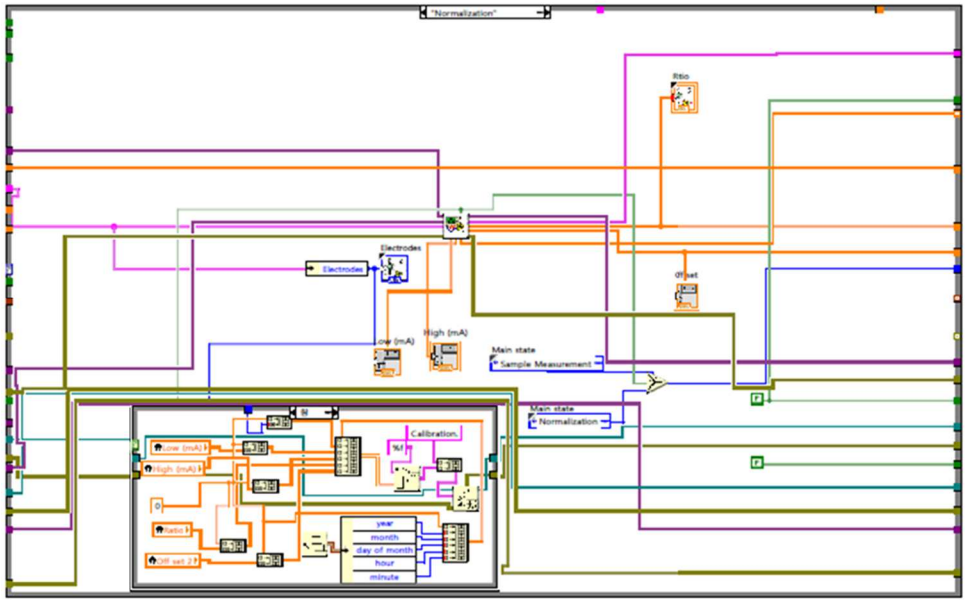
"Normalization"
Rtio
Electrodes
Offset
High (mA)
Main state
Sample Measurement
Normalization
Calibration
year
month
day of month
hour
minute

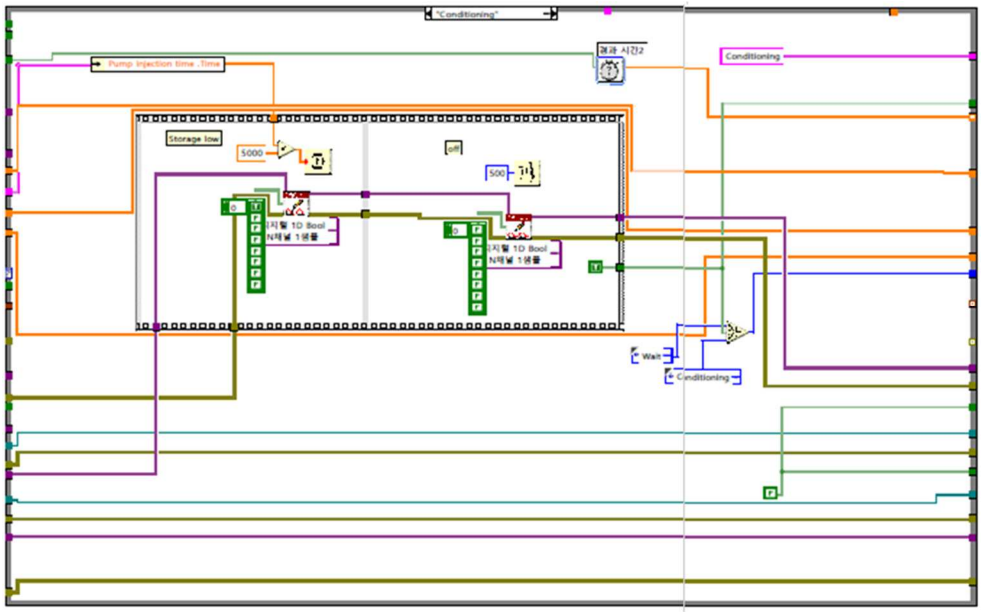
"Conditioning"
Pump Injection time .Time
Storage low
5000
Conditioning
Wait
Conditioning

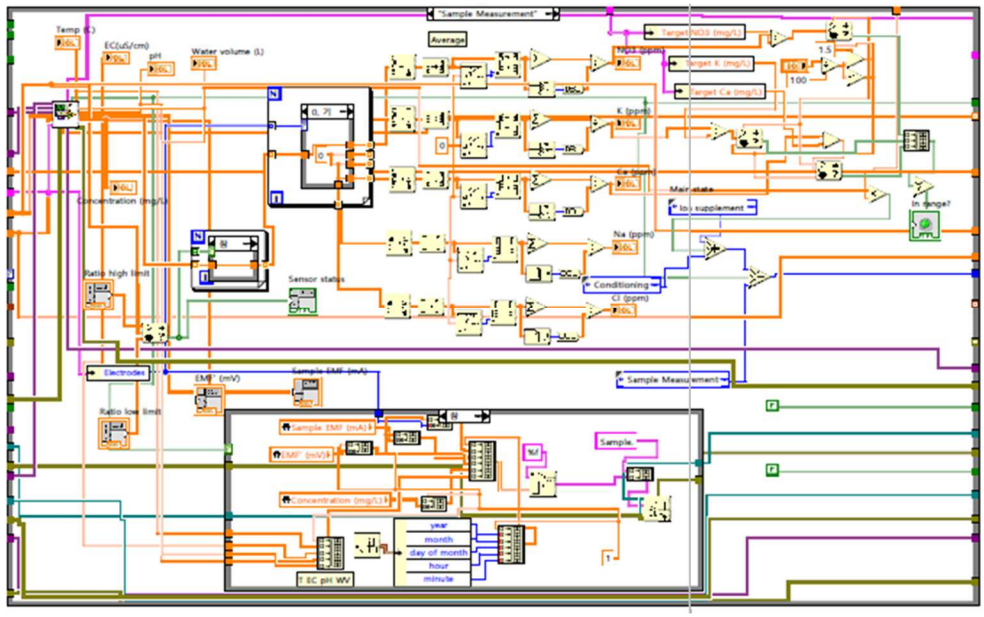
"Sample Measurement"
Temp (C)
EC(uS/cm)
pH
Water volume (L)
Average
Concentration (mg/L)
Ratio high limit
Sensor status
Electrodes
EMF (mV)
Ratio low limit
Conditioning
Sample Measurement
Sample
year
month
day of month
hour
minute
T EC pH WV

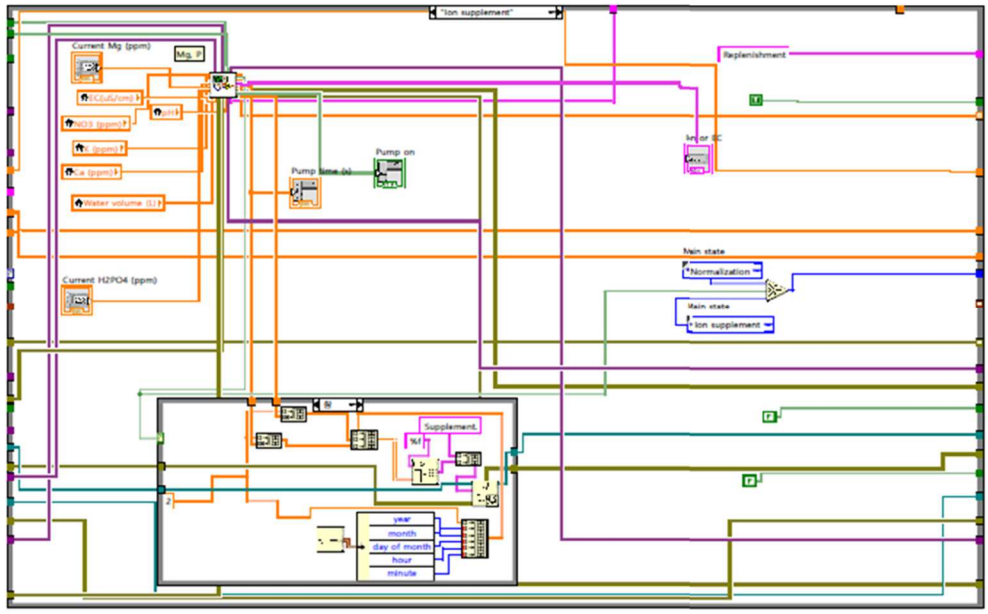
"Ion supplement"
Current Mg (ppm)
Mg_P
Pump time (s)
Pump on
Replenishment
Main state
Normalization
Main state
Ion supplement
Current H2PO4 (ppm)
Supplement
year
month
day of month
hour
minute

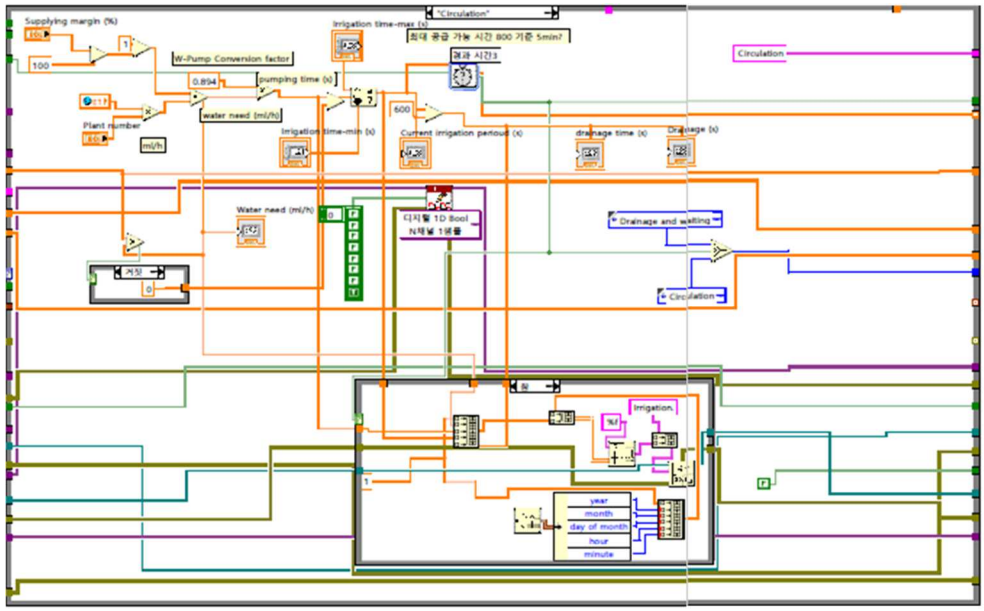
"Circulation"
Supplying margin (%)
Irrigation time-max (s)
W-Pump Conversion factor
pumping time (s)
water need (ml/h)
Plant number
Irrigation time-min (s)
Current irrigation period (s)
drainage time (s)
Drainage (s)
Circulation
Water need (ml/h)
Drainage and waiting
Circulation
Irrigation
year
month
day of month
hour
minute

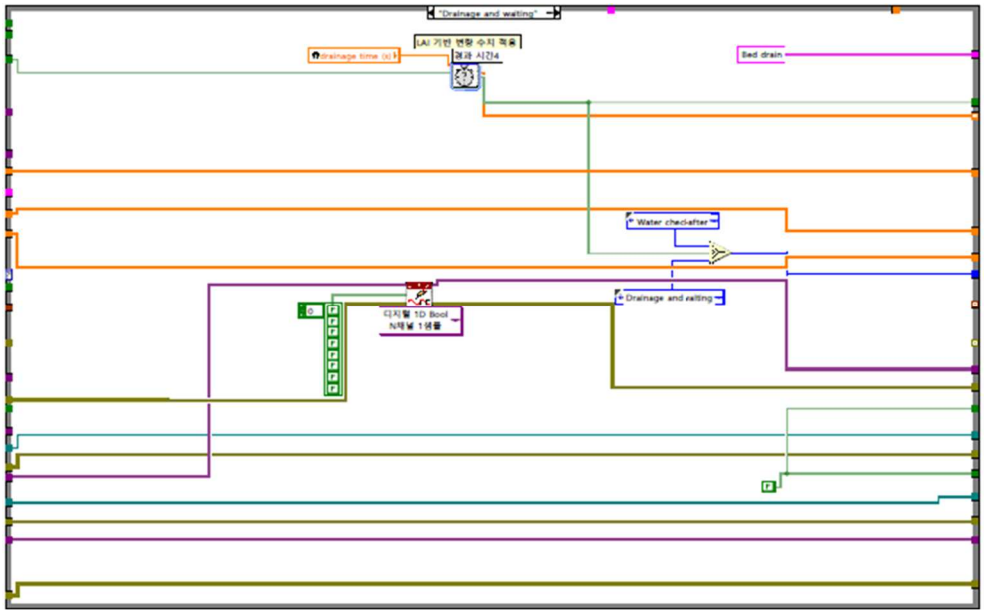
"Drainage and waiting"
drainage time (s)
Bed drain
Water check after
Drainage and waiting
디지털 1D Bool
N채널 1샘플

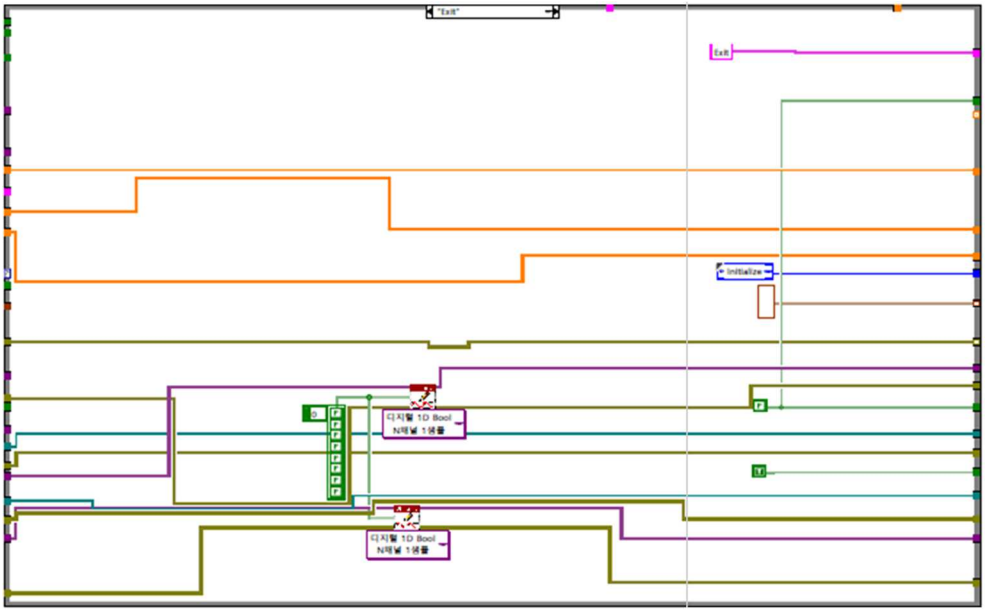
"Exit"
Exit
Initialize
디지털 1D Bool
N채널 1샘플
디지털 1D Bool
N채널 1샘플

개별 이온 및 작물 생육 센싱 기반의 정밀 수경재배 양액 관리 시스템

조 우 재

ABSTRACT IN KOREAN

현재의 순환식 수경재배 시스템에서 양액의 분석과 보충은 전기전도도(EC, electrical conductivity) 및 pH를 기반으로 수행되고 있으며, 양액의 공급은 작물의 생육 상태에 대한 고려 없이 항상 일정한 시간 동안 펌프가 동작하여 공급되는 형태이다. 그러나 EC 기반의 양액 관리는 개별 이온 농도의 동적인 변화를 감지할 수 없어 반복되는 보충 중 불균형이 발생하게 되어 양액의 폐기를 야기하며, 고정된 시간 동안의 양액 공급은 작물에 대해 과잉 또는 불충분한 물 공급으로 이어져 물 사용 효율의 저하를 일으킨다. 이러한 문제들에 대해, 개별 이온 농도에 대해 부족한 성분만을 선택적으로 보충하고, 작물의 생육 정도에 기반하여 필요한 수준에 맞게 양액을 공급하는 정밀 농업에 기반한 양액 관리를 수행하면 물과 비료 사용 효율의 향상과 양액의 재사용 기간 증진을 기대할 수 있다. 본 연구의 목적은 자동으로, 그리고 가변적으로 작물 생육 정보에 기반하여 양액 공급량을 제어하고, 작물 생장에 적합한 조성에 맞게 현재 양액의 이온 농도 센싱에 기반하여 적절한 수준만큼의 물과 개별 양분 비료를 보충할 수 있는 정밀 수경재배 양액 관리 시스템을 개발하는 것이

다. 해당 목표를 달성하기 위해, 변이하는 물과 양분 요구량을 측정할 수 있는 모니터링 기술들을 분석하고 각 모니터링 기술들에 대한 검증을 수행하였다. 먼저, 작물의 물 요구량을 실시간으로 관측할 수 있는 영상 기반 측정 기술을 조사하였다. 영상 기반 분석 활용을 위해 박막경 기반의 순환식 수경재배 환경에서 자라는 상추의 이미지들을 전체 베드에 대해 수집할 수 있는 영상 모니터링 시스템을 구성하였고, 수집한 영상 중 상추 부분만을 excess green (ExG)과 Otsu 방법을 통해 분리하여 투영작물면적 (CC, canopy cover)을 획득하였다. 영상 처리 기술의 적용성 평가를 위해 직접 분석한 투영작물면적 값과 이를 비교하였다. 비교 검증 결과에서 투영작물면적 측정을 위한 영상 수집 및 분석이 수확 전까지의 상추에 대해 적용 가능함을 확인하였다. 이후 수집한 투영작물면적과 기온, 상대습도, 일사량을 기반으로 생육 중인 상추들이 요구하는 물의 양을 예측하기 위해 Penman-Monteith 방정식 기반의 증산량 예측 모델을 구성하였으며 실제 증산량과 비교하였을 때 높은 일치도를 확인하였다. 개별 이온 농도 측정과 관련하여서는, 이온선택성전극 (ISE, ion-selective electrode)를 이용한 수경재배 양액 내 이온의 연속적이고 자율적인 모니터링 수행을 위해 2점 정규화, 인공신경망, 그리고 이 둘을 복합적으로 구성한 하이브리드 신호 처리 기법의 성능을 비교하여 분석하였다. 분석 결과, 하이브리드 신호 처리 방식이 가장 높은 정확성을 보였으나, 센서 고장에 취약한 신경망 구조로 인해 장기간 모니터링 안정성에 있어서는 가장 높은 정밀도를 가진 2점 정규화 방식을 센서 어레이에 적용하는 것이 적합할 것으로 판단하였다. 또한, 주어진 개별 이온 농도 목표값에 맞는 비료 염 및 물의 최적 주입량을 결정하기 위해 의사결정트리 구조의 비료 투입 알고리즘을 제시하였다. 제시한 비료 투입 알고리즘의 효과에 대해서는 순차적인 목표에 대한 보충 및 특정 성분에 대해 집중적인 변

화를 부여한 보충 수행 실험을 통해 검증하였으며, 그 결과 제시한 알고리즘은 주어진 목표값들에 따라 성공적으로 양액을 조성하였음을 확인하였다. 마지막으로, 제시되었던 센싱 및 제어 기술들을 통합하여 NFT 기반의 순환식 수경재배 배드에 상추 재배를 수행하여 실증하였다. 실증 실험에서, 종래의 고정 시간 양액 공급 대비 57.4%의 양액 공급량 감소와 상추 생육의 촉진을 확인하였다. 동시에, 개발 시스템은 NO_3, K, Ca, Mg, 그리고 P에 대해 각각 4.9%, 1.4%, 3.2%, 5.2%, 그리고 14.9% 수준의 변동계수 수준을 보여 EC기반 보충 방식에서 나타난 변동계수 6.9%, 4.9%, 23.7%, 8.6%, 그리고 8.3%보다 대체적으로 우수한 이온 균형 유지 성능을 보였다. 이러한 결과들을 통해 개발 정밀 관비 시스템이 기존보다 효율적인 양액의 공급과 관리를 통해 양액 이용 효율성과 생산성의 증진에 기여할 수 있을 것으로 판단되었다.

주요어: 자동화 시스템, 폐루프 제어, 순환식 수경재배, 작물영상 모니터링, 정밀 양액 공급, 이온 기반 양액 보충

학번: 2015-30385